

Functional Modulation of Activated Protein C using DNA-Aptamers

DISSERTATION

zur

Erlangung des Doktorgrades (Dr. rer. nat.)

der

Mathematisch-Naturwissenschaftlichen Fakultät

der

Rheinischen Friedrich-Wilhelms-Universität Bonn

vorgelegt von

Nasim Shahidi Hamedani

Aus

Hamedan, Iran

Bonn, Februar 2017

Angefertigt mit Genehmigung der Mathematisch Naturwissenschaftlichen Fakultät der
Rheinischen Friedrich-Wilhems-Universität Bonn

1. Gutachter: Prof. Dr. Bernd Pötzsch

2. Gutachter: Prof. Dr. Diana Imhof

Tag der Promotion: 07.02.2017

Erscheinungsjahr: 2017

Abstract

Aptamers are single stranded DNA or RNA oligonucleotides which are able to interact with their designated target molecules with high affinity and specificity. The in-vitro procedure used for aptamer selection from a randomly designed oligonucleotide library is named Systematic Evolution of Ligands by EXponential enrichment (SELEX). Since aptamers, in comparison to antibodies, bind to larger surface structures, these molecules have the potential to better discriminate between the enzymatically inactive zymogen and active enzymes. Indeed, it has been previously shown that a DNA-aptamer selected against activated protein C (APC) possesses a high selectivity over zymogenic protein C.

APC is a serine protease which is generated from zymogenic protein C by thrombin-mediated proteolytic activation on the surface of endothelial cells. APC performs its anticoagulant activity by proteolytic inactivation of activated factors V (FVa) and VIII (FVIIIa) which act as procoagulant cofactors within the blood coagulation cascade. Besides its anticoagulant functions, APC shows anti-inflammatory and anti-apoptotic activities which lead to endothelial barrier stabilization. Mild and moderate forms of inherited PC-deficiency predispose patients to an increased risk of venous thromboembolism while severe forms are associated with the development of purpura fulminans, a severe and potentially life-threatening thromboinflammatory disease comparable to severe sepsis. In severe sepsis acquired PC-deficiency plays a central role in the development of microvascular thrombosis leading to multiorgan failure. Substitution of septic patients with plasma-purified PC or a recombinant version of APC has been shown to improve outcome in terms of mortality rates. An increased incidence of bleedings, however, restricted the substitution of APC in patients with septicemia. Recombinant APC variants with impaired anticoagulant activity but intact cytoprotective properties are potentially safer drugs for the treatment of severe septicemia. Alternatively, specific ligands that selectively inhibit the anticoagulant activity of APC might offer several advantages over genetically engineered APC-variants.

To increase the probability to select distinct APC binding sequences with divergent functional activities we used a capillary electrophoresis (CE)-based SELEX strategy. In addition different randomized ssDNA-libraries were applied, including a G-rich library to increase the likelihood of selecting G-quadruplex containing aptamers. The SELEX technology was further improved by developing a novel method for single-stranded DNA (ssDNA) production, allowing the convenient and rapid purification of ssDNA.

A previously identified consensus motif dominated the selected aptamer pools despite using two differently structured randomized DNA-libraries during CE-SELEX. However, a G-quadruplex forming sequence raised up when using a G-rich DNA-library. Evaluation of the impact of identified aptamers on the amidolytic activity of APC combined with competition experiments using heparin as competitor revealed the so-called basic exosite of APC, which mediates its anticoagulant functions, as exclusive binding site. Further functional analysis clarified that, despite sharing the same binding site, different aptamers alter the functions of APC in different ways. Most interestingly, the G-quadruplex-based aptamer protected APC from inactivation by plasma protein C inhibitor while the other APC-specific aptamers rather accelerated this process.

To conclude, the described aptamers may be useful for fast and efficient inhibition of APC under APC-mediated bleeding situations. Since the anti-apoptotic and anti-inflammatory functions of APC are most likely not influenced by aptamer-binding, such aptamers may be used as an adjuvant therapy in hemophilia in which APC inhibition might at least partially compensate the absence or reduced activity of FVIII or FIX. Furthermore, the availability of specific ligands with high discriminatory power between the zymogenic and active form of APC might be useful for the quantification of the active enzyme in biological fluids.

Table of Content

Abstract	1
Chapter 1: General introduction and outline.....	1
1.1. Blood coagulation system	2
1.2. Regulation of the coagulation system.....	3
1.3. Activated protein C.....	4
1.3.1. APC structure	4
1.3.2. APC anticoagulant activity	5
1.3.3. APC cytoprotective activity	6
1.4. Aptamers	7
1.4.1. Aptamer selection procedure	8
1.4.2. Capillary electrophoresis (CE)	9
1.4.3. Capillary Electrophoresis-based SELEX (CE-SELEX)	11
1.5. Single-stranded DNA production	12
1.6. Aptamers against coagulation factors	14
1.6.1. Thrombin binding aptamers	16
1.6.2. Factor IXa binding aptamer.....	16
1.6.3. Anti-vWF aptamers	18
1.6.4. Anti-APC aptamers.....	18
1.7. Aims and outlines of the thesis	19
Chapter 2: Chapillary electrophoresis for the selection of DNA aptamers recognizing activated protein C.....	20
2.1. Abstract	22
2.2. Introduction.....	22
2.3. Materials.....	23
2.3.1. Capillary electrophoresis	23
2.3.2. Polymerase chain reaction (PCR).....	23
2.3.3. Agarose gel.....	24
2.3.4. ssDNA production	24
2.3.5. Filter retention analysis	25
2.4. Methods	25

2.4.1.	Installation and conditioning of a new capillary	26
2.4.2.	CE-based isolation of target-binding ssDNA-molecules	27
2.4.3.	PCR-based amplification of selected ssDNA	29
2.4.4.	Asymmetric PCR and isolation of ssDNA	29
2.4.5.	Filter retention experiment	30
2.5.	Notes	31
Chapter 3: Capture and Release (CaR): A simplified procedure for one-tube isolation and concentration of single-stranded DNA during SELEX.....		35
3.1.	Abstract	37
3.2.	Main manuscript	37
3.3.	Electronic supplementary information (ESI+)	43
3.3.1.	Chemicals and reagents	43
3.3.2.	Prediction of DNA hybridization profiles and design of capture-molecules	43
3.3.3.	Binding of capture-molecules to streptavidin-coated magnetic beads (SMB).....	45
3.3.4.	Assessment of binding and adverse release of capture molecules to /from SMB using fluorescence measurements	45
3.3.5.	Exponential amplification and asymmetric PCR	46
3.3.6.	Production of asymmetrically amplified IHT1-library for evaluation purposes	47
3.3.7.	Assessment of quality and purity of ssDNA after asymmetric PCR/ CaR during basic assay evaluation	47
3.3.8.	Quantification of streptavidin released from the SMB	49
3.3.9.	CE-SELEX against APC and FXIIIaA.....	49
3.3.10.	Yield and purity of ssDNA as produced by asymmetric PCR/ CaR during SELEX	50
3.3.11.	Filter retention assay.....	51
3.3.12.	Cloning and sequencing	52
3.3.13.	Production of identified individual aptamers by asymmetric PCR/ CaR and determination of binding affinity	52
3.3.14.	In silico folding predictions	55
3.3.15.	Determination of the reusability of loaded SMB	55
Chapter 4: Modifying substrate specificity of the serine protease activated protein C using excite-modulating aptamers.....		55
4.1.	Abstract	58
4.2.	Main manuscript	58

4.3.	Supplementary information	64
4.3.1.	Chemicals and materials	64
4.3.2.	Capillary electrophoresis-(CE)-SELEX	65
4.3.3.	Next generation sequencing and data analysis	65
4.3.4.	In silico secondary structure predictions	65
4.3.5.	Detection of G-quadruplex formation by Thioflavin T-staining.....	66
4.3.6.	Determination of dissociation constants and binding competition experiments.	66
4.3.7.	OECA-based binding competition experiments.....	67
4.3.8.	APC amidolytic assay.....	67
4.3.9.	FVa and FVIIIa inactivation assays	67
4.3.10.	Thrombin generation assay.....	68
4.3.11.	APC anticoagulant activity in whole blood	68
4.3.12.	APC-APC-inhibitor complex formation testing.....	69
4.4.	Supplementary tables and figures	69
	Abbreviations	79
	Bibliography.....	82
	Acknowledgement	91
	Curriculum Vitae.....	92

Chapter 1

General introduction and outline

1.1. Blood coagulation system

The occurrence of vascular injury requires rapid clot formation in order to prevent hemorrhage. In the case of damaged endothelium, platelets adhere to the sub-endothelium and, subsequent to instantaneous activation of the haemostatic system, fibrin production occurs, which forms a mesh over the platelet plug, sealing the site of injury. The explosive activation of the haemostatic system is due to the so-called 'cascade' system of coagulation in which inactive zymogens and cofactors are sequentially activated by proteolytic cleavage¹.

The coagulation cascade, which was proposed for the first time in 1964, is explainable as a model consisting of the interlinked so-called intrinsic and extrinsic pathways (Figure 1.1).

The physiologically more important extrinsic pathway involves tissue factor (TF) and factor VII (FVII). Upon vascular injury, cells expressing membrane-bound tissue factor come into contact with activated factor VII (FVIIa) within the blood. The resulting TF-FVIIa complex, as a potent activator of the coagulation cascade, activates two substrates, namely, factor IX (FIX) and factor X (FX)^{1,2}. In turn, activated factor X (FXa) activates minute amounts of prothrombin to thrombin³.

Thrombin is the key enzyme of the coagulation system due to its biologically important functions such as platelet activation, fibrinogen conversion to fibrin, and feedback amplification of the plasmatic coagulation cascade. Indeed, thrombin activates the coagulation co-factors VIII and V. Activated FVIII (FVIIIa) serves as a cofactor of FIXa within the 'tenase' complex, which is a contraction of "ten" and the suffix "-ase". This means that the substrate FX gets activated through cleavage by the complex. Accordingly, together with FXa, activated FV (FVa) forms the prothrombinase complex which activates prothrombin to thrombin^{1,4}.

At the final stage of the coagulation cascade, fibrinogen is converted by the act of thrombin to insoluble fibrin. The multi-step procedure starts with thrombin cleavage of fibrinogen to form soluble fibrin monomers. The newly formed fibrin mesh is stabilized by cross-linking catalysed through action of thrombin-activated coagulation factor XIII (FXIII)¹.

The currently reputed model of in vivo coagulation agrees on the central role of tissue factor as the main coagulation initiator. As described above, this model asserts the rapid amplification of thrombin as an essential step in the development of a stable clot and the dependence of the model on coagulation factors and cellular elements ². On the other hand, however, activation of the intrinsic pathway involves activation of factor XII (FXII) at negatively-charged surfaces exposed to the blood stream due to endothelial injuries. In the further course, activated FXII (FXIIa) activates Factor XI (FXI) which in turn activates FX, closing the link between both, the extrinsic and intrinsic pathways ².

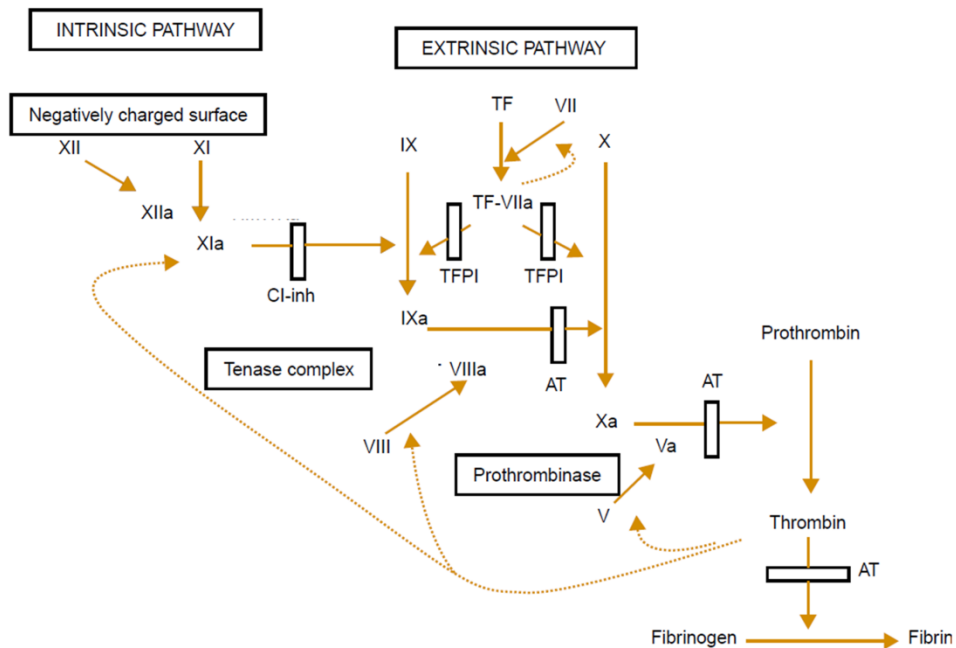


Figure 1.1. The cascade model of coagulation with its intrinsic and extrinsic pathways. C1-inh : C1-inhibitor. TF : tissue factor. TFPI : tissue factor pathway inhibitor. AT : antithrombin, modified from Norris, 2003 ¹.

1.2. Regulation of the coagulation system

The rapid and efficient activation of blood coagulation is essential to avoid blood loss. However, to prevent a generalized activation of coagulation and excess fibrin deposition, local and transient activation of the system at the site of vascular injury is required. To achieve this goal, various regulatory mechanisms are exerted either by enzymatic inhibition or by modulation of the activity of the cofactors.

As described above, the TF-VIIa complex as a potent initiator of the extrinsic pathway activates both, FIX and FX. A specific inhibitor of this complex is named the tissue factor pathway inhibitor (TFPI). TFPI is a multi-domain protein which is released from

endothelial cells and megakaryocytes and binds to the TF-VIIa complex subsequent to binding to FXa⁵. The anticoagulant activity of TFPI reduces intravascular procoagulant activity in the very early stage and thereby down-regulates thrombin formation⁶.

Many of the activated coagulation enzymes are inhibited by the serine-protease inhibitor antithrombin, which mainly forms irreversible complexes with FXa and thrombin. At this, the inactivation of free thrombin and FXa by antithrombin occurs faster than that of thrombin and FXa bound to activation complexes which ensures the clearance of active enzymes from circulation and restriction of their activity to the site of vascular injury and corresponding clot formation¹. Heparin and heparin-like molecules from the endothelial cell surface stimulate the activity of antithrombin towards both enzymes⁵.

Another important system for the regulation of blood coagulation is the protein C (PC) anticoagulant pathway.

1.3. Activated protein C

1.3.1. APC structure

Protein C is a vitamin K-dependent plasma protein which was purified for the first time from bovine plasma as described by Stenflo in 1976⁷. APC is generated from zymogenic protein C by thrombin-mediated proteolytic activation⁸.

Thrombomodulin (TM), which is expressed on the vascular endothelium, forms a 1:1 complex with thrombin which in turn activates PC bound to endothelial protein C receptor (EPCR) on the surface of endothelial cells. Circulatory APC is consisting of a light- and heavy-chain molecule held together by a single disulfide bond. The anticoagulant activity of APC is directed through irreversible proteolytic inactivation of FVa and FVIIIa, thereby inhibiting further thrombin generation⁹.

Human PC consists of 419 amino acids and undergoes post-translational modifications including β -hydroxylation at Asp⁷¹, N-linked glycosylation at residues 97, 248, 313 and 329 and gamma-carboxylation of nine glutamic acid residues in the amino terminus, the so called Gla domain¹⁰.

Thrombin cleavage of the zymogen PC at Arg¹⁶⁹ leads to elimination of the activation peptide (residues 158–169) and APC generation. The interaction of APC with different plasmatic and cellular proteins are directed by various amino acids embedded in domains termed exosites that are distinct from the active site triad consisting of His²¹¹, Asp²⁵⁷ and Ser³⁶⁰ that is characteristic for all coagulation enzymes⁸. The so-called basic exosite, consisting of the 37-loop, the 60-loop, and the 70–80-loop is involved in the proteolytic inactivation of factors Va and VIIIa^{11,12}. Furthermore, a negatively charged exosite, which consists of acidic residues of the 162 helix is responsible for the interaction of APC with

protease activated receptor-1 (PAR-1), mediating the anti-apoptotic and anti-inflammatory properties of APC¹³ (Figure 1.2).

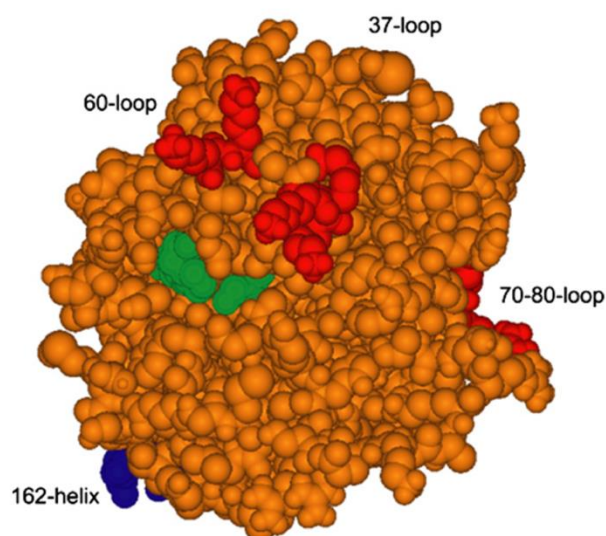


Figure 1.2. Space-filling model of the APC. The basic exosite consisting of basic residues of the 39-loop, the 60-loop, and the 70–80-loop are presented in red, while acidic residues of the 162 helix are exposed in blue. The green part located in the center of the molecule belongs to the catalytic triad. This model is configured based on the 1AUT structure from the crystal structure of APC deposited in the Protein Data Bank¹³.

1.3.2. APC anticoagulant activity

APC performs its anticoagulant activity by irreversible proteolytic inactivation of activated FVa/ FVIIIa. The two cleavages responsible for FVa inactivation by APC occur at Arg³⁰⁶ and Arg⁵⁰⁶ in a sequential order including the first rapid cleavage at the Arg⁵⁰⁶ site followed by a slower cleavage at the Arg³⁰⁶ site¹². The exact mechanism by which APC inactivates FVa is unclear but according to the findings of some experiments, the main structures of APC that take part in cleavage of the Arg⁵⁰⁶ site are the 39-loop (Lys³⁷-Lys³⁹) and the 70-80-loop (particularly Arg⁷⁴ and Arg⁷⁵)¹⁴. In the presence of protein S (PS), the cleavage of Arg³⁰⁶ is accelerated by 20-fold and the presence of FXa protects FVa from inactivation by APC through selective blockage of the Arg⁵⁰⁶ cleavage site¹⁵.

APC-mediated inactivation of FVIIIa takes place at the homologous sites Arg³³⁶ and Arg⁵⁶², located on the A1 and A2 subunits, respectively. Tendency for cleavage site selectivity is directed by the presence of other coagulation factors. While FIXa inhibits cleavage at the A2 site (Arg⁵⁶²), FX protects FVIIIa from inactivation through cleavage at the A1 site (Arg³³⁶)¹⁶. Unlike FVa, a cleavage on each of the cleavage sites leads to almost complete

inactivation of FVIIIa. Protein S (PS) enhances the cleavage rate at the Arg⁵⁶² site approximately 5 fold, however, it has only a moderate effect towards the Arg³³⁶ site¹¹.

FV promotes inactivation of FVIIIa by acting in synergy with PS as a cofactor of APC in the inhibition of the FVIIIa - FIXa complex. A mutant form of FV known as FV_{Leiden}, is less susceptible to proteolysis by APC due to amino acid substitution at Arg⁵⁰⁶ and the mutated FV does not display this anticoagulant cofactor activity. Since cleavage at Arg⁵⁰⁶ of FV by APC is prerequisite for its cofactor function, FV-Leiden has a 10-fold less efficiency as an APC-cofactor in the degradation of FVIIIa¹⁷. It has been also described by Castoldi et al. that the procoagulant effects of the FV_{Leiden} mutation is not only due to insensitivity of FVa to APC-mediated proteolysis but also to the loss of the above mentioned APC cofactor activity¹⁸.

Although the APC-mediated FVIIIa inactivation was confirmed in several investigations, spontaneous dissociation of A2 domain of FVIIIa might be the primary mechanism of FVIIIa inactivation due to the short plasmatic half-life of FVIIIa (~ 2 min)¹⁹.

1.3.3. APC cytoprotective activity

APC cytoprotective activities include anti-inflammatory activity, anti-apoptotic activity and protection of the endothelial barrier. These cytoprotective effects mostly require the two receptors EPCR and protease activated receptor-1 (PAR-1).

The APC anti-inflammatory effect can be conveyed into the effect on endothelial cells and the effect on leukocytes. APC inhibits the release of inflammatory mediators from leukocytes and endothelial cells and down-regulates vascular adhesion molecules, leading to reduced leukocyte adhesion and tissue infiltration and, consequently, decreasing damage to the tissue²⁰.

Breakdown of the monolayer of endothelial cells which separates the blood from underlying tissue plays a key role in inflammatory processes such as sepsis. APC enhances the endothelial barrier integrity by binding to EPCR and activation of PAR-1, leading to subsequent inhibition of inflammatory gene expression in endothelial cells²¹. In animal and human studies, APC proved to inhibit endotoxin-induced pulmonary injury and inflammation due to inhibition of leukocyte accumulation and chemotaxis²².

In addition to an improved survival rate in murine endotoxemia models, a large randomized clinical trial also suggested the pharmacologically beneficial effects of APC in reducing mortality in sepsis⁸. The PROWESS trial has urged approval of drotrecogin alfa (recombinant human activated protein C, Xigris®, Eli Lilly) by the Food and Drug administration (FDA) in the clinical treatment of adults suffering from severe sepsis in the last quarter of 2001²³. However, subsequent studies in 2010 showed a lack of efficiency of APC in septic shock treatment and an increased incidence of bleeding. As a result, it was withdrawn from the market^{24,25}. The increased incidence of bleedings was related to

the anticoagulant activity of APC as conducted by the basic exosite apart from the cytoprotective related exosite.

According to the above described findings that the anticoagulant and anti-inflammatory effects of APC are directed by distinct subdomains²⁶, the increased incidence of bleeding that encompassed the use of Xigris® may be controllable by the use of APC-specific inhibitors which affect the anticoagulant activity of APC while cytoprotective effects remain active. Furthermore, a specific ligand which interferes with the anticoagulant activity of APC might be helpful as an adjuvant therapy in hemophilia patients to compensate the lack of FVIII. In addition, having a specific ligand which could bind to APC with high affinity might be helpful in promoting diagnostic test systems to capture and detect the level and activity of APC in biological fluids. In this regard, aptamers represent a potent alternative to conventional antibodies.

1.4. Aptamers

Aptamers (from the Latin *aptus* - fit, and Greek *meros* - part) are oligonucleotide or peptide molecules which can bind to their target with high affinity and specificity²⁷. Nucleic acid aptamers (aptamers) are single-stranded DNA (ssDNA) or RNA oligonucleotides which can shape to specific three-dimensional structures including stems, loops, or G-quadruplexes²⁸. Based on their 3D structures, aptamers are able to bind to various molecular targets such as small molecules, proteins, nucleic acids, and even whole cells²⁹. The folding of the nucleic acid provides numerous interactions depending on the ligand which is responsible for aptamer-target binding such as electrostatic bonding, van der Waals interactions, hydrogen bonding, base stacking effects and hydrophobicity or combination of these bindings³⁰. For protein targets, the aptamer binding site is mostly on the surface of the target whereby non-covalent interactions lead to maximum binding through optimum complementarities²⁹.

The binding affinity of aptamers varies from the low nanomolar range for larger target molecules such as proteins to the micromolar range for small chemicals. A high selectivity of aptamers for their targets was described in many publications. In aptamers selected against coagulation factors, an active form-selectivity has been observed¹³. Moreover, the so-called enantiomer-selectivity which refers to the discriminatory power of an aptamer between two enantiomer molecules was also reported for aptamers³¹.

Aptamers not only show comparable binding affinity for their target molecules, but also offer advantages over antibodies as they can readily be produced by chemical synthesis which reduces batch to batch variation, and show adequate stability to a wide range of pH and organic solvents³². Modification of aptamers may lead to increased stability in biological fluids or binding enhancement³³. Some modifications specific for RNA aptamers such as changing of the 2'-OH groups of ribose to 2'-F or 2'-NH₂ groups or 2'-O-methyl substituted nucleotides protect them from nuclease degradation³⁴. A 3'-end

capping such as inverted thymidine (3'-idT) or making a 3'-3' linkage as well as executing 5'-caps by amine, phosphate or polyethyleneglycol (PEG) protect oligonucleotides from exonucleases^{35,36}.

1.4.1. Aptamer selection procedure

Systematic Evolution of Ligands by Exponential Enrichment (SELEX), which was described for the first time in 1990^{27,37} is a technology for in vitro selection of high affinity nucleic acid aptamers recognizing a designated target molecule²⁸. SELEX consists of repetitive cycles of selection, partitioning and amplification of binding sequences to enrich specific sequences with reasonable binding affinity. Normally the procedure starts with a nucleic acid library which consists of a random region flanked by two primer binding sites necessary for the amplification step. Through incubation of the random library with the target molecules, by chance, some sequences are able to bind to the target molecules. These specific sequences will be eluted from the target molecules after the partitioning step and amplified by a PCR reaction. The partitioning step is the most crucial step of the SELEX procedure. This step, in which the strong binding DNA-molecules are separated from unbound or weakly bound sequences, may influence the yield of selection, also due to the potential contamination of bound sequences with unspecific oligonucleotides (Figure 1.3).

Depending on the used DNA or RNA library for selection, a reverse transcription step is needed to transcribe RNA oligonucleotides to DNA strands which are necessary for the amplification process. The resulting double-stranded DNA has to be transformed into a new oligonucleotide pool by separating the relevant ssDNA or by in vitro transcription and subsequent purification of the synthesized RNA. This new pool of selected single-stranded oligonucleotides is used for incubation with the target molecules in the next round of SELEX²⁸. Generally 8 to 12 selection cycles are needed to reach to high affinity aptamers. As assessed by measurement of the crude binding affinity, the enriched final pool will be subjected to the cloning and sequencing step to identify individual aptamers. Representative aptamer-clones are then chosen and used in binding assays to characterize their binding features in terms of affinity and specificity.

Sequence truncation for identifying the minimal binding motif is an important step to narrow down the critical binding domains. As assessed by predicted 2D structures, redundant regions are removed, and the properties such as binding affinity or specificity of the truncated aptamer checked.

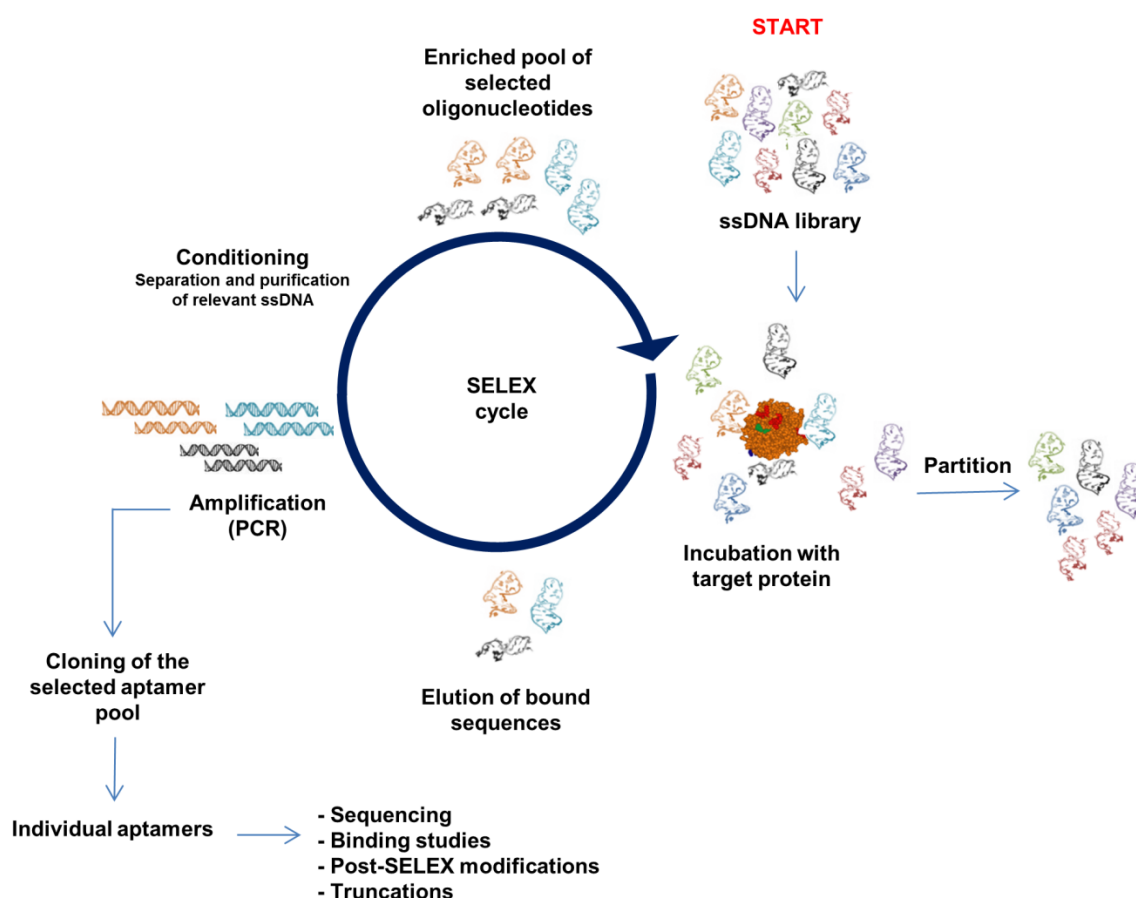


Figure 1.3. Schematic representation of DNA aptamer selection. The starting point of each SELEX procedure is incubation of a synthetic random DNA oligonucleotide library with target molecules followed by repetition of the iterative steps of selection, amplification and preparation of single-stranded DNA. In the selection step, binding sequences are partitioned from unbound and/or weakly bound oligonucleotides. The target-bound oligonucleotides are eluted and subsequently amplified by PCR. A new enriched pool of selected oligonucleotides is generated by preparation of the relevant ssDNA from the PCR products. This new enriched pool is used for the next SELEX round. Generally, 6 to 20 SELEX rounds are required for the selection of high affinity, target-specific aptamers. Assessment of the enrichment of target specific oligonucleotides indicates the plateau of the SELEX procedure and the enriched library is subjected to cloning and sequencing to obtain individual aptamers.

1.4.2. Capillary electrophoresis (CE)

Electrophoresis involves an electrical field to attract or repulse the ingredients of a mixture in an electric field. It was introduced as a separation technique by Tiselius in 1937 and led to the Nobel Prize in chemistry in 1948³⁸. Primary application of open tubes for electrophoresis was described by Hjertén in 1967 which continued in the early 1980s

electrophoresis buffer. The sample is injected into the capillary column and separated under high voltage applied to both ends of the capillary column. (B) In fused-silica capillaries, positively charged buffer ions are attracted to the negatively charged silanoate groups (Si-O⁻). This forms two inner layers of cations. Under the high voltage applied between the ends of the capillary, the more mobile layer which is distant from the silanoate groups moves in the direction of the negatively charged electrode, resulting in a constant bulk flow of electrolytes called the electroosmotic flow (EOF). Although the EOF is always toward the electrode having the same charge as the capillary wall, positively charged molecules move faster due to the electrophoretic attraction to the negatively charged electrode while negatively charged molecules are retained longer because of their contradictory electrophoretic mobility. Therefore, molecules are separated by mass/charge ratio within the flow.

In fused-silica capillaries, silanol groups (Si-OH) which are attached to the interior wall of the capillary, are ionized through a first conditioning step using alkaline solution like KOH or NaOH. The silanoate groups (Si-O⁻) attract positively charged buffer ions to form two inner layers of cations, called the diffuse double layer. Under the high voltage applied between the ends of the capillary, the outer layer which is distant from the silanoate groups and therefore more mobile, moves in the direction of the negatively charged electrode, resulting in a constant bulk flow of electrolytes called the electroosmotic flow (EOF). This EOF represents the main trigger responsible for the mobility of injected materials within the capillary. Due to the greater force of the EOF than the electrophoretic mobility of the compounds, all injected molecules migrate from the inlet (anode) to the outlet (cathode) of the capillary³⁸. As a result of the electrophoretic attraction to the negatively charged electrode, positively charged molecules move faster while negatively charged molecules are retained longer because of their contradictory electrophoretic mobility. Therefore, depending on its mass and charge, each specific molecule possesses a specific retention time under the conditions defined by the electrophoresis setup³⁹.

1.4.3. Capillary Electrophoresis-based SELEX (CE-SELEX)

Conventional SELEX normally involves the immobilization of the target protein. Despite the advantages accompanied with immobilized targets such as efficient partitioning of bonded sequences from non-binders, some draw backs such as the need of so called counter selection to exclude sequences that show cross-reactivity to the applied solid support has to be mentioned. Another disadvantage of target immobilization may be the masking of specific structures which may affect the selection. Thus, homogenous selection methodologies such as capillary electrophoresis-based SELEX (CE-SELEX), which allows the selection of aptamers against free targets are an advantage and also provide a high resolving power that reduces the desirable number of cycles for selection to 4 to 6 cycles instead of 8 to 12 cycles when using conventional selection schemes^{41,42}.

Potential disadvantages of CE-SELEX are the limitation of the sample volume which leads to restriction of the total number of ssDNA-molecules that can be introduced into the capillary, the difficulty of selecting aptamers against basic or low molecular weight target molecules, or thermal band broadening of CE because of Joule heating which restricts the ion composition of the partitioning buffer³⁹. Furthermore, the optimal conditions must be determined for each individual protein, randomized library and selection buffer^{41,43}.

During the first step of CE-SELEX, a randomized ssDNA-library is incubated with the target molecule in free solution. After a certain incubation time, the mixture containing free target molecules, target-ssDNA complexes and free ssDNA is injected into a primed capillary. The loaded capillary is placed to span two reaction tubes filled with neutral to basic conductive buffer. In the case of the replacement of the negatively charged electrode in the end of the capillary, the positively charged free target proteins migrate faster while the negatively charged non-bound library retains longer within the capillary. Collecting the outlet fraction at the retention time specific for target-bound ssDNA offers the opportunity of gathering target-binding DNA-aptamers.

Collected sequences are then amplified and generated single-strands subjected to the next round of the selection procedure. Usually 4 to 6 cycles of selection are required for the enrichment of an aptamer-pool showing peak bulk binding affinity. Subsequent analysis of included single aptamer-sequences by either cloning/sanger-sequencing or next-generation sequencing approaches finally leads to the identification of candidate sequences to be tested for binding affinity and specificity.

1.5. Single-stranded DNA production

After partitioning step of SELEX procedure, the enriched pool is subjected to the PCR amplification to increase the copy number of specific sequences. Double strand sequences resulted from PCR amplification could not be introduced to the next selection cycle before single strand production has been performed.

Several procedures have been described indicating single strand production from double strand PCR products such as alkaline-based denaturation of biotinylated PCR-products after immobilization onto streptavidin-coated magnetic beads (SMB) or enzymatic strand digestion after asymmetric PCR^{44,45}. Apparently, all of these procedures do accompany with their advantages and drawbacks. For example, alkaline-based treatment requires final neutralization or solvent exchange of the final product to achieve suitable ssDNA for proceeding with the next selection cycle.

Biotin streptavidin separation including alkaline treatment is another rapid and efficient method in which PCR amplified double strands are immobilized onto SMBs using biotinylated forward or reverse primer followed by separation of desired non-biotinylated

strand from immobilized biotinylated one using alkaline treatment (NaOH). Further steps such as ethanol precipitation can increase ssDNA concentration. The possibility of releasing of biotinylated non-target strand and/or streptavidin due to the alkaline treatment is the major drawback of this method which results to loss of tertiary structure of specific strand due to re-annealing of complementary strand or introduction of a secondary target for selection, respectively^{45,46}.

Lambda exonuclease selectively digests phosphorylated strand from 5' to 3' end with high affinity to phosphorylated 5' end rather than the hydroxylated 5' end. The procedure is fast and efficient however, subsequent purifications such as phenol/chloroform extraction for lambda exonuclease elimination results in reduction in the yield of ssDNA production⁴⁵.

Recently, we introduced a novel fast and convenient principle for the purification of ssDNA named Capture and Release (CaR) which has been described extensively in **chapter 3**⁴⁷. Briefly, short biotinylated oligodeoxynucleotides, that are complementary to the 3'-end of the target single stranded oligodeoxynucleotides (aptamers), are bound to streptavidin magnetic beads. Incubation of the loaded streptavidin magnetic beads with asymmetric PCR mixtures results in capturing of the ssDNA which can be easily released after washing by alteration of temperature and ion strength conditions (Figure 1.5).

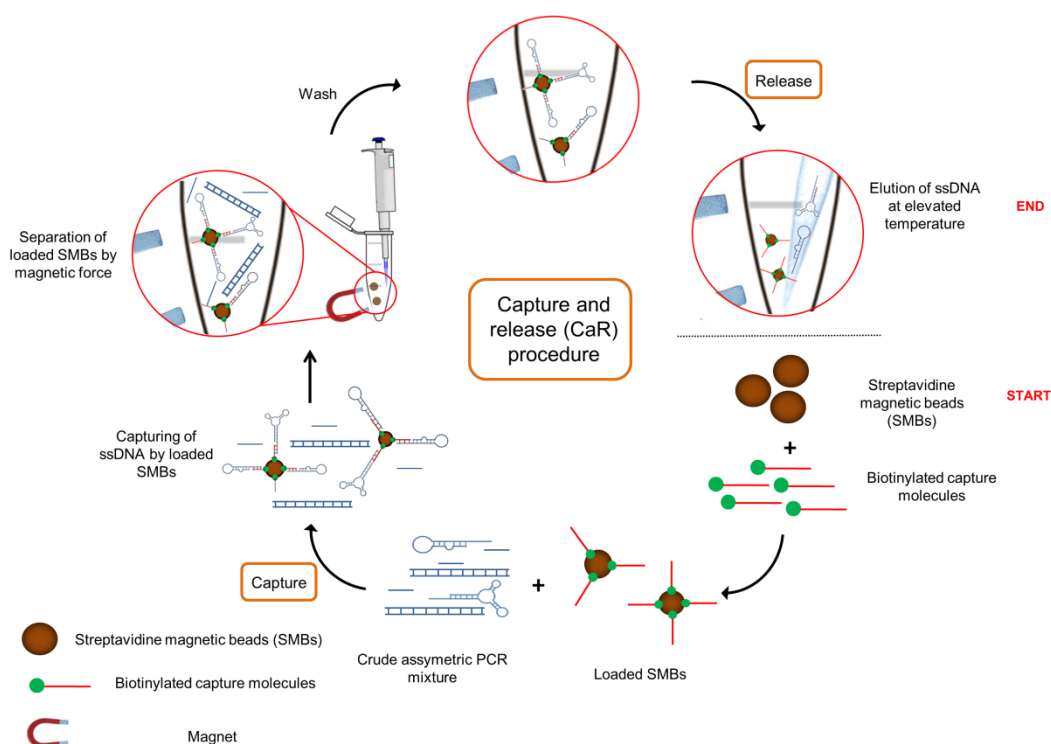


Figure 1.5. Principle of capture and release (CaR) procedure. Single-stranded DNA (ssDNA) is captured from crude asymmetric PCR mixture using streptavidin magnetic beads (SMBs) loaded with short biotinylated DNA molecules complementary to the 3' end of the ssDNA. Captured

ssDNA is released after washing by increasing the temperature and lower the ion strength conditions.

1.6. Aptamers against coagulation factors

Anticoagulation is an important therapeutic strategy for the prevention and treatment of thrombotic disorders.

Heparin, is widely used as a parenteral antithrombotic due to its low cost and ease of monitoring. However, numerous shortcomings accompany heparin as it bears the risk of hemorrhage and heparin-induced thrombocytopenia⁴⁸. Warfarin, a member of the vitamin K antagonists, is an oral anticoagulant with a narrow therapeutic window and requires individualized dosing based on the international normalized ratio (INR). Due to the narrow therapeutic index and necessity for frequent laboratory monitoring associated with warfarin, there has been a desire for the development of new and effective anticoagulants. Among novel anticoagulants (NACs) direct thrombin and FXa inhibitors were designed. Some of these direct thrombin inhibitors are administered parenterally, including argatroban and bivalirudin; however, oral administration of dabigatran increases patient compliance in long term use. Having idarucizumab (Praxbind®) in hand as a monoclonal antibody designed for the reversal of anticoagulant effects is another advantage of dabigatran.

Also direct acting factor Xa inhibitors are used for prophylaxis and/or treatment of embolic diseases. Andexanet-alpha which is a modified recombinant derivative of FXa, acts as an antidote for direct inhibitors of factor Xa including apixaban, rivaroxaban and edoxaban^{49,50}. Lack of specific laboratory parameters available to monitor the anticoagulant impact is a major drawback of FXa inhibitors⁵¹. Conventional coagulation monitoring assays such as activated partial thromboplastin time (aPTT) and prothrombin time (PT) are unable to accurately measure the degree of anticoagulation in patients undergoing therapy with NACs. Therefore, management of bleeding complication mostly comprises basic principles of bleeding management, including rapid assessment of the source, cause, and severity of bleeding, cessation of anticoagulation therapy and, if possible, reversal of anticoagulation effects, using specific antidote^{52,53}.

To overcome the major drawbacks of NACs, an optimal anti-thrombotic drug which is safe, non-toxic and well adjustable is needed. Other optimal characteristics that might accompany with an anti-thrombotic drug are rapid onset of action, predictable dose-response, selectivity for a specific biological target and reversible action⁵⁴. Among different researches for finding reasonable novel candidate molecules, aptamers appear as an emerging class of future anticoagulants. Chemical modifications of aptamers such as amino- or fluoro- modification at the 2' position of pyrimidines as well as 3' inverted deoxythymidine caps make RNA aptamers resistance to nuclease degradation. Conjugation of polyethylene glycol and other moieties lead to the reduction in aptamer

renal clearance during in vivo utilization. The general concept of antidote control of aptamers relies on Watson-Crick base pairing which alter the 3D structure of the aptamer, leading to loss of target binding affinity⁵⁵. On the other hand, aptamers can be used as capturing ligands to quantify the circulating level of certain coagulation factors in plasma as well as other biological fluids. For example, the application of an oligonucleotide (aptamer)-based enzyme capture assay (OECA) allows rapid quantification of circulating levels of APC under pathological conditions such as hip-replacement surgery. The test platform quantifies the activity of aptamer-captured APC through hydrolysis rates of a fluorogenic peptide substrate⁵⁶.

Several aptamers have been selected against different coagulation factors such as thrombin, activated protein C, FVIIa and FIXa (Table 1.1).

Table 1.1. Binding properties and application of selected aptamers against blood coagulation proteins

Target	Oligo type	Binding affinity [nM]	Binding site	Application	Reference
Human thrombin	α -DNA	~ 200	Fibrinogen binding site of thrombin	Thrombin procoagulant function Inhibition	57
Human thrombin	α -RNA	9.3	Heparin binding site of thrombin	Thrombin-catalysed fibrin-clot inhibition	58
Human thrombin	α -DNA	0.5	Heparin binding site of thrombin	Inhibition of thrombin-mediated activation of platelets and FV/VIII	59
Human Factor IXa	RNA	0.65	EGF1 and/or EGF2 domain of FIX	Inhibition of FX cleavage by FIXa-FVIIa	60
VWF	DNA	>20	GPIb α binding domain on vWF	Inhibition of vWF-dependent platelet activation	61,62
VWF	Modified DNA/RNA oligonucleotide	2 nM*	GPIb α binding domain on vWF	Inhibition of vWF-dependent platelet activation	63

APC	RNA	~ 100	Not clear	Inhibition of APC anticoagulant function	64
APC	DNA	0.47	Heparin binding site	Inhibition of APC anticoagulant function	13

* The binding affinity has been determined for A1 domain of VWF

1.6.1. Thrombin binding aptamers

The first DNA-aptamer against thrombin has been selected in 1992 by Bock et al ⁵⁷. This aptamer, which was named later as HD1, interferes with thrombin catalyzed conversion of fibrinogen to fibrin. The structure of the aptamer, which was solved by structural analysis, is an antiparallel G-quadruplex and conducts it to one of the anion binding site of thrombin, named exosite I. The second thrombin-recognizing aptamer, which possesses a RNA structure, was selected two years later by Kubik and colleagues ⁵⁸. Another DNA based thrombin binding aptamer which bears a G-quadruplex structure and binds to the heparin binding exosite of thrombin, known as exosite II, was identified by the same group ⁵⁹. Later on, a bivalent aptamer consisting of the two DNA aptamers coupled via a poly- dA linker has been described as the most potent aptameric thrombin inhibitor. It binds to both anionic exosites without blocking the active site of the enzyme ⁶⁵. This bivalent aptamer, HD1-22, has been used for the measurement of plasma thrombin levels. Through incubation of primed plasma samples in microtiter plates pre-coated with HD1-22, thrombin is captured and detected using a thrombin-specific fluorogenic peptide substrate. Compared to the available thrombin measurement techniques, which are based on the measurement of thrombin-antithrombin complexes (TAT) or prothrombin activation peptides (F1.2) as two cumulative markers in plasma, using an aptamer-based capturing assay for direct measurement of circulating levels of active thrombin better reflects the real time coagulation status ⁶⁶.

1.6.2. Factor IXa binding aptamer

An aptamer specific for FIXa has been described in 2002 by Rusconi et al ⁶⁰. This RNA aptamer, which is reinforced against nucleases by using 2'-fluoropyrimidines, was assessed in both in vitro and in vivo studies. The binding site and the impact of the aptamer on blockade of intrinsic and extrinsic coagulation pathways are controversially discussed. Although Rusconi et al. have an impression that the FIXa aptamer blocks either intrinsic or extrinsic pathway probably through binding protease and EGF2 domains of factor IXa, later experiment conducted by Gopinath et al. revealed that this aptamer

specifically blocks the extrinsic coagulation pathway with emphasizing on binding domain of the Gla and EGF1 domains on factor IXa⁶⁷. Rusconi et al also reported the binding site of EGF2 domain on FIXa for aptamer⁶⁰. The concept of using a complementary oligonucleotide as an aptamer-specific antidote was first described for the FIXa aptamer (Figure 1.5) and currently assessed in clinical trials. REG1 (Regado Biosciences) is an anti-FIXa aptamer system containing the aptamer pegnivacogin (RB006) and anivamersen (RB007) in which RB007, the complementary oligonucleotide antidote, binds to RB006 by Watson-Crick base pairing and neutralizes its anti-FIXa activity⁶⁸. In a phase 1a study after intravenous injection of RB006 in healthy volunteers and in phase 1b study demonstrating the efficiency of RB006 as well as the-RB007 antidote in patients with stable coronary artery disease, no major bleeding or any other serious adverse events were observed^{69,70}. A subsequent phase 2a clinical trial demonstrated the effectiveness of the REG1 system when combined with platelet-directed therapy in patients suffering from stable cardiac artery disease (CAD), while a phase 2b (RADAR) study revealed the effectiveness of RB006 in patients with acute coronary syndrome (ACS) undergoing cardiac catheterization⁷¹. A randomized multicenter phase 3 trial planned to randomly allocate 13200 patients undergoing percutaneous coronary intervention and to compare the effectiveness of the REG1 system to bivalirudin faced early termination with 3232 patients due to severe allergic reaction in 1% of patients receiving REG1. Thus, according to the limited events and low statistical power resulting from the premature termination of the study, there was no evidence that using the REG1 system reduces ischaemic events or bleedings when compared to bivalirudin⁷².

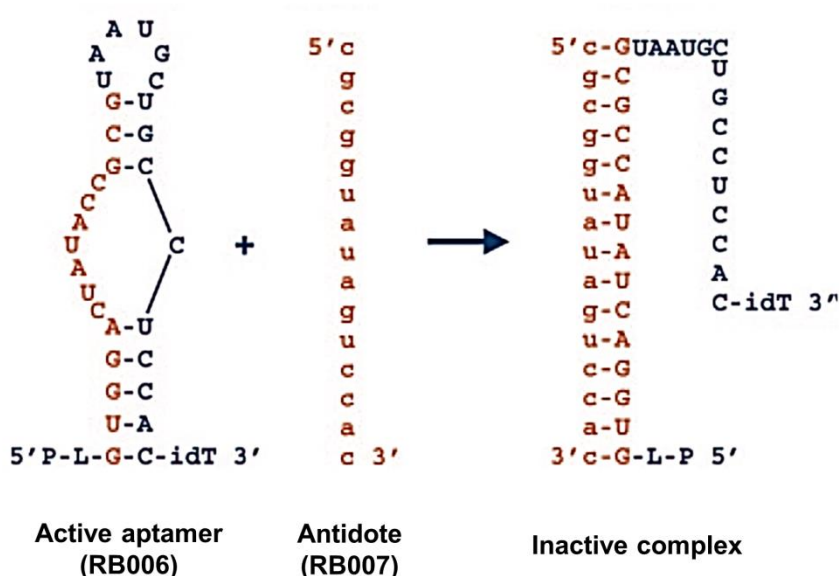


Figure 1.5. The REG1 anticoagulation system which is composed of the anti-FIXa aptamer pegnivacogin (RB006) and the oligonucleotide antidote to RB006, anivamersen (RB007). Antidote

RB007 and the motif within RB006 which pairs to RB007 shown in red. P indicates polyethylene glycol; idT, inverted deoxythymidine; modified from Nimjee et al., 2006⁷³.

1.6.3. Anti-vWF aptamers

ARC-1172 is a DNA-aptamer recognizing von-Willebrand factor (vWF). The aptamer can strongly inhibit vWF-mediated platelet adhesion due to inhibition of the vWF A1-domain and platelet GPIb α membrane receptor interaction. Furthermore, by using specific antidote molecules, platelet functions could be efficiently restored⁶¹. Later on, ARC-1779, a DNA/RNA-based aptamer was introduced. The molecule included a 5'- conjugation of PEG while the aptamer still showed high binding affinity to A1 domain of vWF⁶³. The first phase 1 clinical trial which investigated safety, pharmacokinetics and pharmacodynamics of the aptamer in healthy volunteers started in 2007 and was successfully completed in the same year (NCT00432770) (<http://clinicaltrials.gov>). Then, the next evaluation study suggested dose- and concentration-dependent inhibition of vWF activity and platelet function of ARC1779 without a significant increase in bleeding⁷⁴. In a phase 2 clinical trial started in 2008 in 36 patients undergoing carotid endarterectomy (CEA), intravenous injection of the aptamer was effective in reducing cerebral embolism⁷⁵. To conclude, between the years 2007 and 2010, among six registered clinical trials considering phase 1 and 2 clinical trials of ARC-1779, one had been withdrawn and three phase 2 trials have been terminated due to the reason that the enrollment into studies was slower than expected.

1.6.4. Anti-APC aptamers

The first aptamer selected against APC was described in 1998⁶⁴. The non-modified RNA aptamer consisted of 167 nucleotides and showed an intermediate binding affinity to APC (KD = ~ 100 nM). However, the selectivity of the aptamer over zymogenic protein C was not evaluated. In 2009, the selection of DNA aptamers against APC was described. The aptamers showed enhanced affinity for APC in the subnanomolar range and a 200- to 400-fold lower binding affinity to PC¹³. According to the fact that DNA aptamers are fundamentally more resistant to enzymatic degradation in the plasma or whole-blood matrix compared to non-chemically modified RNA aptamers, a longer half-life in these matrices can be expected. Using the truncated aptamer variant HS02-52G, an oligonucleotide-based enzyme capture assay (OECA) was developed and validated. The assay allows the measurement of APC plasma levels under clinical conditions with a lower limit of detection of 22 pg/mL (0.4 pM)⁵⁶. Furthermore, HS02-52G aptamer binds to basic exosite of APC without affecting the anti-apoptotic and cytoprotective functions of the active enzyme. Thus the selective inhibition of the anticoagulant activity of APC offers a potential application of HS02-52G to stop APC-induced bleeding complications in patients receiving recombinant APC.

1.7. Aims and outlines of the thesis

Aptamers are single-stranded DNA or RNA molecules which bind to their designated target molecules with high affinity and specificity. The ease of production and reduced batch to batch variability make aptamers interesting diagnostic tools as well as clinically applicable agents. Enzymes involved in the blood coagulation process are multi task proteins containing several functional domains. Activated protein C (APC) is a serine protease with plasmatic and cellular functions. Beside its role in inactivation of FVa and FVIIIa, it has cytoprotective effects which include anti-inflammatory and anti-apoptotic activities. The interactions of APC with FVa and FVIIIa are directed by the so-called basic exosite while the acidic exosite is involved in the interaction with protease activated receptor-1 (PAR-1), mediating the anti-apoptotic and anti-inflammatory properties of APC. Interference with each domain may lead to alteration of enzyme functions either by steric hindrance or allosteric inhibition.

The aim of this study was first to identify aptamers that specifically recognize APC and then to elucidate the effect of these aptamers on the different functions of APC.

The first priority to achieve aptamers that possess a high binding affinity is to set up a selection method accompanied with high efficiency and resolution of separation. To accomplish this goal, CE-SELEX was performed which accompanied with numerous advantages such as using target proteins in native free conformation and a high resolving power which leads to higher conversion rate of specific sequences in shorter time. Consecutive steps of a selection procedure as well as the evaluation of the binding affinity of selected aptamers to APC are described in **chapter 2**.

Single-stranded DNA production is a crucial step during the aptamer selection procedure in order to provide an enriched library of aptamers needed for the next selection round. Accordingly, in **chapter 3**, a convenient and rapid method for ssDNA production named Capture and Release (CaR) that allows direct isolation and concentration of ssDNA from asymmetric PCR-mixtures without the need for post-processing and conditioning steps is introduced. This method is described in the context of the CE-SELEX procedure but may also be implemented in other applications that require the generation of ssDNA.

Due to the fact that different functions of APC such as anticoagulant and cytoprotective effects are directed by distinct exosites, selective modulation of APC functions might be applicable according to the binding site of each specific ligand. Furthermore, as aptamers, in comparison to antibodies, bind to larger surface structures, binding of aptamers to the same or overlapping regions might cause distinct effects on the anticoagulant function of APC. Accordingly, in **chapter 4** the selection and characterization of DNA-aptamers against APC using the established CE-SELEX and CaR methods is described. In addition a comprehensive functional characterization of the newly identified APC-aptamers has been performed. The found aptamer-mediated alterations of the anticoagulant functions

of APC opens the horizon in the prevention of APC-induced bleeding such as in trauma-induced coagulopathy and supportive treatment approach in hemophilic patients.

Chapter 2

Capillary electrophoresis for the selection of DNA aptamers recognizing activated protein C

Adapted from

Hamedani, N.S., and Muller, J. (2016). Capillary Electrophoresis for the Selection of DNA Aptamers Recognizing Activated Protein C. *Methods in molecular biology* (Clifton, N.J.) *1380*, 61-75.

2.1. Abstract

Capillary electrophoresis-based SELEX (CE-SELEX) is an efficient technique for the isolation of aptamers binding to a wide range of target molecules. CE-SELEX has a number of advantages over conventional SELEX procedures such as the selection of aptamers can be performed on non-immobilized targets, usually within a fewer number of selection cycles. Here we describe a complete procedure of CE-SELEX using activated protein C (APC) as the target protein.

2.2. Introduction

Aptamers are single stranded DNA or RNA molecules which are able to bind to different target molecules ranging from small organic molecules to entire organisms. Aptamers are typically selected from randomized libraries of nucleic acids using a procedure termed **Systematic Evolution of Ligands by Exponential Enrichment (SELEX)** which was introduced for the first time in 1990^{27,37}. The SELEX-procedure consists of multiple rounds of selection, partitioning and amplification which are repeated to allow for the enrichment of aptamers with high binding affinity. This procedure will be completed by cloning and/or sequencing, and evaluation of individual aptamer sequences⁷⁶.

During conventional SELEX, targets need to be immobilized onto solid supports to allow for efficient separation from non-binding ssDNA-molecules. However, further progressions led to the development of homogenous methods, such as capillary electrophoresis (CE)-SELEX, which allow the selection of aptamers against free targets⁷⁷.

In CE-SELEX, the random library is incubated with the target molecules in free solution and then the mixture containing free target molecules, target-ssDNA complexes and free ssDNA is injected into a capillary column and separated under high voltage. Collecting the outlet fraction at the retention time specific for target-bound ssDNA brings about the opportunity of gathering target-binding DNA-aptamers.

Besides homogeneous conditions, this kind of selection has additional advantages such as a high resolving power that reduces the number of cycles needed for selection to 4 to 6 cycles instead of 8 to 12 cycles when using conventional selection schemes⁴². However, also potential disadvantages do accompany CE-SELEX such as limitation in the total

number of ssDNA-molecules introduced to the capillary or the difficulty of selecting aptamers against basic or low molecular weight target molecules⁴³.

In this chapter, a protocol for CE-SELEX of DNA-aptamers against activated Protein C (APC) is described. Although elucidated for the use of a ProteomeLab *PA 800* System (Beckman Coulter, Krefeld, Germany), the described principles are also applicable when using other CE-systems.

2.3. Materials

2.3.1. Capillary electrophoresis

1. ProteomelabTM PA 800 capillary electrophoresis (Beckman Coulter, Inc., Fullerton, CA, USA) equipped with UV/PDA detector.
2. Bare fused-silica capillary, 67 cm total length, 50 cm effective length, 50 μm inner diameter (i.D.), 375 μm outer diameter (o.D.) (Beckman Coulter, Inc. Brea, CA, USA).
3. Plastic vials, 0.5 ml.
4. Glass vials, 2 ml and caps (Beckman Coulter, Inc. Brea, CA, USA).
5. Random ssDNA-library IHT1: 5'- AAG CAG TGG TAA GTA GGT TGA - N₄₀ - TCT CTT CGA GCA ATC CAC AC -3'. Order 1 μmol synthesis scale followed by PAGE purification. Store lyophilized powder at 2-8°C until dissolved. Aliquot and store resolved stock solutions (e.g. 100 μM) at $\leq -20^\circ\text{C}$ until used.
6. Separation buffer: 25 mM Tris-HCl, 10 mM NaCl, 1 mM KCl, 1 mM CaCl₂ and 1 mM MgCl₂, pH 8.3 (see **Note 1**) (see **Note 2**).
7. Human activated protein C (APC) (e.g. Haematologic Technologies, Essex Junction, Vermont, USA). Store stock solutions as indicated on label until used (see **Note 3**).
8. Vivaspin[®]6 centrifugal concentrators with 10,000 Da MW cut-off (Sartorius Stedim, Goettingen, Germany).
9. Washing buffers: 0.1 N NaOH; 0.1 N HCl; ultrapure water.

2.3.2. Polymerase chain reaction (PCR)

1. Thermal cycler.
2. HotStarTaq *Plus* DNA polymerase including buffers.

3. Amplification primers targeting the fixed sequences of the library in full length, HPLC purified. Store lyophilized powder at 2-8 °C until dissolved. Aliquot and store resolved stock solutions (e.g. 100 µM) at < -20°C until used.
4. Deoxynucleotide triphosphates solution, 25 mM of each. Aliquote and store stock solutions at -20°C until used.
5. PCR tubes 0.2 ml.

2.3.3. Agarose gel

1. LE Agarose.
2. Tris Borate-EDTA buffer: 50 mM Tris, 45 mM boric acid, and 0.5 mM EDTA, pH 8.4.
3. 10 mg/mL Ethidium bromide. Aliquot and store stock solutions. Add adequate amount of ethidium bromide to agarose cooled to 50-60°C to reach a final concentration of 0.5 µg/ml (see **Note 4**).
4. DNA molecular weight marker XIII, 50 base pair ladder.
5. Loading buffer for gel electrophoresis: 40% succrose, 0.1% Xylene cyanol and 0.1% Bromophenol blue. Store stock solutions at 4-8°C until used.

2.3.4. ssDNA production

1. NanoDrop® ND-1000 UV/Vis-Spectrophotometer (Thermo Scientific).
2. Thermomixer.
3. Magnetic beads separator.
4. Streptavidin-coated magnetic beads (SMB), Dynabeads M-280 Streptavidin (Life Technologies, Karlsruhe, Germany). Store the vial upright to keep the beads in liquid suspension since drying of the beads will result in reduced performance. Store the vial at 2-8°C, avoid freezing.
5. 5' -biotinylated capture molecules, complementary to a part of the 3' primer-binding section of the IHT1 library: 5'-Biotin-GTG TGG ATT GC-3'. Store lyophilized powder at 2-8°C until dissolved. Aliquot and store resolved stock solutions (e.g. 100 µM) at -20°C until used.
6. Binding and washing buffer 1 (B&W 1): 5 mM Tris-HCl, 1 M NaCl, 0.5 mM EDTA, pH 7.5.
7. Binding and washing buffer 2 (B&W 2): 5 mM Tris-HCl, 1 M NaCl, pH 7.5.

8. Washing buffer: 10 mM Tris-HCl, 20 mM NaCl, pH 7.5.
9. 5 M NaCl-solution.
10. Protease-free bovine serum albumin (BSA). Store at 4°C.
11. SMBs storage buffer: 1x PBS, 0.1% BSA, 0.02% NaN₃, pH 7.4.

2.3.5. Filter retention analysis

1. Phosphorimager.
2. Dot-Blot system, e.g. Minifold® I Blotting System (Whatman, USA).
3. T4 polynucleotide kinase.
4. Phosphorimager screen and matching cassette.
5. γ -³²P ATP (PerkinElmer, Rodgau, Germany).
6. Dulbecco's phosphate buffered saline containing 0.5 mM MgCl₂ 0.9 mM CaCl₂.
7. Illustra microspin G-25 columns.
8. Nitrocellulose membranes, 0.45 μ m pore size.
9. Yeast tRNA, 10 mg/ml.

2.4. Methods

During the first step of CE-SELEX, the randomized library is incubated with the target molecule (e.g. APC). After incubation, a small volume of the sample is injected into a primed, silica-fused capillary for CE-based separation of non-binding from target-bound sequences. The loaded capillary is then placed to span two reaction tubes filled with neutral to basic conductive buffer solution. During separation under high voltage applied between the tubes, positively-charged buffer ions that are attracted to the negatively charged surface of the capillary do migrate to the cathodic end, resulting in a constant bulk flow of electrolytes that is called the electroosmotic flow (EOF) and represents the main trigger responsible for the mobility of injected materials within the capillary. Because the force of the EOF is greater than the electrophoretic mobility of the compounds, all injected molecules migrate from the inlet (anodic) to the outlet (cathodic) of the capillary³⁸. Due to the electrophoretic attraction the positively charged molecules move faster while negatively charged molecules are retained longer because of their contradictory electrophoretic mobilities. Therefore, depending on its mass and charge, each specific molecule possesses a specific retention time under the conditions defined by the electrophoresis setup³⁹. The negatively-charged ssDNA sequences which show binding affinity to the faster moving target protein molecules migrate at retention times that are shorter than that of the bulk non-binding ssDNA-library molecules. Thus, target-

binding sequences can be collected from the outlet of the capillary within the so-called collection window that is the time between the start of the separation and the time that unbound sequences reach the outlet.

Collected sequences are amplified and generated single-strands introduced to the next round of the above described CE-SELEX-procedure. Usually 4 to 6 cycles of selection are required for the enrichment of an aptamer-pool showing peak bulk binding affinity. Subsequent analysis of included single aptamer-sequences by either cloning/Sanger-sequencing or next-generation sequencing approaches finally leads to the definition of candidate sequences to be tested for binding affinity by filter retention analysis.

Due to the lower amount of ssDNA that is injected into the capillary, in comparison to other selection methods, an increased risk of contamination with non-target-specific sequences stemming from capillary and/ or instrument contaminations must be considered. The most critical source of contamination are the unbound library-sequences which migrate in spatial proximity to the desired specific aptameric sequences. As the amount of the specific sequences is trivial when compared to the bulk library sequences, contamination of the outlet of the capillary with non-binding sequences obviously reduces selection efficiency. Another source of contamination are the PCR-products from previous rounds of selection. Thus, rigorous separation of pre- and post-PCR areas as well as pre- and post-PCR materials is needed to avoid potential contaminations of evolved pools with previous-generation sequences.

Within the following sections, the main general procedures for the selection of DNA-aptamers against APC by CE-SELEX are described. Please consult the manual of the used CE-system / software for specific technical details.

2.4.1. Installation and conditioning of a new capillary

Install a new capillary for each individual selection. The following points describe the most critical steps during installation and use of a new capillary when running the Beckman Coulter *PA 800* System.

1. Remove seal retainer clips as well as the aperture plug and the O-ring from the cartridge. Firmly remove the used capillary by pulling it out from the cartridge inlet side. Insert the new capillary into the outlet side of the cartridge with the end utmost from the capillary detection window (near to the cartridge window).
2. Push the capillary carefully into the cartridge base until it appears at the inlet. Protect detection window of the capillary from breakage (see **Note 5**).
3. Once the end of the capillary appears in the inlet side of the cartridge, pull it from the inlet side until the detection window appears centered within the cartridge window.

4. Insert the capillary seal clips over the capillary at both inlet and outlet side. Use the Capillary Length Template to accordingly cut both ends of the capillary using the cleavage stone. In doing so, adjust the ends of the capillary to be one millimeter shorter than the electrodes within the final CE-Cartridge assembly. Then re-install the aperture plug and O-ring.
5. Check the capillary ends under magnification and re-cut/ re-adjust the capillary in case of angled or denticulated ends.
6. Condition the capillary before the first use. For silica-fused capillaries, use the conditioning program described below:

Reagent	Presseure	Voltage	Duration
NaOH, 0.1 M	20 psi	----	4 min
Air drying	20 psi	----	2 min
ddH ₂ O	20 psi	----	2 min
Separation buffer	20 psi	----	4 min
Separation buffer	----	15 kV with 2 min ramping time	6 min

2.4.2. CE-based isolation of target-binding ssDNA-molecules

2.4.2.1. Incubation of ssDNA-library and APC

1. Dilute the starting library in separation buffer to yield a concentration of 25 μ M in final volume of 20 μ l (see **Note 6**). Use a final concentration of 0.5 μ M of selected ssDNA pools during the subsequent cycles (see **Note 7**).
2. Heat the thus diluted library to 90°C for 5 min using one single PCR tube and let it to return to the room temperature to allow for proper folding the random ssDNA-molecules.
3. Centrifuge the PCR tube shortly.
4. Spike the APC target-protein into the ssDNA pool to reach the final concentration of 0.5 μ M for the first cycle and incubate the mixture for 30 min at RT (see **Note 8**) (see **Note 9**).

2.4.2.2. Injection into capillary and separation of components under EOF

1. Wash both ends of capillary and electrodes with distilled water and dry it using cotton swabs.
2. Place the single PCR tube containing target-ssDNA-mixture in injection site and prepare assembly needed for sample injection.

3. Add 100 µl of separation buffer each into tubes that will be defined and used as the inlet and outlet buffer vials during separation.
4. Adjust the separation temperature for the capillary to 20°C.
5. Perform separation using a program as described below (see **Note 10**):

Step	Reagent	Presseure	Voltage	Duration	Mode of action
1	Target protein-ssDNA mixture	4 psi- inlet	----	5s	Hydrodynamic Injection (see Note 11) (see Note 12)
2	Moving the inlet of capillary from injection vial to an inlet vial containing separation buffer				
3	Separation buffer	20 psi- both inlet and outlet	25 kV ¹	20 min ²	Separation with the positive electrode at the inlet
4	End				

¹ Performing constant voltage should supply constant current during separation (see **Note 13**).

² Duration of separation depends on the retention time of the unbound fraction of ssDNA. Separation must be stop before the unbound ssDNA start to migrate out of the capillary. Determine collection window before start of the actual process for CE-SELEX (see **Note 14**).

6. Remove the collected fraction vial with caution using a new pair of gloves and close cap immediately as any contamination with non-binders will reduce the efficiency of selection.

2.4.2.3. Washing process between the runs

As the separation procedure stops before the migration of unbound sequences out of the capillary, a precise washing step is required to remove the unbound sequences from the capillary while protecting the instrument as well as the surrounding area from contamination by unspecific sequences (see **Note 15**).

1. Use the 0.5 ml plastic vials and buffer trays for washing step (see **Note 16**).
2. Clean the blue vial caps with distilled water and with aid of syringe.
3. Try to fill the vials starting from the bottom to avoid air bubbles.
4. All vials must be capped before starting the electrophoresis.
5. Follow the program indicated below:

Reagent	Presseure	Voltage	Duration	Mode of action
HCl, 0.1M	20 psi	----	5 min	Reverse rinse wash
NaOH, 0.1M	20 psi	----	5 min	Reverse rinse wash
ddH ₂ O	20 psi	----	5 min	Reverse rinse wash
Washing buffer	20 psi	----	5 min	Reverse rinse wash

2.4.3. PCR-based amplification of selected ssDNA

1. Prepare a PCR master mixture containing 0.8 mM dNTPs, 1 mM each forward and reverse primer, 1.5 mM MgCl₂, 1.25 U/reaction HotStart*Taq* DNA polymerase and 20 µl of sample in a total volume of 100 µl.
2. Amplify collected ssDNA in a total of 5 reactions at 95°C for initial activation of HotStart*Taq* DNA polymerase followed by 30 cycles of 95°C for 30 s, 56°C for 30 s and 72°C for 30 s.
3. Pool all PCR mixtures and check the quality by running 10 µl of PCR product mixed with 2 µl of 5x loading buffer on a 2% agarose gel.

2.4.4. Asymmetric PCR and isolation of ssDNA

The production of ssDNA is a crucial step of the SELEX-process. This paragraph describes the application of 'Capture and Release' (CaR) for the isolation of ssDNA from asymmetric PCR mixture (see **Note 17**)⁴⁷. During the approach described here, additional asymmetric PCR is performed on previously amplified selected ssDNA (see subheading 2.4.3).

1. Dilute the yielded PCR products (see subheading 2.4.3) 1 in 10 using distilled water.
2. Add 10 µl of the dilution to 10 PCR vials containing 90 µl of asymmetric PCR master mixture (prepared as described in subheading 2.4.3 but without addition of reverse primers).
3. Perform reactions in a thermal cycler by applying 50 cycles of the temperature profile described in subheading 2.4.3. Check the quality of ssDNA obtained from asymmetric amplification by running a 10 µl sample on a 2% agarose gel.
4. Resuspend the streptavidin magnetic beads by shaking the vial vigorously and take 1 mg of the beads (100 µl of 10 mg/ml stock suspension).
5. Wash the beads three times using B&W 1 buffer and a suitable magnetic device. Incubate the beads in 200 µl B&W 1 containing 1 µM of capture molecules (2 µl of 100 µM stock solution) for 30 min at room temperature. Prevent settling of the beads by shaking at 1200 rpm during incubation.
6. Wash the beads three times using 1 ml of B&W 2.
7. Pool and add the total of 1 ml of the asymmetric reaction mixtures to the loaded SMBs followed by spiking with 5 M NaCl to reach a final concentration of 100 mM.
8. Incubate for 30 min at room temperature. Prevent settling of the beads by shaking at 1200 rpm during incubation.

9. Wash the beads three times using washing buffer.
10. Add 20 μl of pre-heated purified water to the beads and incubate for 2 min at 43°C to release captured ssDNA. Collect supernatant after separation of beads at 43°C.
11. Determine the concentration of obtained ssDNA by nanodrop UV-measurement.
12. Use isolated ssDNA for the next selection cycle.

For storage, resuspend the loaded SMBs in storage buffer and store at 4°C until used.

2.4.5. Filter retention experiment

1. Add 5 to 10 pmol of purified ssDNA to a master mixture containing 5 μl T4 PNK buffer (10x), 2 μl T4 polynucleotide kinase (T4 PNK, 10 U/ μl), 2 μl γ -³²P ATP (3.3 μM ; 10 $\mu\text{Ci}/\mu\text{l}$) in a final volume of 50 μl .
2. Incubate the mixture for 30 min at 37°C.
3. Prepare the G-25 columns by resuspending the resin by vortexing. Twist off the bottom closure and centrifuge at 735 x g for 1 min.
4. Pipett the labeling reaction to the top-center of the resin. Avoid disturbing the resin bed (see **Note 18**).
5. Purify the labeling reaction by centrifugation at 735 x g for 2 min. Discard used G25 column.
6. Check the removal of unbound radioactivity as well as the integrity of the labeled DNA by PAGE-analysis.
7. Dilute the ³²P-labeled DNA 1:10 with 1x D-PBS, heat it up to 90°C for 5 min followed by cooling down to room temperature (see **Note 19**). This temperature treatment is necessary for obtaining stable conformation of ssDNA at room temperature.
8. For each aptamer pool or single sequence to be tested, prepare a dilution series of the target protein (APC) in D-PBS containing 0.1% BSA and 10 μM yeast t-RNA. Pipette 24 μl of each dilution into a single well of a microtiter-plate. Always include a buffer-only sample. Run all analysis in at least duplicated. Add 1 μl of pre-diluted ³²P-labeled to each of the designated wells.
9. Cover the plate using parafilm and incubate it at 37°C for 30 min.
10. Soak the nitrocellulose membrane in freshly prepared 0.4 M NaOH followed by washing with 1x D-PBS (without BSA and tRNA).
11. Transfer the pre-treated nitrocellulose membrane into the Dot-Blot system, apply the vacume and wash each well three times using 150 μl of 1x D-PBS.
12. Use a 8-channel pipette to transfer 20 μl of the incubation mixtures to individual wells of the prepared blotting assembly.

13. Wash each well three times using 150 μl 1x D-PBS to remove non-target-bound sequences.
14. Remove membrane from the device and allow to air dry.
15. Pipett 0.8 μl of the used dilution of each applied ^{32}P -labeled DNA onto the same or another nitrocellulose membrane. These spots represent the total amount of radioactivity (i.e. labeled DNA) that was introduced to each well. Cover membranes by using a thin plastic foil, assemble with screen and close cassette (see **Note 20**).
16. Scan screen using the phosphorimager and quantify the single dots relative to the corresponding 100% spots. (Figure 2.1).
17. Use 4-parametric regression analysis for calculation of K_D -values. Sigmoidal curve patterns are needed to yield reliable results.

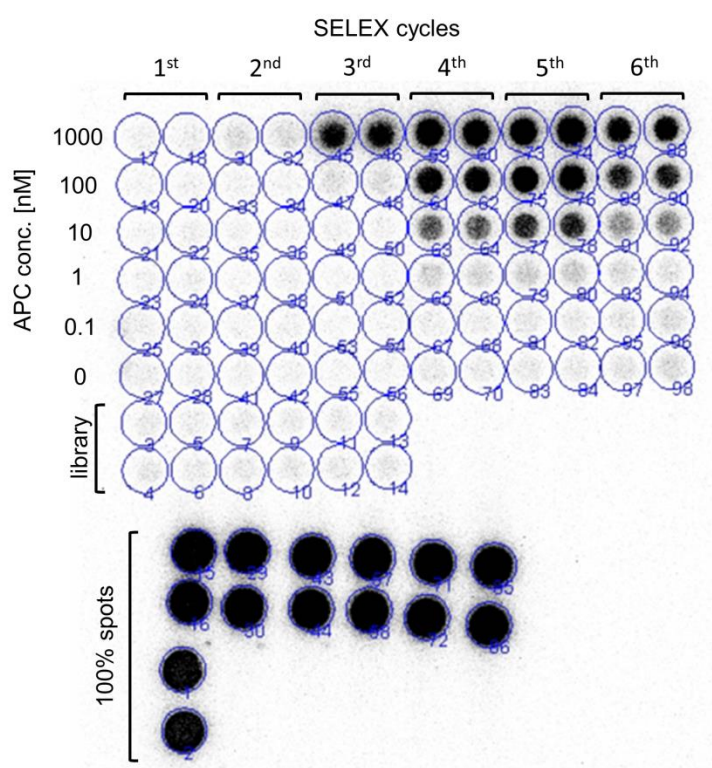


Figure 2.1. Example of Dot-Blot images for the assessment of pool binding affinities over performed selection cycles. For testing of the starting random library, the indicated APC-concentrations were applied in a transposed pattern (wells 3 to 14). The 100% spots were arranged in accordance with the according to the applied sample wells. The shown data revealed highest percentage of binding and affinity of the aptamer pool gathered after five cycles of selection.

2.5. Notes

1. All buffers should be prepared in ultrapure water using analytical grade reagents. Buffers should be filtered before use as present particles may interfere with proper electroosmotic flow or even plug the used capillary.

2. The composition of the buffer and the salt concentration can be varied according to the selection conditions. The current set by a certain voltage is a function of salt concentration in the separation buffer. However, exceeding more than the maximum tolerated current (300 mA) can harm the interface block of the instrument.
3. As changing of the composition of the used selection buffer can not only interfere with aptamer-binding but also produce fluctuations in the electropherogram, we strongly recommend to change the buffer of the used APC using Vivaspin®6 concentrators by three consecutive addition of the separation buffer in the same volume as introduced APC followed by centrifugation at 2000 g in 4°C. The resulting APC concentration might be determined using NanoDrop® ND-1000 UV/Vis-Spectrophotometer regarding to the APC extinction coefficient of $E_{1\text{ cm}, 280\text{ nm}}^{1\%} = 14.5$.
4. The major drawback of ethidium bromide is its mutagenic potential. When used, ethidium bromide solution should therefore be handled with caution.
5. Always use gloves while installing a new capillary as finger print reduces detection sensitivity in capillary window. Handle the capillary with caution as the detection window is fragile.
6. No peak in electropherogram might be a sign of an air bubble at the bottom of the sample vial or insufficient quantity of sample in sample microvial. In these cases, remove the air bubble or increase the sample volume up to 100 µl, respectively.
7. The concentration of random library has a significant impact on the initial number of unique sequences introduced to the target and the capillary. Due to the presence of multiple copies of binding sequences after the first selection cycles, a reduced concentration of ssDNA (e.g. 0.5 µM) during the consecutive selection cycles will not affect the efficiency of the selection.
8. Injection of a sample with a different salt concentration than that of the separation buffer produces fluctuation in baseline of the electropherogram. Therefore, ensure that the incubation mixture of the ssDNA and the target protein corresponds to the composition of the selection buffer.
9. Gradually reduce the protein concentration with each selection cycle. It has been previously shown that the efficiency of enrichment of best binders is directed by the stringency of the selection that is increased by reduction of the protein concentration⁷⁸. As the target concentration decreases, the presence of high affinity aptamers in the collected pool increases while the considerable point is the practical lower limit which means that once the target protein concentration drops below the k_d value of the aptamer with highest binding affinity, further

decreasing in the protein concentration has no significant or only a slight impact on further enrichment ⁷⁹.

10. Under a certain condition applied to the capillary and by using the same buffer system, each target protein, bound fraction of the library- target protein and unbound ssDNA migrate at a certain time. In case of APC as the target protein, determination of the collection window required separate injections of protein and library in order to assess individual retention times (Figure 2.2). In our opinion, collection of target-binding sequences should be already stopped when the bulk library sequences become detectable by UV-measurements.

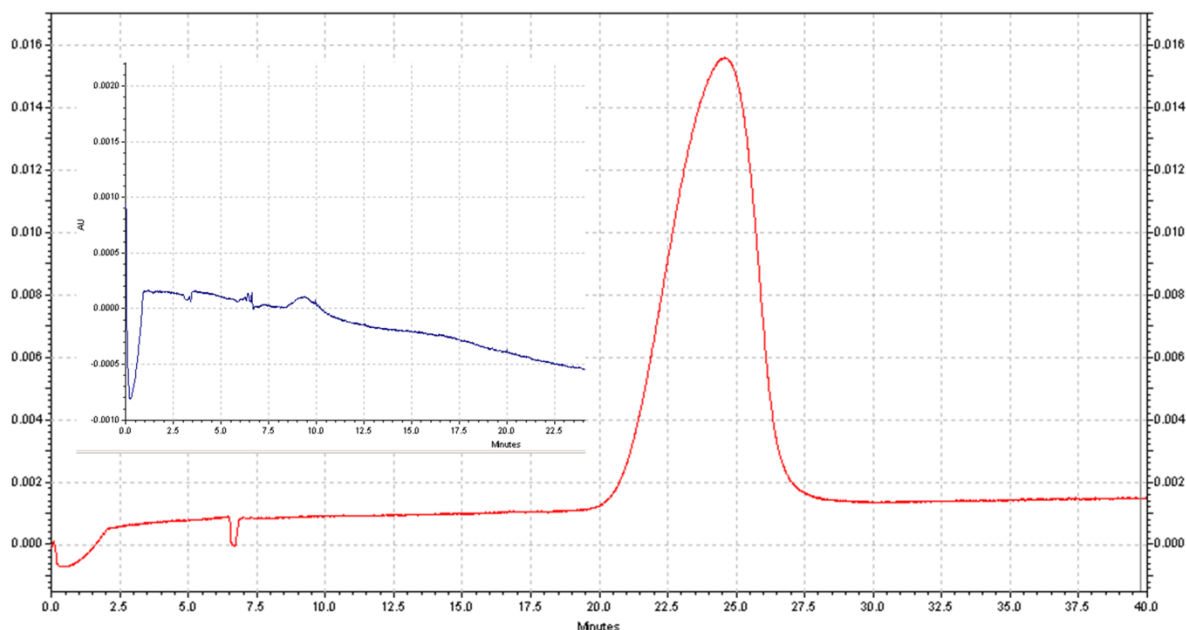


Figure 2.2. Determination of aptamer collection window. Electropherograms obtained from separate injections (4 psi, 5 seconds) of the IHT1 random library (25 μ M) with UV detection at 254 nm and activated protein C (2 μ M) with UV detection at 214 nm (inlet).

11. There are two different possibilities for samples injection: 1) Hydrodynamic injection 2) Electrokinetic injection. In hydrodynamic injection, an applied pressure for a certain time introduces the sample to the capillary column which is known as the most frequently used injection technique. In electrokinetic injection, an applied current or voltage for a certain time causes the sample to migrate into the capillary column. This kind of injection is mostly applied for high viscosity materials which is not common in CE-SELEX ⁴⁰.
12. The volume of the sample introduced to the capillary (V_{inj}) by hydrodynamic injection is a function of the capillary inner diameter, the viscosity of the buffer, the applied pressure and injection time. The loaded volume can be calculated using the Hagen-Poiseuille equation ³⁹:

$$V_{inj} = \frac{\Delta P d^4 \pi t_{inj}}{128 \eta L}$$

Where

ΔP = pressure difference across the capillary

d = capillary inside diameter

t_{inj} = injection time

η = buffer viscosity

L = total capillary length

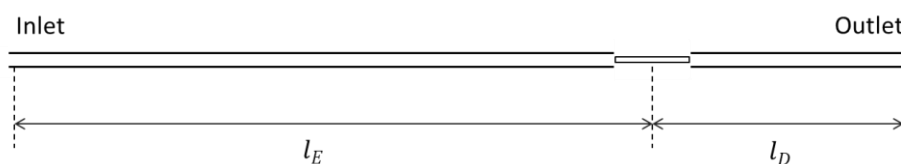
13. Low or unsteady current might be an indicator of a plugged capillary. One solution is to rinse the capillary with ddH₂O at 100 psi for 10 min. Change the capillary to a new one in case the problem persists⁸⁰.
14. As the retention time indicated in an electropherogram is the migration time of the define compound to the detection window but not to the end of the capillary, the exact time at which each compound reaches to the end of the capillary can be calculated using equation below:

$$x = t_m + \left(\frac{l_E}{l_D} t_m \right)$$

l_D : Capillary length to the detector or effective length

l_E : Capillary length from detection window to the end (which for beckman coulter PA 800 capillaries is constant to 10.2 cm)

t_m : Migration time of the defined compound to the detection window



15. Contamination of collected fractions with unspecific sequences should be considered in SELEX procedures using capillary electrophoresis. Due to the small amount of molecules injected into the capillary, contamination of the outlet with the bulk unbound sequences can negatively interfere with the next SELEX cycle. To avoid such a huge source of contamination, a strategy that prevents the bulk library sequences from reaching the outlet of the capillary is a necessity. Therefore, stopping the EOF during retention of the unbound sequences and flashing out these unbound sequences via the inlet of the capillary is a reasonable measure.

16. As the inlet of the capillary always comes into contact with unbound ssDNA at high concentrations during injection, it should always be assumed as a source of contamination. Thus, physical separation of vials/ rubbers used at the inlet or the outlet of the capillary is strongly recommended. Furthermore, the use of single-use plastic vials instead of glass vials will significantly reduce potential sources of contamination.
17. Capture and Release (CaR) is an efficient procedure for isolation of ssDNA required for each selection cycle. Briefly, short biotinylated oligodeoxynucleotides, that are complementary to the 3'-end of the target single stranded oligodeoxynucleotides produced during asymmetric PCR, are bound to streptavidin magnetic beads. Incubation of the loaded streptavidin magnetic beads with asymmetric PCR mixtures results in capturing of the ssDNA which can be easily released after washing by altering temperature and ion strength conditions⁴⁷.
18. Although the G-25 columns may be applied in conjunction with a fixed-angle rotor, we observed much better performance when using a swing-out rotor.
19. The dilution factor depends on the intensity of radioactivity. For example, after one half life of applied or available radioactivity (14.3 days), the dilution factor may be reduced to 1:5.
20. The incubation time depends on the intensity of the radioactivity that retained on the nitrocellulose membrane. For samples freshly labeled with only little decayed ³²P, incubation for a few hours might be sufficient while low levels of radioactivity may necessitate an overnight incubation.

Chapter 3

Capture and Release (CaR): A simplified procedure for one-tube isolation and concentration of single-stranded DNA during SELEX

Adapted from

N.S. Hamedani, F. Blumke, F. Tolle, F. Rohrbach, H. Ruhl, J. Oldenburg, G. Mayer, B. Potzsch, J. Muller, Capture and Release (CaR): a simplified procedure for one-tube isolation and concentration of single-stranded DNA during SELEX, *Chemical communications (Cambridge, England)* 51 (2015) 1135–1138.

3.1. Abstract

Short biotinylated oligodeoxynucleotides immobilized on streptavidin-coated magnetic beads allow for convenient and rapid purification of single-stranded oligodeoxynucleotides from crude asymmetric PCR mixtures, facilitating the selection of DNA aptamers.

3.2. Main manuscript

The preparation of single-stranded DNA (ssDNA) after PCR-based amplification is a crucial step during the selection of DNA-aptamers, a process also termed as systematic evolution of ligands by exponential enrichment (SELEX)^{57,81}. Currently applied strategies range from asymmetric PCR and enzymatic strand digestion to the most commonly used alkaline-based denaturation of biotinylated PCR-products after immobilization onto streptavidin-coated magnetic beads (SMB)^{44,45,82-84}.

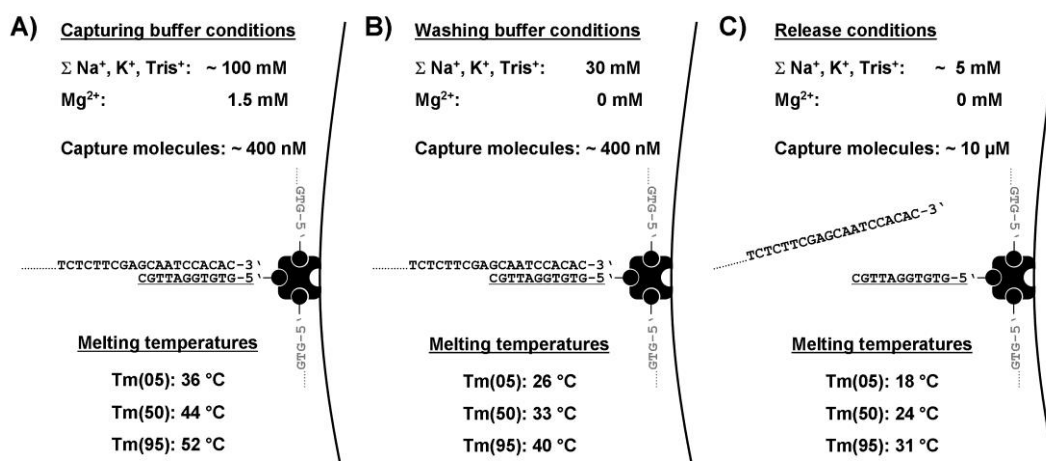
The possibility to directly purify PCR-products even from crude reaction-mixtures might be the main reason for the common utilization of the SMB-based method. Separation of strands is usually done by alkaline-treatment rather than heat-denaturation, because of the massive release of streptavidin into solution at elevated temperatures^{45,84}. However, in this case final neutralization or solvent exchange of the product is required to proceed with the selection cycle. Furthermore, due to the strong association between biotin and streptavidin, SMBs are usually used once, significantly increasing costs.

In principle, asymmetric PCR represents the method of choice for direct generation of ssDNA,⁸⁵ followed by gel-electrophoresis for the selective extraction and purification of ssDNA from dsDNA and reaction components⁴⁵. Not least due to the short length of random libraries used for SELEX (< 100 nts), however, loss of ssDNA during the purification processes is high. Moreover, gel components and conceivably applied nucleic-acid dyes are additional sources of potential contamination⁸⁶.

In order to combine the advantages of asymmetric PCR with SMB-based concentration and purification, we established a novel approach, named capture and release (CaR) that facilitates purification of ssDNA from crude PCR mixtures. During CaR, short biotinylated oligodeoxynucleotides (capture molecules), complementary to a defined site at the 3'-end of the target-ssDNA are employed. After their immobilization onto SMBs they are added to (pooled) crude asymmetric PCR mixtures. During this step the capture molecules bind to the target-ssDNA and subsequently the beads are washed and finally taken up in a small volume of ultrapure water. Due to the strongly decreased concentration of monovalent and magnesium ions, the melting temperature (T_m) of the immobilized capture-molecules bound to the targets decreases⁸⁷, allowing the release of pure ssDNA

at only moderately increased temperatures, whereby the integrity of the SMBs is preserved (Scheme 3.1).

The CaR method was successfully applied during capillary-electrophoresis (CE)-based SELEX (CE-SELEX)^{76,88}. We employed two distinct ssDNA-libraries (IHT1 and IHT2N) and selected aptamers for two different protein targets, namely activated protein C (APC) and the activated A-subunit of factor XIII (FXIIIa), two key enzymes of the coagulation cascade^{56,89}. For the design of corresponding capture molecules, an online tool for the prediction of DNA thermodynamics was used⁸⁷ (see ESI† for methodological details). As shown in Scheme 3.1 (IHT1) and Figure S 3.1 (IHT2N, ESI†), predicted melting temperatures between the library- and capture molecules mainly depend on the concentration of salt-ions but were also influenced by the concentration of capture molecules present during the different steps of CaR. Due to the inevitable presence of residual amounts of washing buffer associated with the SMB-pellet and the tube, a concentration of 5 mM of monovalent cations was assumed to be present during the final release step.



Scheme 3.1. Principle of CaR and predicted melting temperatures of the IHT1-capture molecules at different buffer conditions during the different steps. A, Capture; B, Wash; C, Release. Tm-values represent the melting temperature at which 5% [Tm(05)], 50% [Tm(50)], or 95% [Tm(95)] of captured ssDNA molecules are predicted to be released from the capture molecules.

We first assessed the basic functionality of CaR using asymmetrically amplified DNA-library IHT1 (ESI†). For capturing of ssDNA molecules, 5'-biotinylated IHT1 capture molecules were bound to SMB (200 pmole/ mg SMB; Figure S 3.2, ESI†). Subsequently, 500 μl of pooled crude asymmetric PCR mixtures were added to 1 mg of SMB that were loaded with capture-molecules (SMB+). After incubation for 30 min at RT, SMB+ were washed and finally resuspended in 20 μl of ultrapure water. The release of captured ssDNA was assessed at RT and three elevated temperatures (37°C, 43°C, and 50°C). After

two minutes of incubation, SMB+ were separated by magnetic force and supernatants collected. Three consecutive elution steps using new batches of water at each temperature were conducted (Figure S 3.3, ESI[†]).

Comparable yields of ssDNA in the low pmole range (low μM concentrations) were released at elevated temperatures with about 90% of the ssDNA being released during the first elution step as determined by UV-measurements (Figure 3.1A). Gel analysis and A260/A280 ratios revealed high purity of isolated single-strands (Figure S 3.3, ESI[†]).

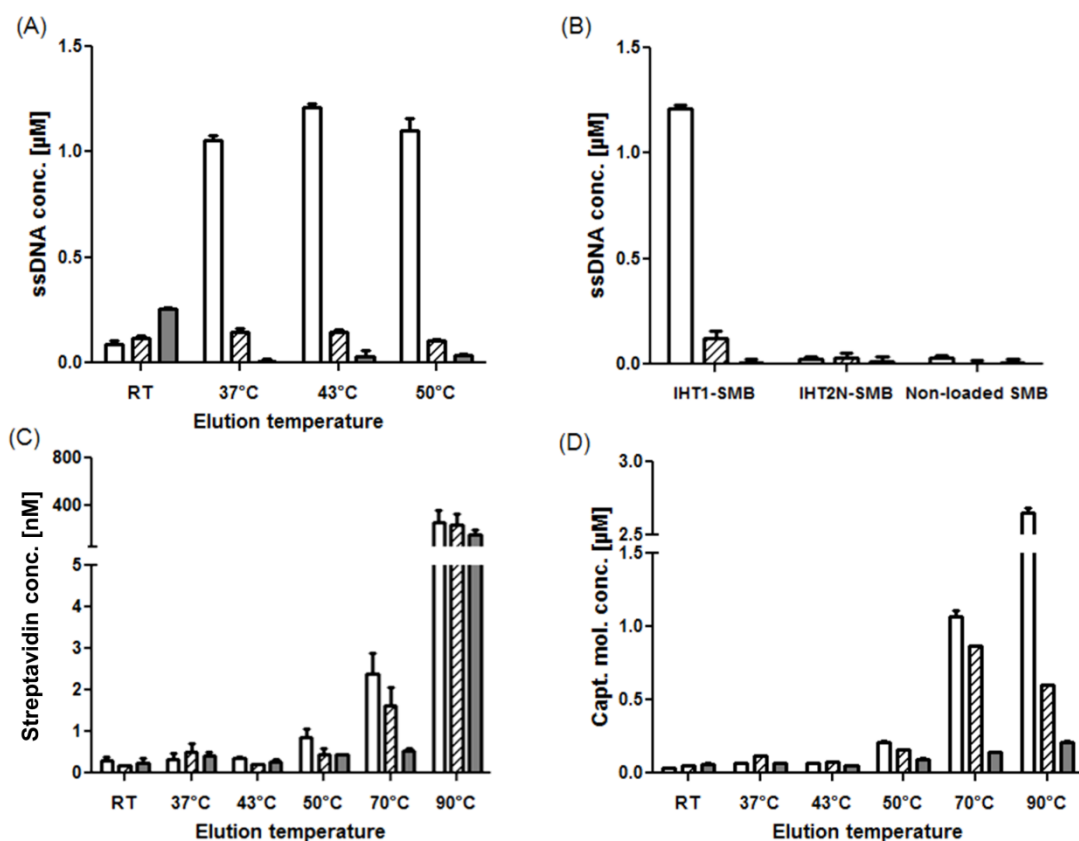


Figure 3.1. Key-characteristics of the CaR procedure. Open bars show results of the first elution, striped bars: 2nd, gray bars: 3rd. A, Yield of ssDNA at different elution temperatures. B, Prove of sequence-specificity. C, Degree of streptavidin-contamination at different elution temperatures. D, Leakage of capture molecules from SMB.

In order to prove the specificity of CaR, non-loaded SMB or SMB loaded with non-complementary IHT2N capture molecules were introduced to the described assay with captured ssDNA released at 43°C (ESI[†]). As shown in Figures. 3.1B and S 3.4 (ESI[†]), only the application of SMB+ enabled the isolation of IHT1-ssDNA from crude asymmetric reaction mixtures, demonstrating the sequence specificity of the assay.

To assess the potential rate of contamination of produced ssDNA with streptavidin, 1 mg of non-loaded SMB in 20 μl of ultrapure water were incubated for 2 min at RT, 37°C, 43°C, 50°C, 70°C or 90°C. After the separation of beads, supernatants were tested for the

presence of streptavidin-(subunits) (streptavidin) by ELISA (ESI⁺). Three consecutive experiments using the same SMBs were performed at each temperature. As shown in Figure 3.1C, even at RT, a detectable amount of streptavidin (~6 fmole [300 pM concentration]) leaked from the SMB during the first elution step. Up to a temperature of 43°C, leakage only marginally increased to a total of ~7 fmole (~350 pM) while a further apparently exponential increase in leakage was observed at temperatures of 50°C or higher.

These data demonstrate that the amount of streptavidin contamination depends on the elution temperature used, the amount of SMB used, and the total yield of ssDNA. For instance, when considering an elution temperature of 43°C and a yield of 20 pmol of ssDNA (1 μM concentration), the degree of contamination on a molar basis would be 0.04% (400 ppm) when using 1 mg of SMB.

It has been previously described that the interaction between biotin and streptavidin gets weakened in non-ionic aqueous solutions in a temperature-dependent manner⁴⁶. Thus, besides adverse release of streptavidin from the SMB, also the leakage of biotinylated capture molecules from streptavidin into solution had to be considered. To study this effect, SMB were loaded with 3'-fluorescence-labelled capture molecules (200 pmole/mg) and treated as described for the streptavidin release experiments. The concentration of capture molecules in the supernatants was determined by fluorescence measurements (ESI⁺). Indeed, it was found that significant amounts of capture molecules leaked into solution. Up to an elution temperature of 43°C, however, leaked amounts were limited to a maximum of ~ 2 pmole (100 nM concentration) during the three consecutive experiments, corresponding to a loss of ~ 1% of SMB-bound capture molecules per incubation (Figure 3.1D). Nevertheless, at a yield of 20 pmole of ssDNA (1 μM concentration), the degree of contamination would be up to 10% under these conditions.

In summary, these results demonstrate that ssDNA prepared by SMB-based CaR will be contaminated with streptavidin and biotinylated antisense molecules.

The contamination of ssDNA-preparations with SMB-derived streptavidin has also been described for the, in comparison to heat denaturation, more gentle alkaline (NaOH)-based denaturation of immobilized PCR-products^{83,84,90}. For example, Civit et al. achieved ssDNA-concentrations of ~ 40 nM while the contaminating concentration of streptavidin, as also measured by ELISA, was reported to be ~ 150 pM⁸⁴. This corresponds to ~ 3,750 ppm, an approximately 10-fold higher rate than observed in the present study. However, due to the use of different SMB and/ or different (mainly qualitative) methods for the detection of streptavidin in different studies, a more comprehensive comparison of contamination rates appears to be difficult. The same is true for the following adverse effect.

Since alkaline conditions also negatively affect the interaction between biotin and streptavidin, the NaOH-based denaturation of SMB-bound PCR-products also leads to the

contamination of ssDNA with released double-stranded PCR-products and/ or (re-annealing) complementary strands^{45,83}. While biotinylated capture molecules exclusively bind to their corresponding target-region at the 3'-end of the isolated aptamers. Thus, in comparison to NaOH-denaturation of full-length complementary strands, binding of released capture molecules will, if at all, lead to considerably lower interference with the tertiary structure of the selected aptamers.

In contrast to the previously described methods for ssDNA-generation, the characteristics of CaR determine that potential aptamers that find their 3'end involved in intra-molecular folding patterns may not be efficiently captured and therefore be sorted out during selection. Indeed, one might argue that, at least during the first cycle of CaR-based SELEX, aptamers are not solely selected for target binding but also with respect to proper annealing to the applied capture molecules. Due to the presence of high overall sequence diversity at coincidentally high frequency of identical or similar sequence patterns during the first selection cycles, however, this appears to be more of a fact than a problem.

Using the IHT1 and IHT2N ssDNA libraries, asymmetric PCR/ CaR was applied during CE-SELEX to obtain DNA-aptamers recognizing activated protein C (APC) and the activated A-subunit of factor XIII (FXIIIa) ^{56,89}. Since APC was used successfully during previous selections ⁶⁴, this enzyme was mainly considered as a model target for evaluation purposes. In contrast, the selection of aptamers against FXIIIa has not been described so far. In total, 6 selection cycles were performed during 3 independent selections (APC targeted by IHT1 and IHT2N, FXIIIa targeted by IHT1, ESI⁺). The yield and purity of ssDNA obtained during the different cycles of IHT1- and IHT2N-based selections was found to be comparable (Tables S 3.1- S 3.3, ESI⁺). After selection, the starting- and enriched libraries were radioactively labelled in order to (i) sensitively assess the purity of prepared ssDNA by PAGE and (ii) to determine the binding affinity by filter retention analysis (ESI⁺).

As shown in Figures. 3.2A and 3.2B, distinct bands as determined by denaturing PAGE confirmed the high quality of CaR-prepared ssDNA. More importantly, filter retention analysis revealed successful enrichment of DNA aptamers by CaR-SELEX binding to APC or FXIIIa. Highest apparent binding affinities of gathered pools were obtained after 4 to 6 cycles of selection (Figures. 3.2C and 3.2D).

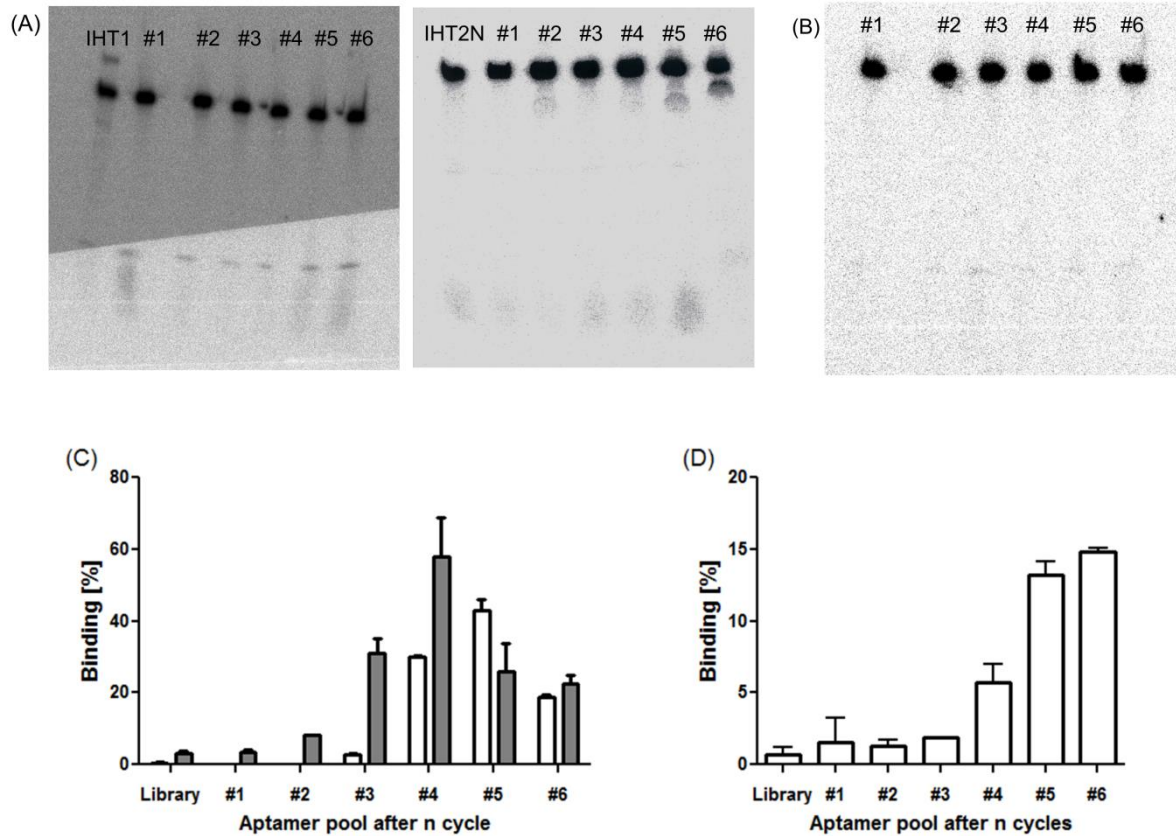


Figure 3.2. Quality of CaR-produced ssDNA (aptamers) and target binding patterns. A, B, PAGE analysis of radioactively labelled original IHT1 and IHT2N libraries and aptamer pools obtained after 1 to 6 selection cycles (A, APC-SELEX; B, FXIIIAa-SELEX). Different background levels on the screen on the left were caused by an artefact during exposure. C, D, Filter retention analysis. C, Percentage of binding of IHT1- (open bars) and IHT2N- (closed bars) derived aptamer pools to APC (100 nM). D, Binding of IHT1-derived aptamer pools to FXIIIAa (100 nM).

Cloning and sequencing of the selected aptamers led to the identification of individual sequence clones from which ssDNA was produced by CaR (Figure S 3.5, ESI[†]) and tested by filter retention analysis. As shown in Figure S 3.6 (ESI[†]), determined binding affinities of all individual sequences were within the high picomolar to low nanomolar range. As expected, in silico two-dimensional DNA folding analysis indicated that the 30-ends of found aptamers are accessible to the used capture molecules (Fig. S 3.7, ESI[†]).

Having shown the usefulness of CaR during aptamer selection and single clone ssDNA-production, we next focused on the reusability of the applied SMB⁺ for ssDNA-production. For this purpose, asymmetrically amplified ssDNA (clone #1 of the IHT1-based selection against APC, Figure S 3.5, ESI[†]) was pooled and aliquotes of 500 μ l each introduced to repetitive CaR using the same batch of SMB⁺ (ESI[†]). As shown in Figure S 3.8 and Table S 3.4 (ESI[†]), comparable yields of highly pure ssDNA were achieved during four consecutive experiments.

In conclusion, we introduced a novel fast and convenient method for the purification of ssDNA. In contrast to previously described applications, CaR allows isolation and concentration of ssDNA from crude reaction mixtures in a single tube without the need for any post-processing steps like pH-adjustment or sample purification. Thus, we believe that, not least due to its scalable nature, the combination of asymmetric PCR and CaR will also be implemented in other applications that require the generation of ssDNA in the future.

3.3. Electronic supplementary information (ESI[†])

3.3.1. Chemicals and reagents

Protease-free bovine serum albumin (BSA), biotin-labelled BSA, rabbit whole antiserum against streptavidin, and all general chemicals were purchased from Sigma-Aldrich (Taufkirchen, Germany). HRP-labelled goat anti-rabbit antibodies were purchased from Dako (Hamburg, Germany). Streptavidin-coated magnetic beads (Dynabeads M-280 Streptavidin) were purchased from Life Technologies (Karlsruhe, Germany). Recombinant human activated protein C (APC) was purchased from Eli Lilly (Giessen, Germany). Recombinant human activated FXIII A subunit (FXIIIAa) was purchased from Zedira (Darmstadt, Germany). The randomized ssDNA libraries IHT1 (5'- AAG CAG TGG TAA GTA GGT TGA - N₄₀ (25% each A/G/C/T) - TCT CTT CGA GCA ATC CAC AC -3') and IHT2N (5'- GAT TGT TAC TGT CAC GAG GAT- N₄₀ (40% G, 20% each A/C/T) - ATA GCA CAT TAG TTC AGA TAC -3') were synthesized and PAGE-purified by Microsynth (Balgach, Switzerland). IHT1 and IHT2N-amplification primers (targeting the shown fixed sequences of the libraries in full length) and the below described capture molecules were synthesized and HPLC-purified by Eurogentec (Seraing, Belgium). The used BM chemiluminescence substrate was purchased from Roche (Mannheim, Germany).

3.3.2. Prediction of DNA hybridization profiles and design of capture-molecules

The fraction of DNA duplexes (capture molecule - target ssDNA) over temperature ('melting curves') of a given sequence under given buffer conditions (concentration of capture-molecules, monovalent ions, and Mg²⁺ ions) was assessed using the 'DNA thermodynamics & hybridization' tool available on the 'biophysics' sub-domain of idtdna.com (<http://biophysics.idtdna.com>). This sub-domain runs stable and tested software to be included into the IDT SciTools collection⁸⁷. Details on applied formulas and calculations can be found at <http://biophysics.idtdna.com/HelpMelt.html>. The applied software returned the predicted fractions of duplex (0 to 1) over an integer temperature range of 0 to 100°C. No absolute accordance to real-world conditions was expected. However, obtained values were used as a basis for the design of the IHT1- and IHT2N-

capture-molecules and to assess the chosen concentration of monovalent cations within the used washing buffer. Based on the returned data (melting profiles), the following sequences were chosen for the capture-molecules:

IHT1-capture-molecule: 5'-Biotin-GTG TGG ATT GC-3'

IHT2N-capture-molecule: 5'-Biotin-GTA TCT GAA CTA AT-3'

Temperatures at which 5%, 50%, or 95% of duplexes (capture molecule - target ssDNA) were predicted to be denatured were assessed from the returned data sets. For the IHT1-capture-molecule, the corresponding values for each step of CaR are shown in Scheme 3.1 of the main manuscript. Figure S 3.1 shows the returned melting profiles at different buffer conditions and derived T_m -values for the IHT2N-capture-molecule.

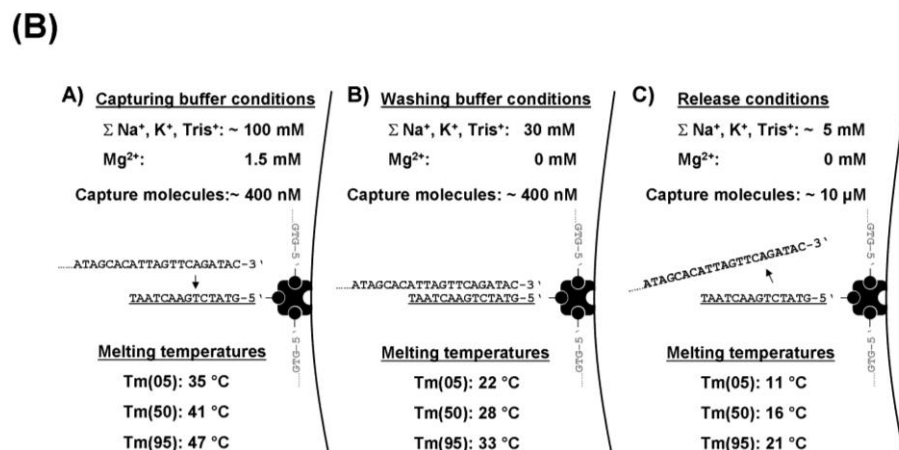
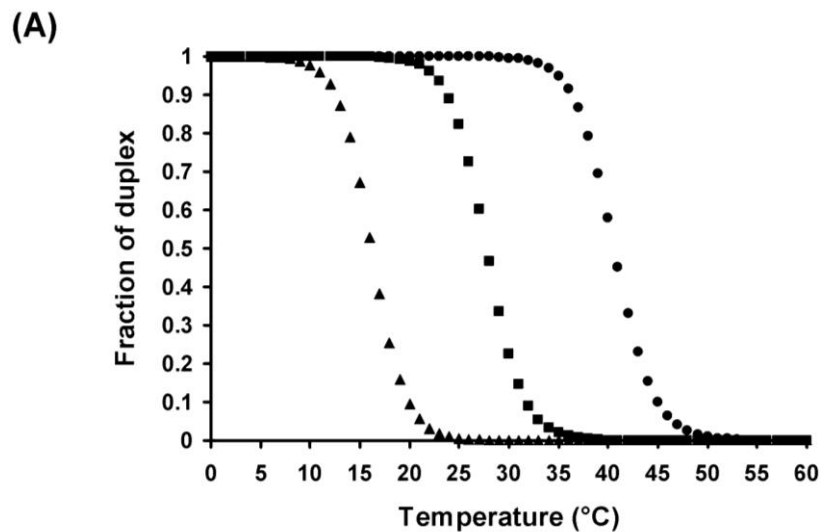


Figure S 3.1. (A) IHT2N-related melting curves (capture molecule - target ssDNA) as predicted by the 'DNA thermodynamics & hybridization' tool. Underlying buffer conditions: Capturing step: circles; Washing step: boxes; Release: triangles. (B) Details on buffer conditions and melting temperatures at which 5% [Tm(05)], 50% [Tm(50)], or 95% [Tm(95)] of captured ssDNA molecules are predicted to be released from the capture molecules.

3.3.3. Binding of capture-molecules to streptavidin-coated magnetic beads (SMB)

5'-biotinylated capture-molecules were bound to SMB as follows. Dynabeads M-280 Streptavidin (SMB) were washed 3x using B&W buffer (5 mM Tris-HCl, 1 M NaCl, 0.5 mM EDTA, pH 7.5) followed by incubation with B&W containing 1 μ M of capture molecules (200 μ l for each mg of SMB > 200 pmole of capture molecules / mg of SMB). The mixture was incubated at RT for 30 min under vigorous shaking to prevent beads from settling. After incubation, SMBs were washed 3x using B&W- (without EDTA). For storage, loaded SMB were suspended in 1 \times PBS, 1 mg/ml BSA, 0.2 mg/ml NaN₃, pH 7.4 and stored at 4°C until used. Before use, the needed amount of stored (loaded) SMB was washed 3x using B&W-.

3.3.4. Assessment of binding and adverse release of capture molecules to/ from SMB using fluorescence measurements

In order to assess the amount of capture-molecules bound to or release from the SMB, 3'-FAM-labelled IHT1-capture-molecules (5'-biotinylated) were applied. After adding to B&W at 1 μ M concentration, each 200 μ l of this solution were incubated with 1 mg of SMB (washed 3x using B&W) for 30 min under vigorous shaking. Subsequently, beads were removed by magnetic force and the amount of FAM-labelled molecules remaining in the supernatant was determined by fluorescence measurements using black 96-well microtiter plates and a Synergy 2 microplate reader (Biotek, Bad Friedrichshall, Germany) and a λ_{ex} 485 / λ_{em} 528 nm filter set.

To assess the temperature-dependent detachment of capture molecules from the SMBs, 3'-FAM-labelled IHT1-capture-molecules (5'-biotinylated) were bound to the SMB as described above. After incubation in ultrapure water (1 mg loaded SMB / 20 μ l) at different temperatures, the absolute amount of fluorescence in the supernatants was measured.

The FAM-labelled IHT1-capture-molecules could be detected down to sub-nanomolar concentrations in TE-buffer (20 mM Tris-HCl, 1 mM EDTA, pH 8.0). Thus, solutions to be tested were diluted in TE-buffer and the relative or absolute amounts of capture-molecules quantified by the standard-curve method.

Regarding determination of SMB-binding-capacity, merely 5% of the total fluorescence remained within the supernatant when using varying amounts of SMB around 1 mg, indicating efficient binding of capture-molecules when using 1 mg of SMB for immobilization of 200 pmole of (non-fluorescent) capture-molecules (Figure S 3.2). Results on the adverse release of capture-molecules from SMB are shown in Figure 3.1D.

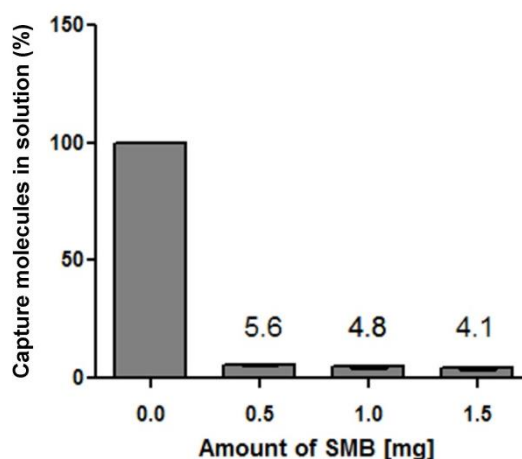


Figure S 3.2. Binding of 3'-fluorescently-labelled capture molecules to SMB introduced in different amounts. Values represent the relative amount of fluorescence that remained in solution after incubation.

3.3.5. Exponential amplification and asymmetric PCR

Initial exponential amplification of IHT1- or IHT2N-target-molecules was performed in a final volume of 100 μ l using the following reaction mixtures and cycling conditions: 1 x PCR buffer (containing Tris-HCl, pH 8.7, KCl, and $(\text{NH}_4)_2\text{SO}_4$), 1.5 mM MgCl_2 , 200 μ M each dNTP, 1 μ M each forward- and reverse-primer, 1.25 U HotStarTaq *Plus* DNA polymerase, and 20 μ l of the sample. Thermal cycling was done using the following profile: 95°C for 3 min followed by the indicated number of cycles of 95°C for 30 sec, 56°C (IHT1) or 58°C (IHT2N) for 30 sec, and 72°C for 30 sec.

For the production of target single-strands, asymmetric PCR was applied using the reaction mixtures and conditions as described for the exponential amplification but without reverse primers. Ten μ l of a 1 in 10 dilution of previously cycled exponential amplification mixtures were used as template. Before introduction to CaR, pooled reaction mixtures were spiked with a final concentration of 100 mM NaCl (using a 5 M stock solution).

3.3.6. Production of asymmetrically amplified IHT1-library for evaluation purposes

Asymmetrically amplified IHT1-library that was applied for evaluation purposes was prepared as follows. For initial exponential amplification, 10 µl of a 167 nM solution of the original IHT1-ssDNA-library (10^{12} molecules) were added to the mastermix and amplified for 15 cycles. Subsequently, 50 cycles of asymmetric PCR were performed after introduction of 10 µl of 1 in 10 diluted exponential amplification products.

3.3.7. Assessment of quality and purity of ssDNA after asymmetric PCR/ CaR during basic assay evaluation

It should be noted that no special efforts were done to optimize the yield of ssDNA as produced by asymmetric PCR during this study which solely focused on the general functionality of the CaR procedure. Thus, total yields of isolated ssDNA may increase in case of further optimization of the asymmetric PCR procedure.

Single bands of dsDNA or ssDNA were observed when performing gel analysis of asymmetrically amplified IHT1-molecules (Figure S 3.3A, lane 1 and Figure S 3.4, lane 1). In order to assess the release of captured ssDNA at different elution temperatures, 500 µl of crude pooled asymmetric IHT1-reaction mixtures were added to 1 mg of SMB loaded with 200 pmole of IHT1-capture molecules (SMB+). After incubation for 30 min at RT, the SMB+ were washed 3x at RT using 1000 µl of 10 mM Tris-HCl, 20 mM NaCl, pH 7.6 and finally taken up in 20 µl of ultrapure water pre-heated to designated temperature (RT, 37°C, 43°C, or 50°C). After 2 min of incubation in a water bath set to corresponding temperature, SMB+ were separated by magnetic force and supernatants collected. The final elution step was repeated 2x using new batches of water.

As shown in Figure 3.1A of the main manuscript, the majority of captured ssDNA was readily released from the IHT1-capture molecules at elevated temperatures during the first elution step. The quality of achieved ssDNA (see Figure 3.1A for total yields) was determined by gel analysis (Figure S 3.3A) while yield and purity was assessed by triplicate UV-measurements (A_{260}/A_{280} ratios) using a NanoDrop® ND-1000 UV/Vis-Spectrophotometer (Thermo Scientific) (Figure S 3.3B).

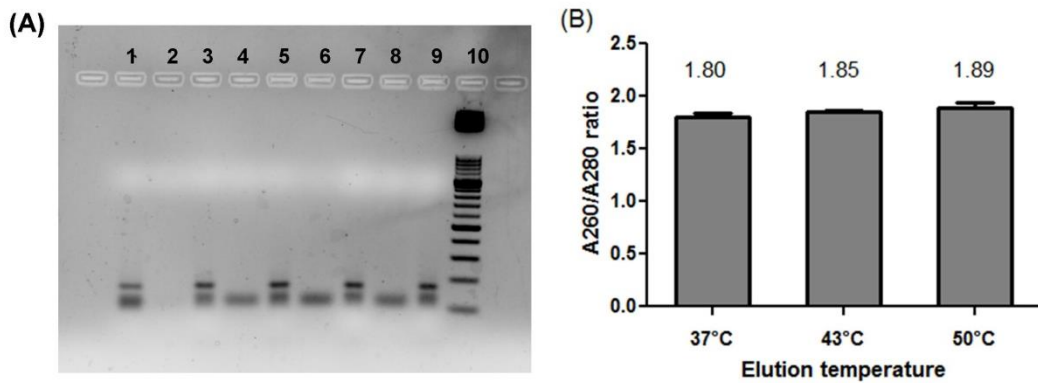


Figure S 3.3. (A) Agarose gel analysis (stained with ethidium bromide) of ssDNA yielded by CaR during the first elution at different temperatures. Lane 1: introduced crude asymmetric IHT1-PCR mixture. Lanes 2, 4, 6, and 8: 1 in 10 dilutions of ssDNA released from the IHT1-capture molecules at RT, 37°C, 43°C and 50°C, respectively. Lanes 3, 5, 7, and 9: corresponding supernatants (asymmetric PCR mixtures) after incubation with SMB+. Lane 10: 50 bp dsDNA ladder. (B) A260/A280 ratios of obtained ssDNA as determined by UV-measurements.

In order to provide further evidence for the proposed principle of CaR, underlying sequence-specificity was verified by the use of SMB loaded with IHT2N-capture molecules during CaR being performed with asymmetrically amplified IHT1-library. Besides SMB loaded with IHT1-capture molecules, also non-loaded beads that were passed through all incubation/ washing steps as described in '*Binding of capture-molecules to streptavidin-coated magnetic beads (SMB)*' (but in the absence of capture molecules), were run in parallel as controls. Again, 500 μ l of crude pooled asymmetric PCR mixtures and 1 mg of SMB were used during each reaction.

As shown in Figure S 3.4, only the use of IHT1-capture molecules yielded detectable amounts of IHT1-ssDNA as determined by gel analysis (see Figure 3.1B for obtained yield). The corresponding A260/A280 ratio was found to be 1.97 for the first elution.

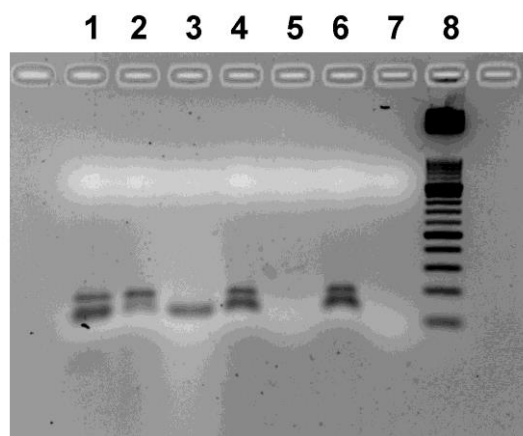


Figure S 3.4. Yield and quality of ssDNA isolated from IHT1 asymmetric amplification by CaR using non-loaded SMB or SMB loaded with specific (IHT1) or non-specific (IHT2N) capture molecules. Lane 1: introduced crude asymmetric IHT1-PCR mixture. Lanes 3, 5, and 7: 1 in 10 dilutions of ssDNA as obtained by the use of IHT1-capture molecules, IHT2N-capture molecules or non-loaded SMBs, respectively. Lanes 2, 4, and 6: corresponding supernatants (asymmetric PCR mixtures) after incubation with loaded or non-loaded SMB.

3.3.8. Quantification of streptavidin released from the SMB

Non-loaded SMB that were passed through all incubation / washing steps as described in '*Binding of capture-molecules to streptavidin-coated magnetic beads (SMB)*' (but in the absence of capture molecules), were applied to assess the potential adverse contamination with streptavidin at different incubation temperatures. Concentrations of streptavidin were measured by an immunoassay as follows. Primarily, Maxisorp microtiter modules were coated with 10 µg/ml BSA-Biotin (100 µl/well) in coating buffer (30 mM Na₂CO₃, 200 mM NaHCO₃ [pH 9.0]) overnight at 4°C followed by 3 times rinsing with 300 µl of washing buffer (1 x PBS [pH 7.4], 3 mM MgCl₂, 0.05 % Tween 20; general washing procedure using an automated plate washer [ELx50, Biotek, Bad Friedrichshall, Germany]). Remaining binding sites were blocked by incubation with blocking buffer (1xPBS [pH 7.4], 2 mg/ml BSA, 0.05 % Tween 20) for 2h at RT. After incubation for 2h at RT, remains were aspirated and sealed modules stored at 4°C until used. To run the assay, standards or samples were diluted in washing buffer containing 1 mg/ml BSA (WB+) and 100 µl of the dilutions were added to the wells and incubated for 1h at RT. After washing, 100 µl of rabbit whole antiserum against streptavidin (diluted 1:2000 in WB+) were added to the wells and also incubated for 1h at RT. Subsequently, wells were washed and 100 µl of HRP-labelled goat anti-rabbit antibodies (diluted 1:2000 in WB+, yielding a final concentration of 0.125 µg/ml) added and incubated for another hour at RT. Finally, after washing, bound HRP was detected using BM chemiluminescence substrate (100 µl well) and a Synergy 2 microplate reader (Biotek, Bad Friedrichshall, Germany). Applied streptavidin standard curves were prepared by half-logarithmic dilution series and showed a linear range from 530 down to 1.7 pM (31.6 down to 0.1 ng/ml). Original samples were diluted in WB+ to match the covered range and the absolute content of streptavidin calculated. The corresponding results are shown in Figure 3.1C.

3.3.9. CE-SELEX against APC and FXIIIa

CE-based separations were performed using a PA800 capillary electrophoresis system (Beckman Coulter, Krefeld, Germany) and 32 Karat software. A 60 cm long (50 cm to the detection window) uncoated fused silica capillary with an inner diameter of 50 µm (Beckman Coulter) was conditioned before the first use and rinsed between runs with an pressure of 50 psi (for 5 min each) with 100 mM HCl, 100 mM NaOH, distilled water, and

selection / separation buffer (25 mM Tris-HCl, 30 mM NaCl, 1 mM KCl, 1 mM CaCl₂ and 1 mM MgCl₂, pH 8.3). Applied ssDNA-libraries (IHT1 or IHT2N) were added to 20 µl of selection buffer in a final concentration of 25 µM (500 pmole) for the first selection cycle and heated to 85°C for 5 min followed by snap cooling on ice. Subsequently, the target protein (either APC or FXIIIa) was added and the mixture was incubated at RT for 30 min before hydrodynamic injection into the capillary (using 4 psi pressure for 5 second, thereby introducing ~ 40 nL of the sample into the capillary). Separation of protein from non-binding ssDNA-molecules took place under electroosmotic flow at a voltage of 25 kV. As determined during previous experiments, the collection window was set during the first 20 min of separation. Samples were collected into tubes containing 150 µl of separation buffer. Library molecules that remained in the capillary were flushed out by reverse rinsing. A total of 120 µl of the collected molecules (6 x 20µl) were exponentially amplified for 30 (IHT1) or 35 (IHT2N) cycles. Subsequently performed asymmetric PCR was routinely conducted for 50 cycles. In case of formation of unwanted by-products (as determined by gel-analysis), however, cycle numbers of asymmetric PCR were reduced to 30 - 45 in order to retain amplification specificity. Subsequently, single reactions were pooled and a total of 500 µl introduced to CaR for isolation of ssDNA. At this, captured ssDNA was eluted at 43°C. A constant amount of enriched library (0.5 µM; 20 pmole) was used during the following selection cycles. In contrast, the concentration of the target enzymes was gradually reduced from 1 µM during the first selection cycle to low nM-concentrations during the sixth (last) cycle.

3.3.10. Yield and purity of ssDNA as produced by asymmetric PCR/ CaR during SELEX

The following Tables S 3.1 - S 3.3 show the yield and purity of ssDNA obtained from asymmetric PCR/ CaR during the process of SELEX as determined by UV-measurements.

Table S 3.1. Yield and purity of ssDNA after each cycle of IHT1-based APC-SELEX.

	1st cycle	2nd cycle	3rd cycle	4th cycle	5th cycle	6th cycle
A260	1.48	1.05	1.022	0.645	1.121	0.811
A280	0.781	0.576	0.542	0.335	0.606	0.426
A260/A280	1.9	1.83	1.89	1.92	1.85	1.90
Conc. [µM]	1.95	1.39	1.34	0.85	1.48	1.07

Table S 3.2. Yield and purity of ssDNA after each cycle of IHT2N-based APC-SELEX.

	1st cycle	2nd cycle	3rd cycle	4th cycle	5th cycle	6th cycle
A260	0.715	1.46	1.06	1.134	1.038	1.185
A280	0.408	0.74	0.535	0.577	0.522	0.631
A260/A280	1.75	1.96	1.98	1.96	1.99	1.88
Conc. [μM]	0.93	1.90	1.38	1.48	1.35	1.54

Table S 3.3. Yield and purity of ssDNA after each cycle of IHT1-based FXIIIAa-SELEX.

	1st cycle	2nd cycle	3rd cycle	4th cycle	5th cycle	6th cycle
A260	0.469	1.048	1.353	1.235	1.130	1.719
A280	0.245	0.530	0.715	0.668	0.601	0.885
A260/A280	1.91	1.98	1.89	1.85	1.88	1.94
Conc. [μM]	0.62	1.38	1.78	1.63	1.49	2.26

3.3.11. Filter retention assay

The affinity of the single-stranded random pools, enriched libraries, and obtained single aptamer molecules was assessed by filter retention assay. Molecules (10 pmole) were radioactively 5'-phosphorylated using 20 U of T4 Polynucleotide Kinase (New England Biolabs, USA) in 70 mM Tris-HCl buffer [pH 7.6] containing 10 mM MgCl₂, 5 mM dithiothreitol, and 300 μ M [γ -³²P]ATP (PerkinElmer, USA) and then purified using G-25 microspin columns (GE Healthcare, Munich, Germany). The integrity of the enriched libraries was qualitatively determined using 12% denaturing polyacrylamide gel electrophoresis.

To determine the dissociation constants, serially diluted APC or FXIIIAa (0-1 μ M) were incubated with 0.5 nM ³²P-labeled ssDNA for 30 min at 37°C in PBS [pH 7.4] containing 1 mg/ml BSA, 10 μ M tRNA, 1 mM CaCl₂ and 50 μ M MgCl₂. After incubation, the reactions were passed through pre-equilibrated 0.45 μ m nitrocellulose membranes followed by three washings using 150 μ l of PBS [pH 7.4] containing 1 mM CaCl₂ and 50 μ M MgCl₂ and then dried out. The retained radioactivity was quantified using a FUJIFILM FLA-3000 PhosphorImager equipped with AIDA Imagequant software (Fujifilm, Düsseldorf, Germany). Data were fitted by 4-parameter logistic curve fit presuming a 1:1 binding

stoichiometry of ssDNA:target protein. K_d values were determined from at least two independent experiments.

3.3.12. Cloning and sequencing

The aptamer pool from the SELEX cycle that showed the highest apparent binding affinity was cloned into pGEM[®]-T vectors (Promega, Mannheim, Germany). For the IHT1- and IHT2N-based selections against APC, 19 and 32 colonies were sequenced, respectively. For the IHT1-FXIIIAa-selection, 32 colonies were sequenced. Sequencing was done using M13 primers and an ABI 3130xl Genetic Analyzer (Applied Biosystems, Darmstadt, Germany).

3.3.13. Production of identified individual aptamers by asymmetric PCR/ CaR and determination of binding affinity

Identified single aptamers were produced from PCR-products using asymmetric/ CaR. Aptamers were radioactively labeled and tested for binding affinity as described above. The capture-efficiency and quality of the yielded ssDNA is demonstrated in Figure S 3.5. The results of the filter retention analysis are shown in Figure S 3.6.

As can be seen in Figure S 3.5, probably due their individual tertiary structures, single monoclonal ssDNA aptamers did not clearly separate from the corresponding double-stranded PCR products during electrophoresis. This was especially true for the FXIIIAa-aptamers and the aptamers #2 and #3 of the IHT2N-based selection against APC. In cases where distinct bands of ssDNA could be assessed, virtually complete capturing of ssDNA from the asymmetric PCR mixtures could be observed.

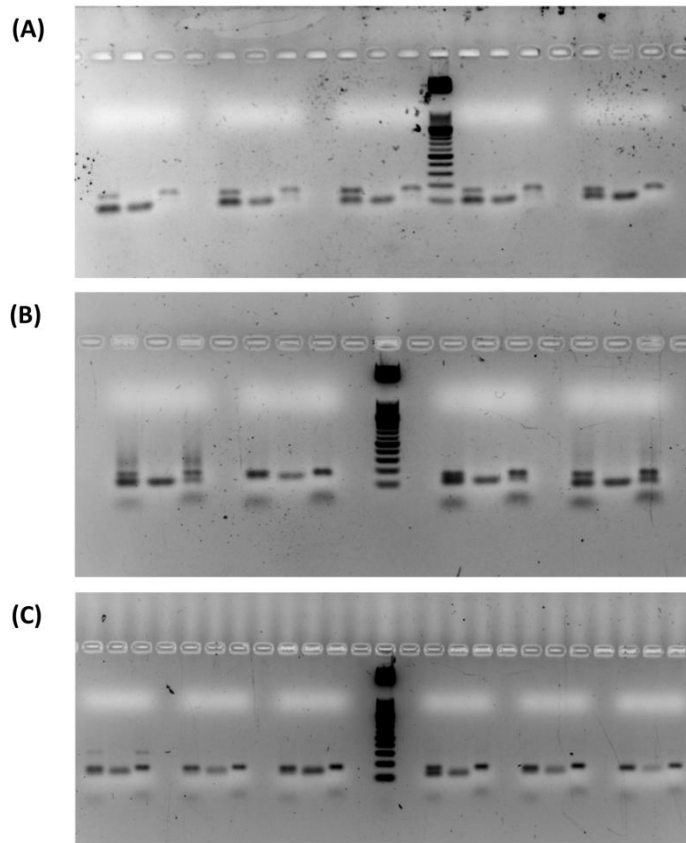


Figure S 3.5. Agarose gel analysis (stained with ethidium bromide) of asymmetric PCR mixtures, obtained ssDNA (1:10 diluted) and supernatants after removal of loaded SMB (from left to right within each group) after introduction of identified single aptamer-clones to asymmetric PCR/ CaR. A, B: selection against APC using the IHT1 (A) and IHT2N library (B) respectively. C, selection against FXIIIAa using the IHT1 ssDNA library. A 50bp dsDNA-ladder was used in each gel.

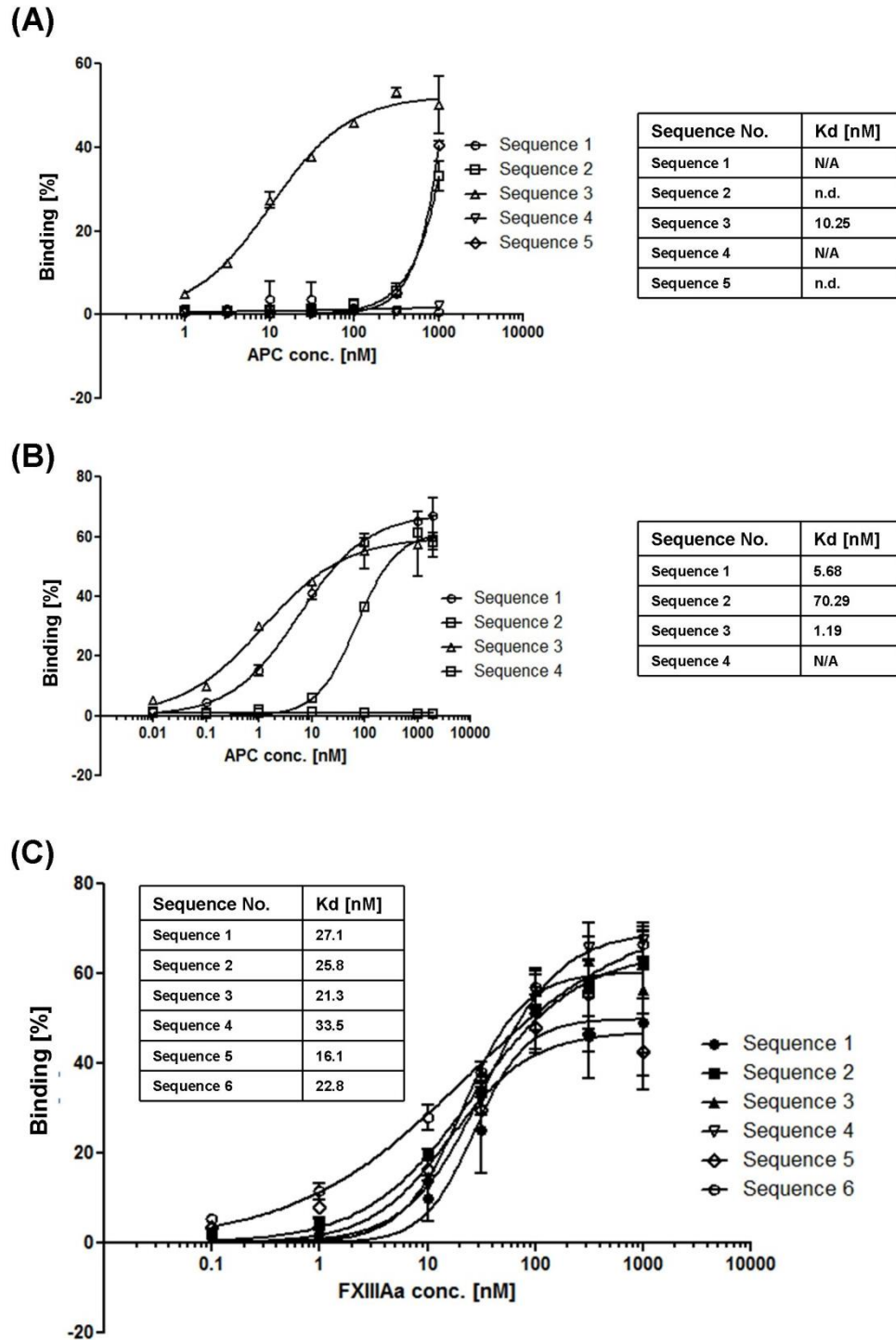


Figure S 3.6. Filter retention analysis of individual aptamers. (A) IHT1-based APC-SELEX. (B) IHT2N-based APC-SELEX. (C) IHT2N-based FXIIIaA-SELEX. Shown K_D -values were determined by 4-parameter logistic curve fit; n.d., not determined; N/A, no binding observed up to 1 μ M.

3.3.14. In silico folding predictions

The mfold web server as available at: <http://mfold.rna.albany.edu/?q=mfold/dna-folding-form> was used at default settings to predict the folding patterns of the identified single aptamers⁹¹. Predicted foldings of the 4 efficiently binding APC-aptamers are shown in Fig. S7. As expected, the 3'-ends of the single sequences appear to be accessible to the corresponding capture molecules. The same was found for the FXIIIAa-binding aptamers (data not shown). However, since these predictions are limited to Watson-Crick base pairing in two-dimensional space, their validity is limited.

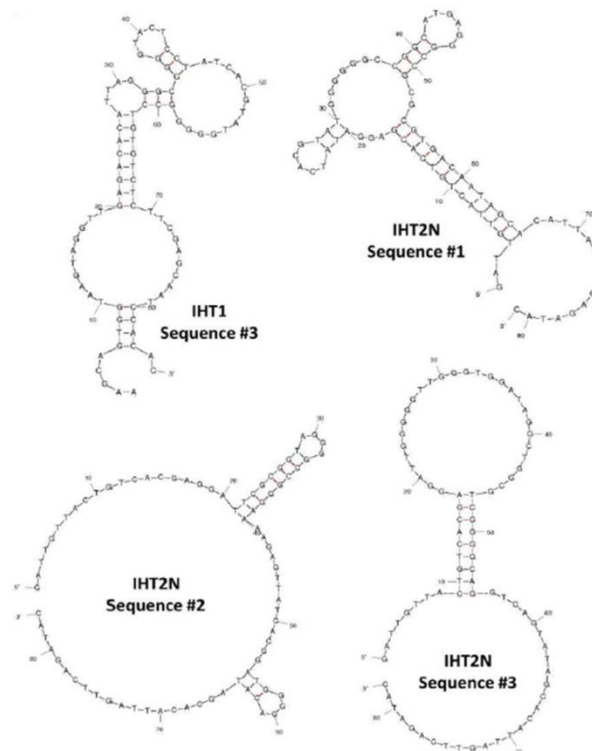


Figure S 3.7. Folding patterns of the identified APC-binding aptamers as determined by mfold.

3.3.15. Determination of the reusability of loaded SMB

Clone #1 identified during IHT1-based selection against APC was used to assess the reusability of SMB loaded with (IHT1) capture molecules (SMB+). After release of captured ssDNA by 3 consecutive incubations with a fresh batches of water, SMB+ were washed and again introduced to the CaR-procedure. In total, 4 cycles of capture and release were performed. As shown in Figure S 3.7, virtually complete capturing of ssDNA from the asymmetric PCR mixtures could be observed. As shown in Table S 3.4, comparable yields and purities were found.

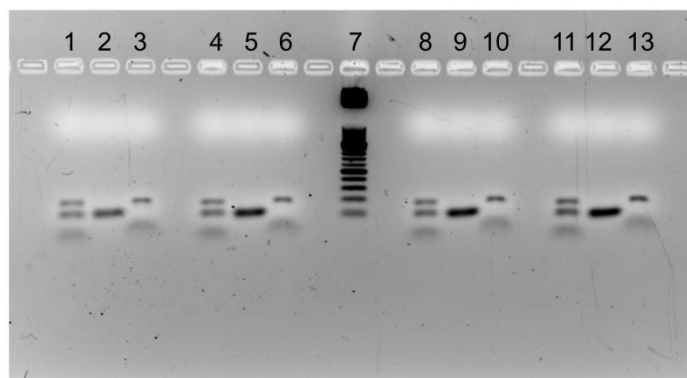


Figure S 3.8. Agarose gel analysis (stained with ethidium bromide) of obtained ssDNA by consecutive usage of SMB+ during CaR. Lanes 1, 4, 8, and 11: introduced crude asymmetric PCR mixture; lanes 2, 5, 9, 12: 1 in 10 dilution of yielded ssDNA when using SMB+ for the first, second, third and fourth time, respectively; lanes 3, 6, 10 and 13: supernatants after incubation of asymmetric PCR mixture with the SMB+ for the first, second, third and fourth time, respectively; lane 7: 50 bp dsDNA ladder.

Table S 3.4. Yield and purity of ssDNA obtained after consecutive use of SMB+.

	1st use	2nd use	3rd use	4th use
A260	0.432	0.513	0.524	0.508
A280	0.214	0.246	0.272	0.261
A260/A280	2.02	2.08	1.93	1.95
Conc. [μM]	0.58	0.68	0.69	0.67

Chapter 4

Modifying substrate specificity of the serine protease activated protein C using exosite-modulating aptamers

Nasim Shahidi Hamedani¹, Fabian Tolle², Heiko Ruehl¹, Behnaz Pezeshkpoor¹, Kerstin Liphardt¹, Johannes Oldenburg¹, Günter Mayer², Jens Müller^{1*}, Bernd Pötzsch^{1*}

4.1. Abstract

Protease exosites act as key regulator elements of protease function. Here we investigated, if the functions of activated protein C (APC) can be modulated by exosite binding aptamers. APC is a multifunctional serine protease that controls blood coagulation and exhibits anti-inflammatory and cytoprotective functions. We showed that APC-aptamers binding to the basic exosite selectively inhibit the anticoagulant functions of APC and can be used to enhance or inhibit the inactivation of APC by endogenous inhibitors resulting in a drastically reduced or enhanced catalytic life of APC. While enhancing the catalytic life of APC offers an interesting approach in the treatment of septicemia and in the prevention of tissue damage after arterial infarction, selective inhibition of the anticoagulant functions of APC is of particular interest in the prevention of APC-induced bleeding such as in trauma-induced coagulopathy and as supportive treatment approach in hemophilic patients.

4.2. Main manuscript

Activated protein C (APC) is a multifunctional serine protease that controls blood coagulation by down-regulation of thrombin formation ⁸. APC is generated from its inactive precursor protein C (PC) on the surface of endothelial cells in a thrombin-dependent manner. This process is augmented, if PC is bound to the endothelial cell protein C receptor (EPCR). APC that is released into the flowing blood acts as an anticoagulant by proteolytic cleavage of the activated cofactors V (Va) and VIII (VIIIa), while APC that remains bound to EPCR expresses cytoprotective functions involving cleavage of protease receptors-1 and -3 (PAR-1/PAR-3) ⁹²⁻⁹⁴.

Dysfunctions of the APC-pathway either inherited or acquired are involved in the pathogenesis of various thrombo-inflammatory diseases. Patients with mild to moderate inherited PC-deficiency are at an increased risk for venous thromboembolism, while severe PC-deficiency is associated with a high risk to develop purpura fulminans, a severe thrombo-inflammatory disorder, affecting the microvasculature of the skin and vital organs ⁹⁵⁻⁹⁷. Acquired APC dysfunction is observed in patients with septicemia where it is involved in the development of microvascular thrombosis leading to severe organ dysfunction and organ failure ^{98,99}. Overwhelming APC formation has been described in trauma patients and seems to be a critical factor in the development of trauma-induced coagulopathy ^{100,101}.

Its involvement in the pathogenesis of various thrombo-inflammatory disorders makes APC and the PC-pathway attractive candidates for therapeutic interventions. A plasma purified PC concentrate is successfully used in the treatment of severe PC-deficiency and of meningococcal septicemia ^{102,103}. A recombinant version of APC, drotrecogin alfa, has

been shown to decrease 28-day mortality in severe sepsis but was withdrawn from the market because the positive outcomes could not be confirmed in follow-up studies^{24,25}. A major complication of APC treatment was the development of bleeding. Since the therapeutic efficacy of APC in the treatment of severe sepsis is mainly based on its cytoprotective properties, mutants were generated showing diminished anticoagulant activities but preserved cytoprotective functions^{104,105}. The catalytic-life of APC in whole blood is approximately 20 min and regulated by two natural inhibitor proteins, namely alpha1-antitrypsin and protein C inhibitor (PCI)^{106,107}. Substitution at Leu¹⁹⁴ generates an APC mutant showing a 4-6-fold prolonged half-life¹⁰⁸. Although these variants suggest therapeutic opportunities, their production is cost intensive and they compete with wild-type endogenous APC for receptor signaling, leading to the need of high dosages.

Modulation of the APC activity by small molecules or other compounds could be an attractive alternative to genetically engineered APC variants. Besides the active center, the basic and acidic exosites of APC are interesting target regions for such an approach. In this study we used the aptamer technology to study if the APC activity can be selectively inhibited and/or the catalytic life of APC modulated. To increase the probability to select distinct APC binding sequences we used several selection strategies. In addition to previously applied conventional SELEX procedures, capillary electrophoresis (CE)-based SELEX (CE-SELEX) was used and different randomized ssDNA-libraries were applied, including a G-enriched library to increase the likelihood of selecting G-quadruplex containing aptamers. Using these approaches, a variety of aptamers has been selected showing binding affinities to APC ranging from 0.2 to 20 nM (Table S 4.1) and no significant binding to the structurally related serine proteases thrombin and activated factor VII as well as to the APC precursor PC (Table S 4.2). Remarkably, a previously described consensus sequence (5'-TATCMCGNATGGGS-3'), that was identified during two independent runs of conventional SELEX, also dominated CE-SELEX (Figure 4.1A). As assessed by next generation sequencing (NGS) (Figure S 4.1), each CE-based selection was dominated by one individual aptamer that contained this consensus sequence. The maximum enrichment comprised more than 80% of sequences independent of the type of library used (Figure S 4.1). Such an enrichment during CE-SELEX appears to be unparalleled and indicates that the degree of heterogeneity achieved during aptamer selection is mainly influenced by the target molecule whereas the applied selection strategy is of minor influence. However, a structurally different APC aptamer (NB3) could be selected from the G-enriched library. Thioflavin T staining of original and selected truncated aptamer variants (Figure S 4.2) confirmed the presence of a G-quadruplex structure within the NB3-aptamer (Figure 4.1B / Figure S 4.3). Furthermore, as assessed by in silico analysis, this putative G4 motif seems not to be involved in intramolecular Watson-Crick base pairing (Figure 4.1A), indicating that aptamer NB3 might indeed be dominated by a G4 structure. This assumption is further supported by the relatively high free energy value (ΔG) of the mfold-based NB3 secondary structure that indicates a

relatively low stability and therefore suggests the presence of an alternate, more stable pattern within the predicted loop-section of the NB3 aptamer.

To localize the binding region of the newly selected aptamers, crossblocking experiments using previously characterized APC binders have been performed. The NB-aptamers compete with the APC-aptamer HS02-52G and unfractionated heparin for binding to the basic exosite as assessed by crossblocking experiments (Figure 4.1C, Figure S 4.4).

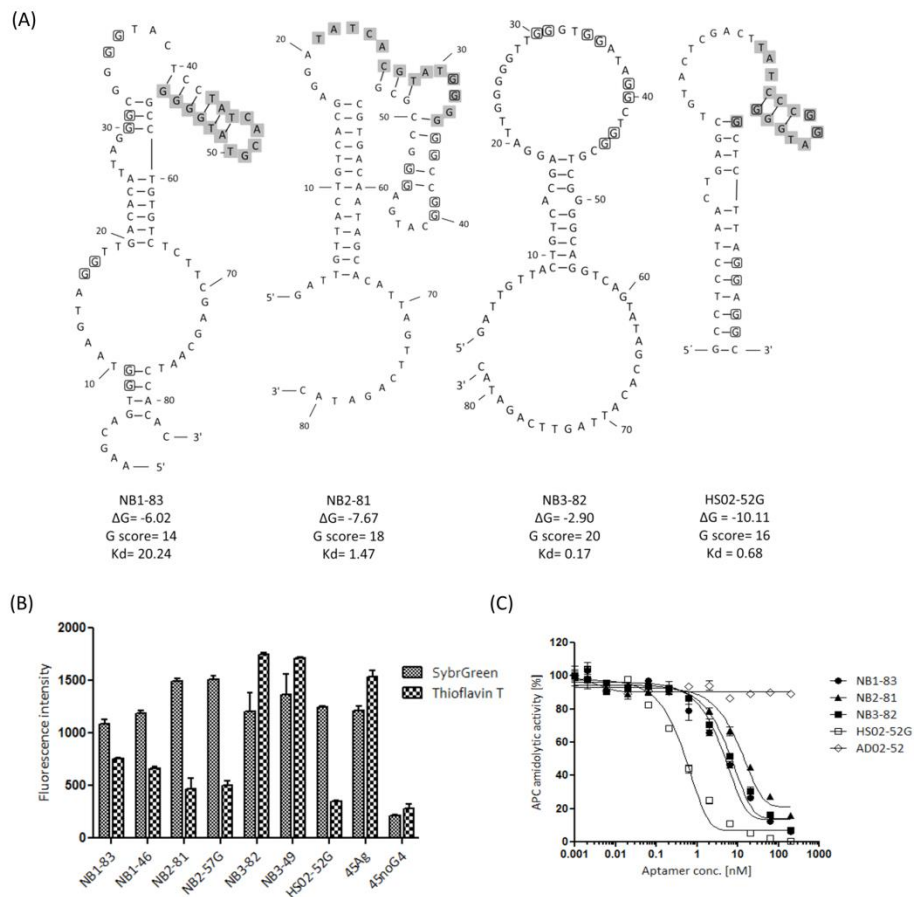


Figure 4.1. Structure and binding characteristics of APC aptamers. (A) In-silico-prediction of secondary structures and key characteristics extracted from m-fold web server on 09/17/2015. The consensus sequence is shown in highlighted format, G-quadruplex forming nucleotides have been defined by a surrounding quadrangle. Dissociation constants (Kd) measured by filter retention assay are shown in nM. (B) G-quadruplex detection assay. SYBRGreen or ThT (1 μ M) were incubated with aptamers at a final concentration of 1 μ M in microtiter plates followed by fluorescence measurement in $\lambda_{ex}/\lambda_{em}$ of 425/500 nm and 497/520 nm for ThT and SYBRGreen, respectively. A G4 forming sequence, 45Ag, was used as positive control while the sequence 45noG4 lacking the ability to form G4 structures was used as negative control. Error bars correspond to standard deviation of three measurements. (C) Unlabeled crossblocking experiments. NB-aptamers at the indicated concentrations were incubated with rAPC (final concentration: 180 μ M). Subsequently the reaction mixture was transferred to wells of a microtiter module coated with HS02-52G aptamers. The amount of APC bound to HS02-52G was

measured through hydrolysis rates of an APC-specific fluorogenic peptide substrate. Results are shown as means of duplicates.

Protein-binding aptamers have been reported to affect molecular interactions distantly from their binding site ¹⁰⁹. Hence, we studied if the APC aptamers interfere with the catalytic center of APC by studying the hydrolysis rates of two distinct peptide substrates. All APC-aptamers led to a partial decrease in conversion rates of the sensitive fluorogenic substrate Pyr-Pro-Arg-AMC, albeit on different levels (Figure 4.2A). With a maximum reduction of 25% NB2- and NB3-aptamers showed a weaker inhibitory effect than NB1 and HS02-52G. Similar results were obtained, when the fluorogenic substrate was replaced by a chromogenic substrate (p-Glu-Pro-Arg-MNA) or if truncated variants of the aptamers were tested (Figure S 4.5). These results strongly suggest that the inhibitory effect of the aptamers on substrate conversion is based on allosteric rather than steric effects and that this effect depends on the individual sequence of the aptamers.

As expected from the proposed binding site, all APC aptamers showed a dose-dependent inhibition of APC-induced FVa cleavage as tested using a prothrombinase assay (Figure 4.2B). Full inhibition was achieved with NB1, NB2, and HS02-52G, whereas full-length NB3 only partially inhibited the APC induced proteolysis of FVa. The lower effect of NB3 is also reflected by the corresponding IC50 values (Table S 4.3). In this experimental approach, the impact of aptamers on the activity of exogenously added APC in a purified system was tested. However, these results not necessarily reflect the in-vivo situation where APC is continuously generated through the thrombin-TM complex and where aptamers might interact with a variety of plasma components and blood cells. To study the influence of the APC aptamers on endogenously generated APC within the plasma matrix, we initiated thrombin formation in plasma in the presence of recombinant thrombomodulin. The results confirmed that all APC aptamers inhibit the anticoagulant activities of APC albeit on a different level. In contrast to the results obtained using the prothrombinase assay, NB3 was found to be a more potent APC inhibitor than NB1 and NB2. Among all APC aptamers tested a truncated version of NB3 (NB3-49) and HS02-52G were found to be the most efficient ones (Figure 4.2C). NB3-49 was found to be an effective APC inhibitor but on a lower level compared to HS02-52G when replacing plasma by whole blood (Figure 4.2D).

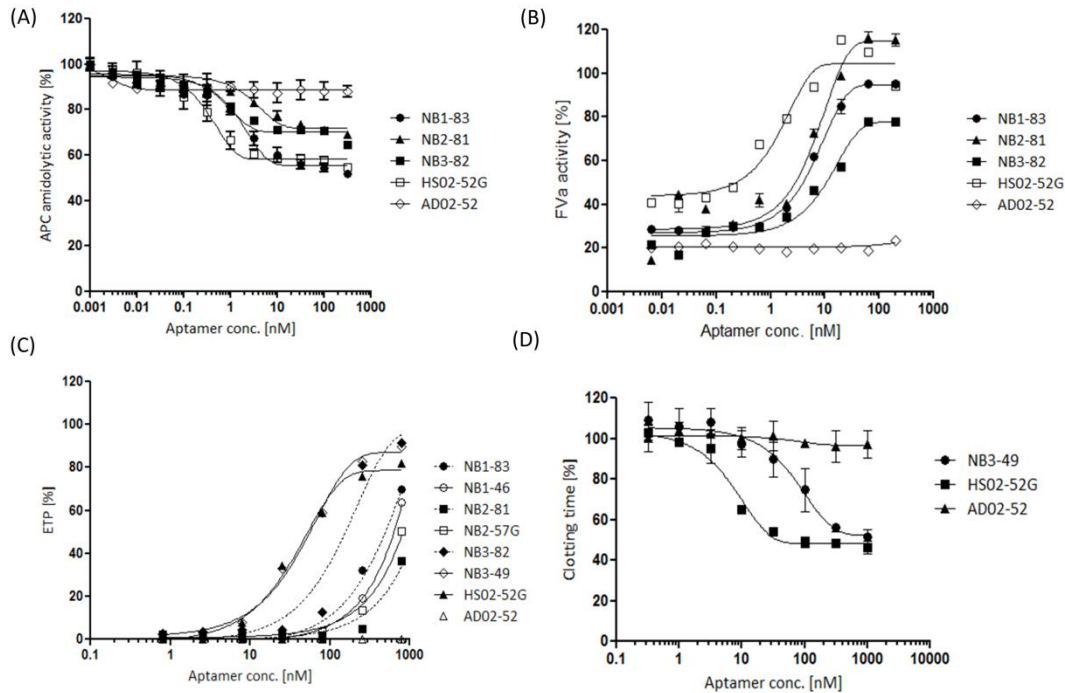


Figure 4.2. Functional properties of APC aptamers. (A) Influence of APC aptamers on peptide substrate conversion. Increasing concentrations of APC aptamers were incubated with rAPC at a final concentration of 180 pM and hydrolysis rates of a fluorogenic peptide substrate (Pyr-Pro-Arg-AMC) were measured. Substrate conversion measured w/o aptamers was set as 100%. (B) Influence of APC aptamers on APC catalyzed FVa-proteolysis. Purified FVa (150 pM) was incubated with rAPC (4.5 pM) in the presence of increasing concentrations of APC-aptamers for 30 min. After addition of FXa (1.3 pM) and prothrombin (25 nM) the amount of thrombin formed was measured through hydrolysis rates of a fluorogenic thrombin substrate. (C) Influence of APC aptamers on the anticoagulant activity of endogenously generated APC in human plasma. Pooled normal human plasma was spiked with rabbit thrombomodulin (2 U/ml) and increasing concentrations of APC aptamers. Subsequently, thrombin formation was initiated by addition of recombinant tissue factor (5 pM) and the time-dependent amount of thrombin generated monitored through the endogenous thrombin potential (ETP). (D) APC inhibiting activities of APC aptamers in whole blood. Contact phase activator (50 μ l) was added to 100 μ l of citrated whole blood containing different concentration of each aptamer. Time to clot formation was detected subsequent to addition of CaCl_2 (25 mM).

A higher stability of the NB3 aptamers containing a stable G4-structure might explain the higher efficacy of this aptamer when compared to the other NB-aptamers. Owing to its substantial Watson-Crick-based stem region, such a stability effect may also determine the high inhibiting capacity of HS02-52G.

However, besides blocking the binding sites for the procoagulant substrates FVa and FVIIIa (Figures S 4.6 – 4.7), the APC activity can also be inhibited by modulating endogenous control mechanisms. Similar to unfractionated heparin, the HS02-52G

aptamer accelerates the rate of APC inactivation by PCI following a template mechanisms¹³. From genetically engineered APC variants it is known that replacement of amino acids at position 194 and 254 generates an APC variant resistant to endogenous inhibition resulting in a prolonged half-life¹⁰⁸. Since these sites are located within or nearby the basic exosite of APC, we studied if the APC NB-aptamers 1-3 influence the inactivation rates of APC similar to HS02-52G. Studying plasma half-life times in the presence of saturating concentrations of the APC aptamers, the aptamers NB1 and NB2 similar as HS02 increased APC inactivation rates but on a lower level (Figure 4.3A). The reduced half-lives correlated well with the increased formation of APC-PCI complexes as tested by a sandwich ELISA. Most interestingly, however, the G-quadruplex-based NB3 aptamer variants, protected APC from APC/PCI-complex formation (Figure 4.3B).

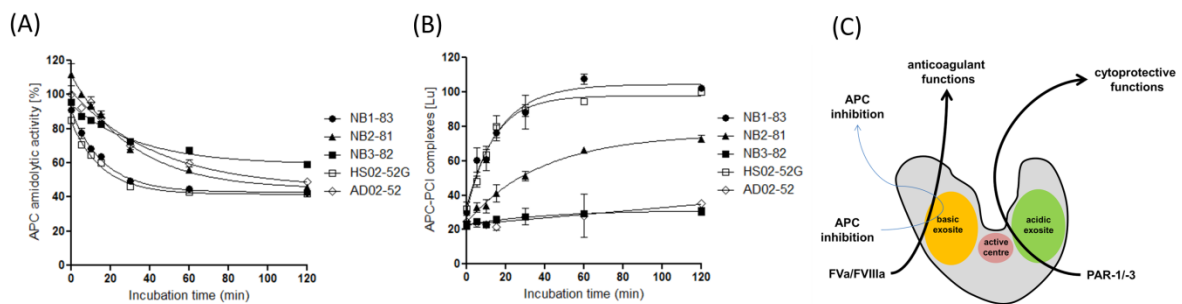


Figure 4.3. Influence of APC aptamers on inhibition of APC by endogenous inhibitors. (A) Recombinant APC (final concentration of 1.9 nM) was spiked to PC-deficient plasma in the presence of 100 nM NB aptamers followed by sub-sampling and capturing of APC using sheep anti-human PC antibody primed plates. Residual activity of APC was measured through fluorogenic peptide substrate conversion. (B) Subsequently, a HRP-conjugated goat anti-human PCI antibody was added to the wells and APC-PCI complex formation was monitored using BM chemiluminescence substrate. The luminescence intensity corresponds to the time point of 120 min incubation of HS02-52G aptamer was considered as 100% value. NB1-83, solid circles; NB2-81, solid triangles; NB3-82, solid squares; HS02-52G (positive control), open squares; AD02-52, open diamonds. Results are shown as means of duplicates. (C) Categorization of APC aptamers based on their impact on functions of APC.

Overall, as outlined in figure 4.3C the aptamers can be categorized in APC anticoagulant activity inhibiting aptamers with and without heparin-like activities and a third class of APC anticoagulant inhibitors inducing resistance to endogenous APC inhibitors. Since the acidic exosite of APC is not involved in aptamer binding the allosteric aptamers show no effect on the cytoprotective functions of APC¹³. These features qualify NB3 as a novel candidate molecule for the development of a specific and potent APC inhibitor as envisaged for the adjuvant treatment of patients with hemophilia^{110–112}. Furthermore, rapid and selective down-regulation of the anticoagulant activity of APC seems to be especially interesting in trauma-induced coagulopathy (TIC) patients where a reversible and short acting APC inhibitor is required and where active-site acting inhibitors bear the

risk to induce an adverse thrombo-inflammatory reaction. Moreover this study shows that aptamers can be used to study and dissect different functional epitopes within a protease exosite not only adding new insights into the architecture and organization of the basic exosite of APC but also showing that aptamers are useful for epitope binning similar to monoclonal antibodies.

4.3. Supplementary information

4.3.1. Chemicals and materials

All basic chemicals were purchased from Sigma-Aldrich (Taufkirchen, Germany). The randomized single-stranded (ss) DNA libraries IHT1 (5'- AAG CAG TGG TAA GTA GGT TGA - N40 (25% each A/G/C/T) - TCT CTT CGA GCA ATC CAC AC -3'), IHT2N (5'- GAT TGT TAC TGT CAC GAG GAT- N40 (40% G, 20% each A/C/T) - ATA GCA CAT TAG TTC AGA TAC -3'), individual aptamers HS02-52G and 3'-biotinylated HS02-52G (5'-GCC TCC TAA CTG AGC TGT ACT CGA CTT ATC CCG GAT GGG GCT CTT AGG AGG C-3'), NB1, NB2, and NB3 (see Table 1 for sequences), as well as the control oligonucleotides AD02-52 (5'-GCC TCC TAA GAG CCC CAT CCG GGA TAA GTC GAG TAC AGC TCA GTT AGG AGG C-3'), 45Ag (5'-GGG TTA GGG TTA GGG TTA GGG TTA GGG TTA GGG TTA GGG -3') and 45noG4 (5'-CAT ACA TAC ATT TCA CAA TTC ACA TTA CAT TCA CAA TCC ATT CAT-3') were synthesized and PAGE-purified by Microsynth (Balgach, Switzerland). IHT1 and IHT2N-amplification primers and 5'-biotinylated capture molecules for the IHT1 library (5'- Biotin-GTG TGG ATT GC-3') and the IHT2N library (5'- Biotin-GTA TCT GAA CTA AT-3') were synthesized and HPLC-purified by Eurogentec (Seraing, Belgium).

The composition of the PBS buffer (1x, pH 7.4) was as follows: 137 mM NaCl, 2.7 mM KCl, 9.6 mM Na₂HPO₄, and 1.5 mM KH₂PO₄. The used D-PBS-buffer (containing 0.9 mM CaCl₂ and 0.5 mM MgCl₂ in the 1x concentrated solution) was purchased as a 10x concentrate at a pH of 5.3 from Sigma (cat. no.: D1283). The pH was adjusted to 7.4 during preparation of the 1x concentrated buffer.. Recombinant human activated protein C (rAPC, Xigris®) was purchased from Eli Lilly (Windlesham, Surrey, UK), recombinant human Factor VIIa (NovoSeven®) was obtained from Novo Nordisk (Bagsværd, Denmark). Argatroban was obtained from Mitsubishi Pharma (Düsseldorf, Germany). Human FVIII was purchased from CSL Behring (Marburg, Germany). Plasma-derived human Protein C (Ceprotin®) was from Baxter (Unterschleißheim, Germany). Unfractionated heparin (UFH) was purchased from Ratiopharm (Ulm, Germany). Human alpha-thrombin, activated human FIX and human FX was from Haematologic Technologies, Inc. (Essex Junction, USA) and was purchased from Cellsystem (Troisdorf, Germany). The aPTT reagent Actin FS was purchased from Siemens Healthcare Diagnostics. Phospholipids was obtained from Rossix (Möln dal, Sweden). G-25 columns were purchased from GE Health Life Sciences (Freiburg, Germany). T4 Polynucleotide Kinase (PNK) was obtained from New England Biolabs (Frankfurt, Germany) and [γ -³²P] ATP was purchased from PerkinElmer (Rodgau,

Germany). The fluorogenic APC peptide substrate PCa 5791 (Pyr-Pro-Arg-AMC) was purchased from Loxo (Dossenheim, Germany) and Fluorogenic FXa substrate, I-1100 (Boc-Ile-Glu-Gly-Arg-AMC) was obtained from Bachem (Weil am Rhein, Germany). The chromogenic APC substrate p-Glu-Pro-Arg-MNA was part of the Berichrom Protein C Kit (Siemens Healthcare, Marburg, Germany). Reagents for thrombin generation (5 pM TF-reagent [PPP-reagent], thrombin calibrator, FluCa buffer and the fluorogenic thrombin substrate Z-Gly-Gly-Arg-AMC) were purchased from Stago (Düsseldorf, Germany). Rabbit thrombomodulin was purchased from Sekisui (Pfungstadt, Germany). Protein C-deficient plasma was purchased from Affinity Biologicals (Ontario, Canada).

4.3.2. Capillary electrophoresis-(CE)-SELEX

All CE separations were performed using the ProteomeLab PA 800 (Beckman Coulter, Inc., Fullerton, CA, USA) as previously described^{47,113}. In brief, 2 independent selections each comprising 6 cycles of CE-SELEX against rAPC were performed using the ssDNA-libraries IHT1 or IHT2N. The concentration of rAPC within the equilibrium mixture with (selected) ssDNA was reduced with each selection cycle to increase stringency. Generation of ssDNA for subsequent selection cycles was isolated from asymmetric PCR mixtures by Capture and Release (CaR) using the IHT1 or IHT2N capture molecules as previously described⁴⁷.

4.3.3. Next generation sequencing and data analysis

NGS was performed using the Illumina sequencing by synthesis technology on a HiSeq 1500 instrument. For adapter ligation with some adaptations, the TruSeq DNA PCR-Free (LT) sample preparation kit (Ref.15037063, Illumina) was used. A detailed description of the sample preparation protocol has recently been published¹¹⁴. Data processing of the raw sequencing data was done by AptalT (Munich, Germany) using the COMPAS software.

4.3.4. In silico secondary structure predictions

The 'DNA folding form' on the mfold web sever available at <http://mfold.rna.albany.edu/?q=mfold>⁹¹ was used at default settings to predict the Watson-Crick-based intramolecular folding patterns of the identified single aptamer sequences. The web-based QGRS mapper software available at <http://bioinformatics.ramapo.edu/QGRS/analyze.php>¹¹⁵ was used at default settings to assess the presence of putative G4-forming sequences (G4 motifs) within the aptamers.

4.3.5. Detection of G-quadruplex formation by Thioflavin T-staining

In general, aptamers and G4-positive (45Ag) or negative controls (45noG4) were heated to 90°C followed by cooling to RT in G4-buffer (50 mM Tris-HCl, pH 7.5 containing 50 mM KCl) and preserved on ice until analyzed.

For PAGE-analysis, 30 pmol of aptamers and controls were mixed with 40% sucrose solution and loaded on native 20% polyacrylamide gels supplemented with 50 mM KCl. Electrophoresis was performed at 4°C for 4 hours at 80 volts in running buffer (Tris Borate, pH 8.3; 89 mM Tris, 89 mM boric acid, and 20 mM KCl) using a MINI Protean Gel System (Bio-Rad, Munich, Germany). Gels were subsequently stained with either SYBRGreen (1x) or thioflavin T (ThT, 1 μ M) in running buffer and bands analyzed using a Chemidoc imaging system equipped with image lab 5.0 software (Bio-Rad).

For analysis in solution, aptamers and controls (1 μ M) were stained in G4-buffer at RT with either ThT (1 μ M) or SYBRGreen (1x) using black 96-well $\frac{1}{2}$ AreaPlate microplates (Perkin Elmer, Rotgau). Fluorescence ($\lambda_{\text{ex}} = 425 \text{ nm} / \lambda_{\text{em}} = 500 \text{ nm}$ for ThT and $\lambda_{\text{ex}} = 497 \text{ nm} / \lambda_{\text{em}} = 520 \text{ nm}$ for SybrGreen) was measured using a 2300 EnSpire Multimode Plate Reader (Perkin Elmer, Rodgau, Germany).

4.3.6. Determination of dissociation constants and binding competition experiments

Determination of binding affinities and binding competition experiments were performed using filter retention analysis as previously described in detail¹¹³. In brief, aptamers were labeled at the 5' end using PNK and [γ -³²P] ATP and labeled molecules purified by the use of G25 columns. For determination of dissociation constants (Kd), APC, PC, FVIIa or human α -thrombin were serially diluted (0-2 μ M) in D-PBS buffer, pH 7.4 containing 0.1% BSA and 10 μ M yeast tRNA (D-PBS+) and ³²P-labeled aptamers added (1 nM final concentration). During HS02-52G competition experiments, increasing concentrations of non-labeled aptamers (0-1 μ M) were incubated with APC (20 nM final concentration) for 10 min followed by addition of ³²P-labeled HS02-52G molecules (1 nM final concentration). For UFH competition experiments, increasing concentrations of non-labeled UFH (0-500 μ M final concentration) were incubated with APC (20 nM final concentration) for 10 min followed by addition of ³²P-labeled aptamers (1 nM final concentration). In general, reaction mixtures were incubated for 30 min at 37°C and subsequently passed through pre-equilibrated 0.45 μ m nitrocellulose membranes followed by three washes using D-PBS+. The radioactivity remaining on the filter was quantified after exposure to a phosphor screen by a FLA 5100 imaging system (Fujifilm Life Science, Düsseldorf, Germany).

4.3.7. OECA-based binding competition experiments

Competition of binding between HS02-52G and the NB aptamers to APC was also assessed using the APC OECA setting as previously described⁵⁶. In brief, increasing concentrations of aptamers (0-100 nM final concentration) were incubated with APC (180 pM final concentration) for 1 h at room temperature (RT). The mixture was then transferred to the wells of microtiter modules primed with immobilized HS02-52G aptamers and incubated for 2 h at RT. After washing, the amount of APC bound to the immobilized HS02-52G aptamers was measured using 100 μ l of 300 μ M of the fluorogenic substrate PCa 5791 ($\lambda_{\text{ex}} = 360 \text{ nm}$ / $\lambda_{\text{em}} = 460 \text{ nm}$) in dilution buffer (10 mM Tris.HCl, 4 mM CaCl_2 , 154 mM NaCl, pH 8.5) and a Synergy 2 microplate reader (Biotek, Bad Friedrichshall, Germany).

4.3.8. APC amidolytic assay

The influence of aptamer binding on the amidolytic activity of APC was assessed in the 96-well format using fluorogenic and chromogenic APC peptide substrates. For fluorogenic measurement, increasing concentrations of aptamers (0-316 nM final concentration) were incubated with rAPC (180 pM final concentration) in assay buffer (10 mM Tris-HCl, 137 mM NaCl, 1 mM MgCl_2 , 1 mM CaCl_2 , 0,1% BSA, pH 7.4) in a total volume of 50 μ l in white F8 Fluoronunc modules (Thermo Fisher Scientific [Nunc], Wiesbaden, Germany). For chromogenic measurement, rAPC (370 pM final concentration) was incubated with increasing concentrations of aptamers (0-100 nM final concentration) in standard transparent 96-well round-bottom plates, pre-coated with BSA (2% BSA in PBS, pH 7.4 containing 0.05% Tween 20). Subsequently, 50 μ l of PCa 5791 or p-Glu-Pro-Arg-MNA at a final concentration of 150 μ M or 140 μ M, respectively were added and substrate hydrolysis rates measured (chromogenic: $\lambda_{\text{abs}} = 405 \text{ nm}$ /fluorogenic: $\lambda_{\text{ex}} = 360 \text{ nm}$ / $\lambda_{\text{em}} = 460 \text{ nm}$) using the Synergy 2 microplate reader (Biotek).

4.3.9. FVa and FVIIIa inactivation assays

To determine the influence of aptamer binding on APC-mediated inactivation of FVa, 150 pM FVa in assay buffer (20 mM Tris-HCl [pH 7.6], 137 mM NaCl, 5 mM CaCl_2 , 1 mg/ml BSA and freshly added 10 μ g/ml phospholipids) was incubated with 0.25 ng/ml (4.5 pM) rAPC in the presence of increasing concentrations of aptamer (0-200 nM). After incubation for 30 min, 25 μ l of the mixture were transferred to a well containing 1.3 pM human FXa and 10 mM fluorogenic thrombin substrate (Pefalour I-1650) and supplemented to a total volume of 75 μ l with assay buffer. Finally, 50 μ l of 25 nM human prothrombin were added

to the reaction mixture and thrombin catalyzed substrate hydrolysis was monitored using Synergy 2 microplate reader and a λ ex 360 / λ em 460 nm filter set.

To determine the influence of aptamers binding on APC-mediated inactivation of FVIIIa a tenase assay was used. This assays measures the FVIIIa-activity through the rate of FXa-formation. In Brief, activated FVIII was prepared by incubation of 1 U recombinant human FVIII with 0.025 U human α -thrombin in PBS buffer ([pH 7.4] 1 mg/ml BSA) in a total volume of 100 μ l. After 2 min of incubation at room temperature, argatroban (final concentration of 100 μ M) was added to terminate thrombin activation. Activated FVIII at a concentration of 0.16 U/ μ l was incubated with 10 nM rAPC in assay buffer (20 mM Tris-HCl [pH 7.6], 137 mM NaCl, 10 mg/ml phospholipids, 5 mM CaCl₂, 1 mg/ml BSA) in the absence or presence of aptamers or controls (0.32–316 nM). After incubation for 30 min, 25 μ l of the mixtures was transferred to the wells of black F16 Fluoronunc modules (Thermo Fisher Scientific, Nunc) containing 3 nM human FIXa and 333 μ M Boc-Ile-Glu-Gly-Arg-AMC in a total volume of 75 μ l assay buffer. Subsequently, 50 μ l 25 nM human FX in assay buffer was added to the wells and the kinetic of FXa-mediated substrate hydrolysis monitored using a Synergy 2 microplate reader.

4.3.10. Thrombin generation assay

Increasing concentrations of aptamers and controls (0 – 800 nM final concentration) were added to pooled normal human plasma spiked with 2 U/ml rabbit thrombomodulin (TM). Plasma samples w/o rabbit TM and aptamers were applied as controls. Thrombin generation in the samples was monitored by calibrated automated thrombography (CAT) using standard reagents (Stago, Düsseldorf, Germany) and a Fluoroskan Ascent FL plate reader (Thermo Scientific) as previously described¹¹⁶.

4.3.11. APC anticoagulant activity in whole blood

Whole blood clotting times were measured using aPTT reagents and the semi-automated 10-channel ball-coagulometer KC10 (Amelung, Lemgo, Germany [now: Diasys, Flach, Germany]). In brief, 100 μ l of citrated whole blood containing different concentration of each aptamer (0.32 - 1 μ M final concentration) and 50 μ l of the contact phase activator Actin FS (Siemens Healthcare Diagnostics) were added to the system-specific cuvettes and incubated at 37°C for 3 min. Subsequently, 50 μ l of 25 mM CaCl₂ solution were added to start the clotting reaction. Time to detectable clot formation was measured mechanically and given in seconds.

4.3.12. APC-APC-inhibitor complex formation testing

The inactivation rates of APC in plasma in the presence and absence of the different APC-aptamers were assessed using a combined functional and immunological assay. In this assay normal human plasma was replaced by PC-deficient plasma to avoid competition between endogenous PC and exogenously added APC for binding to the PC antibodies. PC-deficient citrated plasma was spiked with argatroban and corn trypsin inhibitor (CTI) reaching final concentrations of 100 μM and 25 $\mu\text{g/ml}$, respectively. Subsequently, the plasma was recalcified (10 mM Ca^{2+} final concentration) using a 1 M CaCl_2 stock solution. Primed plasma aliquotes were then spiked with aptamers or controls (100 nM final concentration) and sub-samples taken at the indicated time points. Each sub-sample was diluted 1 to 10 in D-PBS buffer containing 0.1% BSA and 22.2 μM of the APC inhibitor aprotinin and stored on ice. After completion of the sample series, 100 μl of the diluted sub-samples were incubated at RT for 1 h in the wells of microtiter-modules coated with the sheep anti-human PC antibody.

White Maxisorp F8 Fluoronunc microtiter modules (Nunc) were coated with sheep anti-human PC antibody (10 $\mu\text{g/ml}$, 100 $\mu\text{l/well}$) in coating buffer (Na_2CO_3 30 mM, NaHCO_3 200 mM, pH 9) at 4°C overnight. After three times of automated washing (ELx50 microplate washer, Biotek, Bad Friedrichshall, Germany) with D-PBS washing buffer (1x D-PBS, pH 7.4, 0.05% Tween 20; 300 $\mu\text{l/well}$), remaining binding sites were blocked by incubation with 200 $\mu\text{l/well}$ blocking buffer (1x D-PBS, pH 7.4, 2 mg/ml BSA, 0.05 % Tween 20) for 2 h at RT. After incubation, the blocking buffer was aspirated from the wells (using the ELx50 microplate washer) and primed microtiter-modules sealed and stored at 4°C until used.

After washing, the residual activity of the immobilized APC was monitored using a fluorogenic peptide substrate (300 μM) in substrate buffer (100 $\mu\text{l/well}$). Substrate hydrolysis was monitored at 360_{ex}/460_{em} nm by kinetic measurement for 2 h using the Synergy 2 microplate reader (Biotek). Thereafter, a HRP-conjugated goat anti-human PCI antibody (0,5 $\mu\text{g/ml}$; 100 $\mu\text{l/well}$) was added to the wells and incubated for 1h at RT. Subsequent to washing, in order to assess the amount of APC-PCI complexes captured in the wells, BM chemiluminescence substrate (Roche) was added (100 $\mu\text{l/well}$) and luminescence intensity measured at 460 nm using the Synergy 2 microplate reader.

4.4. Supplementary tables and figures

Table S 4.1. Aptamer sequences identified by cloning / sanger sequencing of two distinct selection procedures, IHT1 and IHT2N.

Aptamer	Selecti on library	Sequence (5' to 3')	Binding affinity [nM]
NB1	IHT1	AAGCAGTGGTAAGTAGGTTGACACATTAGGGCGGGGTA CTCCTATCACGTATGGGGCCCTGTGTCTCTTCGAGCAA TCCACAC	20.24
NB2	IHT2N	GATTGTTACTGTCACGAGGATATCACGTATGGGGGGCC GGCATGAGGGCCGCGCTGACAATAGCACATTAGTTCA GATAC	1.57
NB3	IHT2N	GATTGTTACTGTCACGAGGATTGGGGGTTGGGTGGATA GGCTGGCGTCGGGGCAGGTCAGTATAGCACATTAGTTC AGATAC	0.17
HS02-52G	D1	GCCTCCTAACTGAGCTGTACTCGACTTATCCCGGATGG GGCTCTTAGGAGGC	0.68

Table S 4.2. Binding affinities of full length aptamers, truncated variants and HS02-52G to recombinant APC, plasma derived Protein C, as well as the structurally similar serine proteases plasma derived thrombin and recombinant activated factor VII.

Aptamer	rAPC	pPC	pFIIa	rFVIIa
NB1-83	20.24	n.b.	n.b.	n.b.
NB1-46	1.27	n.b.	n.b.	n.b.
NB2-81	1.57	n.b.	n.b.	n.b.
NB2-57	0.95	n.b.	n.b.	n.b.
NB2-57G	0.79	n.b.	n.b.	n.b.
NB2-51	4.72	n.b.	n.b.	n.b.
NB3-82	0.17	n.b.	n.b.	n.b.
NB3-49	0.05	n.b.	> 1 μ M	n.b.
NB3-47	0.07	> 1 μ M	n.b.	n.b.
NB3-49C	0.87	n.b.	n.b.	n.b.
NB3-49CC	0.01	n.b.	> 1 μ M	> 0.1 μ M
HS02-52G	0.68	> 1 μ M	> 1 μ M	n.b.

r, recombinant; p, plasma derived; n.b., no binding. Values are given as means of two measurement.

Table S 4.3. Half maximal inhibitory concentrations (IC₅₀) of full length and truncated APC aptamers on APC amidolytic and anticoagulant activities.

Aptamer	K _d [nM]	IC ₅₀ [nM]		
		Competition experiment using HS02-52G (Filter retention assay) [Fig. S 4.4 A]	Competition experiment using HS02-52G (OECA assay) [Fig. S 4.4 B]	Competition experiment using UFH [Fig. S 4.4 C]
NB1-83	20.24	138.7	4.18	6194
NB1-46	1.27	166.5	3.2	7581
NB2-81	1.47	144.4	10.92	1843
NB2-57G	4.48	129.1	13.10	996
NB3-82	0.17	180.1	5.98	5548
NB3-49	0.05	115.3	6.35	9838
HS02-52G	0.68	46.79	0.49	78410

Aptamer	IC ₅₀ [nM]				
	Amidolytic activity (using Fluorogenic substrate) [Figure S 4.5 A]	Amidolytic activity (using chromogenic substrate) [Figure S 4.5 B]	FVa inactivation assay [Figure S 4.6]	FVIIIa inactivation assay [Figure S 4.7]	Calibrated automated thrombography [Figure 4.2C]
NB1-83	1.74	1.83	6.63	14.38	627.6
NB1-46	1.31	0.86	5.93	11.22	n.b.
NB2-81	3.54	3.03	6.96	38.48	n.b.
NB2-57G	2.47	2.87	90.85	43.01	n.b.
NB3-82	0.86	4.37	11.64	13.12	150.8
NB3-49	1.16	0.90	13.53	8.26	46.56
HS02-52G	0.36	0.32	1.52	4.91	35.65

n.b., no binding. Values are given as means of two measurement.

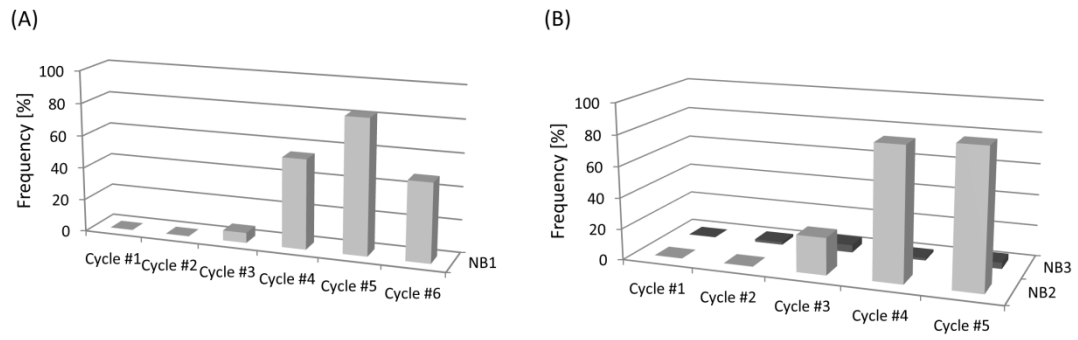
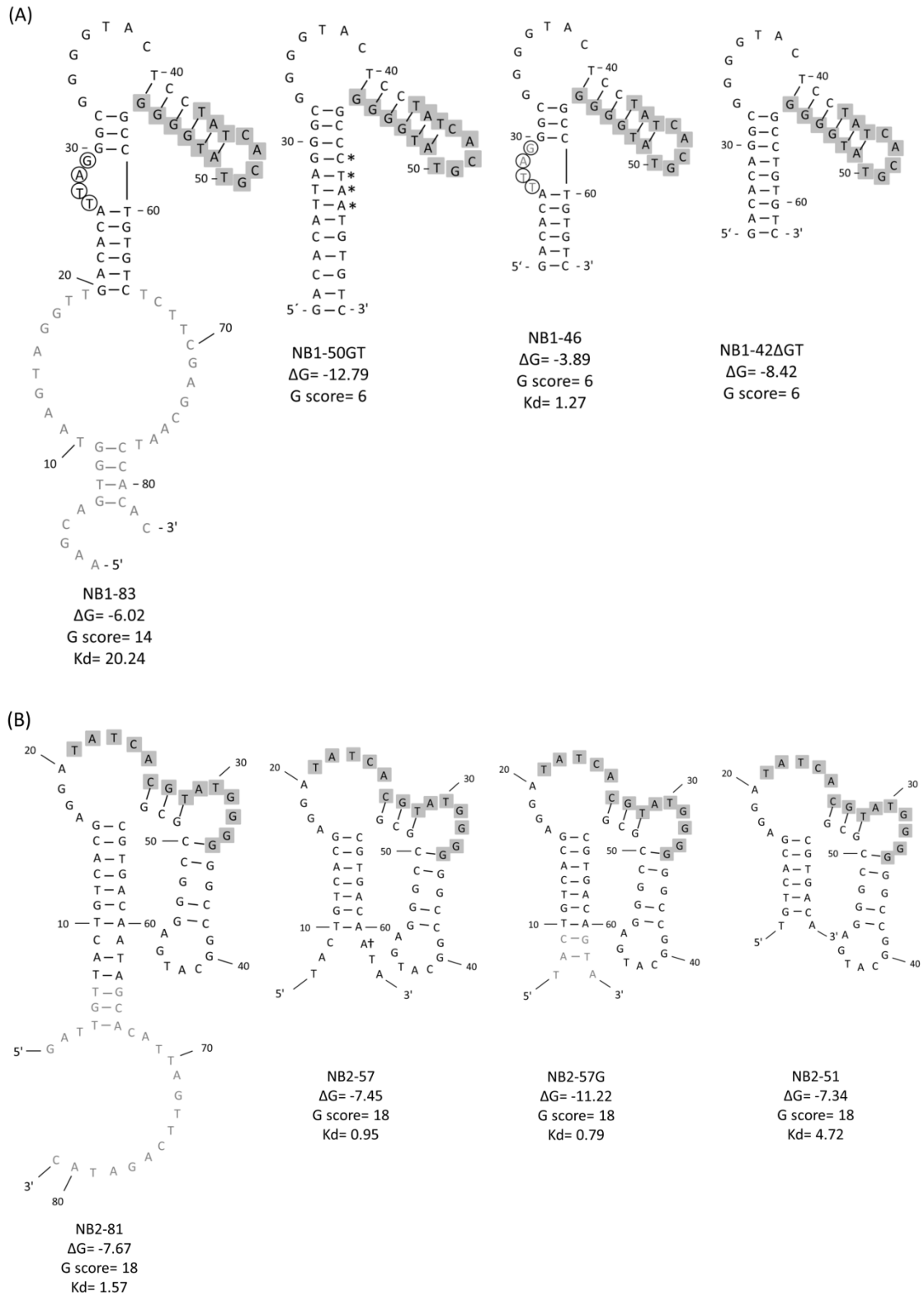


Figure S 4.1. Monitoring of CE-SELEX by next generation sequencing. The evolution profiles of the most abundant sequences identified from (A) IHT1-based selection and (B) IHT2N-based selection.

Chapter 4: Modifying substrate specificity of APC using aptamers



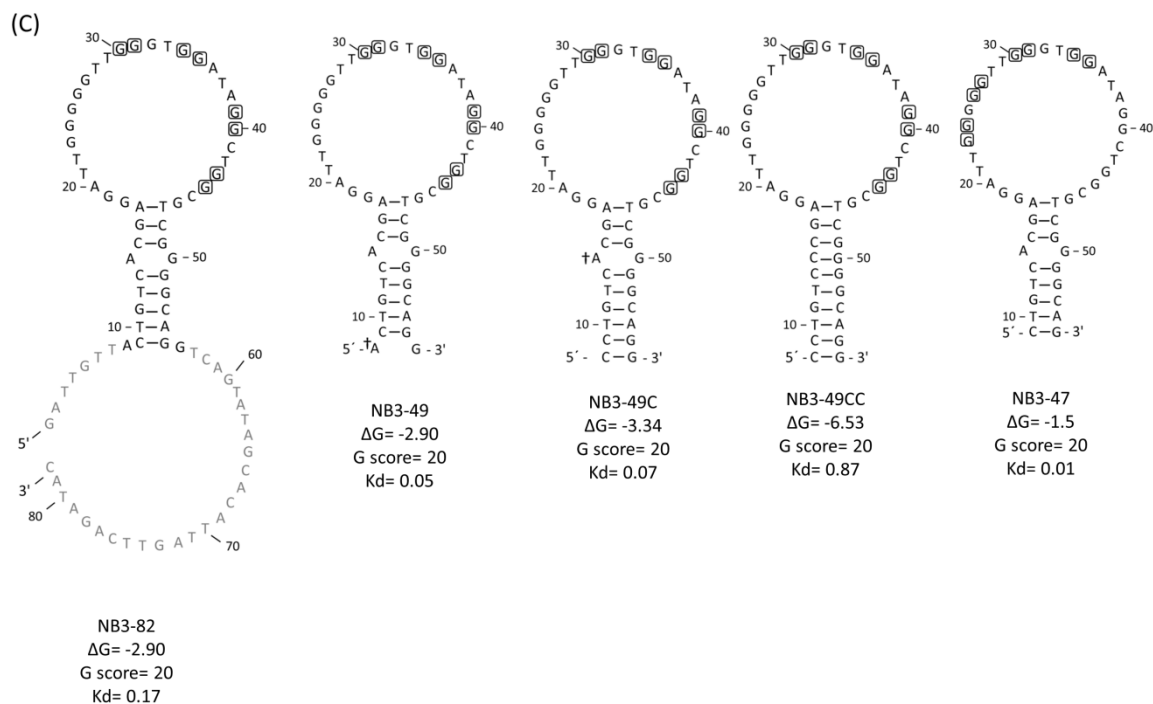


Figure S 4.2. In-silico-prediction of secondary structures and key characteristics of full-length and truncated variants of NB1 (A), NB2 (B), and NB3 (C) extracted from m-fold web server on 17.09.2015. In each group, the numbering follows the same order as full-length aptamer. The consensus sequence highlighted in gray. Each circle or quadrangle represents the incorporation of the intended nucleotide in a bulge and G-quadruplex forming motif, respectively. Addition of complementary nucleotides was specified with * while nucleotides replaced by a complementary nucleotide (according to the Watson-Crick base pairing) marked with †. Dissociation constant (Kd) is shown in nM.

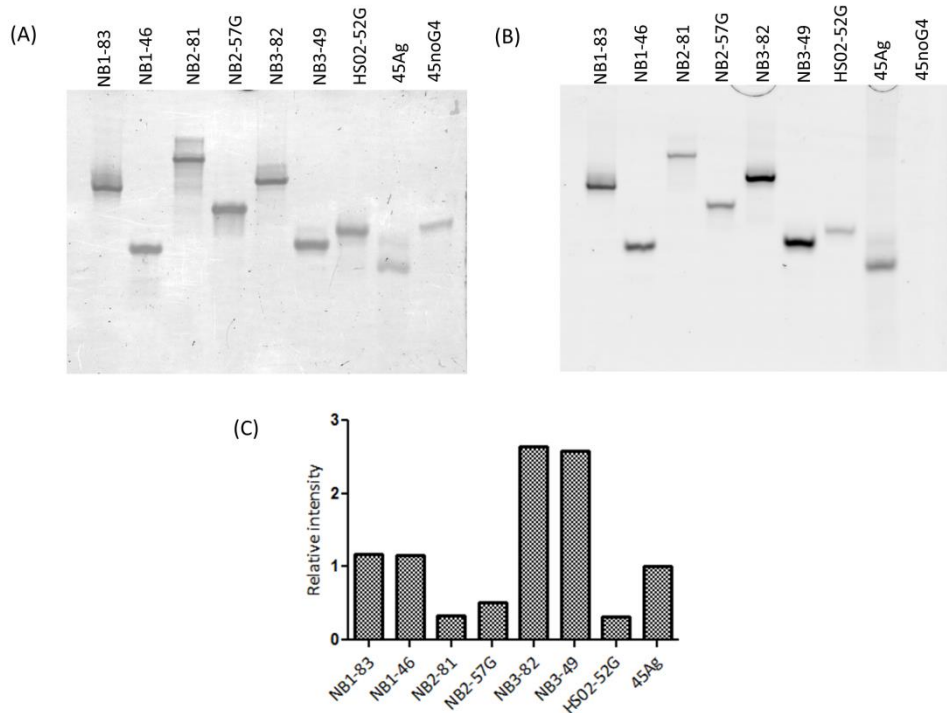


Figure S 4.3. G-quadruplex analysis. (A) Non-denaturing polyacrylamide gel electrophoresis (20% acrylamide gel supplemented with 50 mM KCl) for G-quadruplex structure detection using SybrGreen (1x) staining or (B) Thioflavin T (1 μM) staining. (C) The fluorescence enhancement resulting from polyacrylamide gel electrophoresis stained by Thioflavin T. The intensity of the 45Ag band used as positive control was considered for intensity normalization. (D) Fluorescence enhancement of SybrGreen (1x) and Thioflavin T (1 μM) incubated with NB aptamers and related truncated variants. Error bars correspond to standard deviation of three measurements.

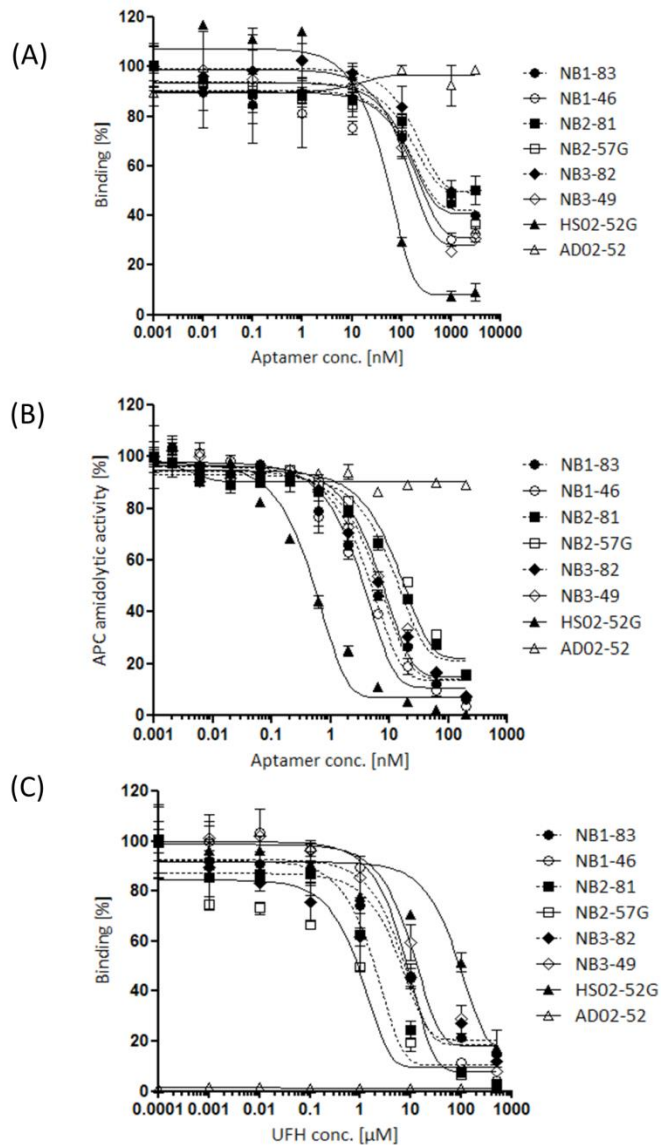


Figure S 4.4. Binding competition experiment. (A) Increasing concentrations of NB aptamers were incubated with rAPC at a final concentration of 20 nM followed by addition of radioactively labeled HS02-52G as the competitor. The reaction mixture passed through nitrocellulose membranes and remaining radioactivity was quantified. (B) NB aptamers as competitors were incubated with rAPC at a final concentration of 180 pM followed by transferring the mixture to the wells primed with immobilized HS02-52G aptamers. Residual amount of APC after washing was measured using an APC-specific fluorogenic substrate. Reduced APC amidolytic activity is an indicator of the replacement of NB aptamers by capturing ligand, HS02-52G. (C) Increasing concentrations of unfractionated heparin (UFH) were incubated with rAPC (20 nM final concentration) followed by addition of radioactively labeled NB aptamers. The reaction mixture passed through nitrocellulose membranes and remaining radioactivity was quantified. The intensity in the wells without competitor was defined as 100% value. Values are given as means of two measurements.

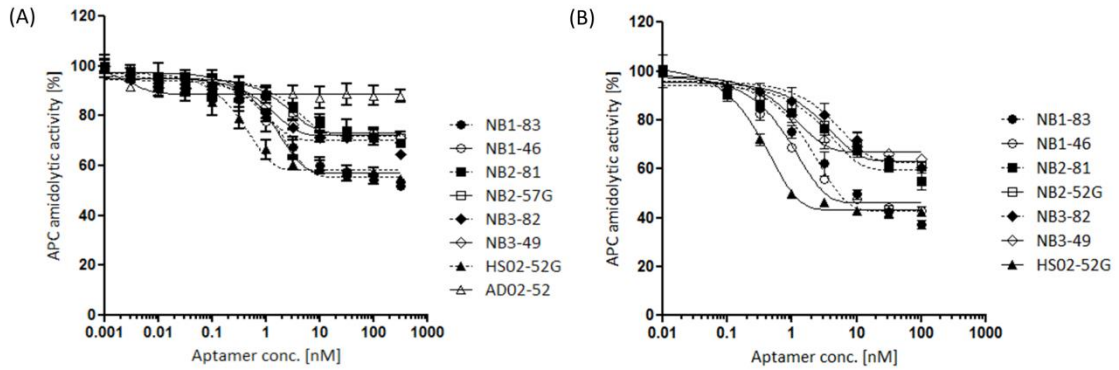


Figure S 4.5. Influence of APC-aptamers and truncated variants on APC amidolytic activity. Recombinant APC (180 pM) was incubated with increasing concentrations of APC-aptamers and cleavage rates of the (A) fluorogenic peptide substrate (Pyr-Pro-Arg-AMC) at a final concentration of 150 µM or the (B) chromogenic peptide substrate (p-Glu-Pro-Arg-MNA) at a final concentration of 140 µM measured. HS02-52G and AD02-52 were used as positive and negative controls, respectively. Data are shown as means of duplicates.

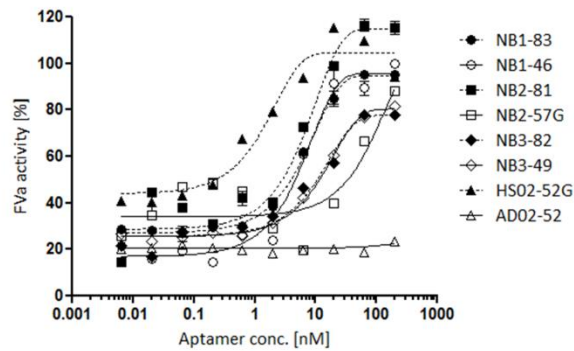


Figure S 4.6. The impact of increasing concentrations of the full-length NB aptamers and truncated variants on APC-mediated inactivation of FVa. Purified factor Va (150 pM final concentration) was incubated with 4.5 pM rAPC in the presence of NB aptamers. Thrombin catalyzed substrate hydrolysis was monitored in the prothrombinase/tenase assay. Aptamers HS02-52G and AD02-52 have been used as positive and negative controls, respectively. All results are shown as means of duplicates.

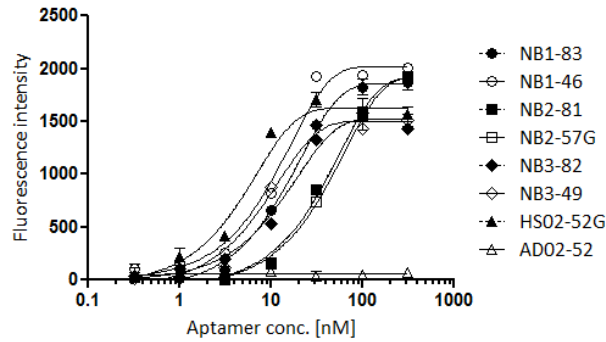


Figure S 4.7. The impact of increasing concentrations of the full-length NB aptamers and truncated variants on APC-mediated inactivation of FVIIIa. Thrombin activated FVIII (0.16 U/ml) was incubated with APC (10 nM) in the presence of different concentration of aptamers or negative control, AD02-52G. FXa-catalyzed substrate conversion was monitored after addition of FIXa and FX in final concentration of 2 nM and 8.3 nM, respectively.

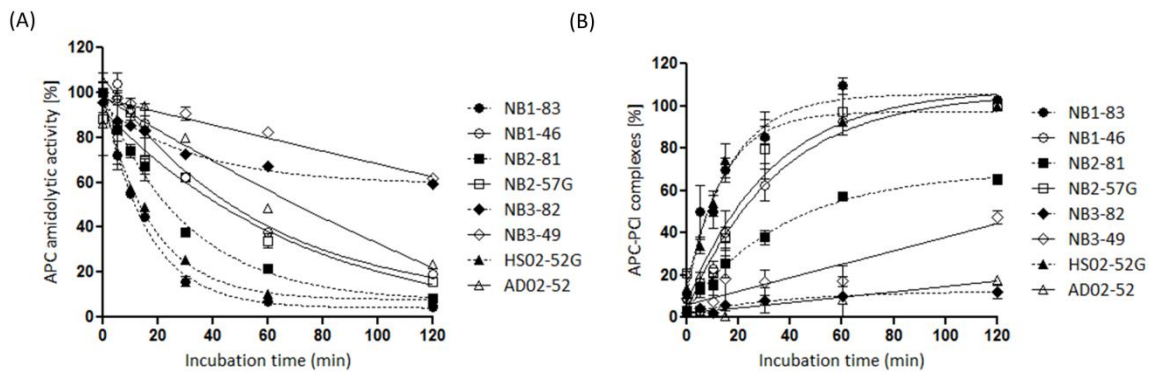


Figure S 4.8. Influence of APC aptamers and truncated variants on inhibition of APC by PCI. (A) Recombinant APC (final concentration of 1.9 nM) was spiked to PC-deficient plasma in the presence of 100 nM NB aptamers followed by sub-sampling and capturing of APC using sheep anti-human PC antibody primed plates. Residual activity of APC was measured through fluorogenic peptide substrate conversion. (B) Subsequently, a HRP-conjugated goat anti-human PCI antibody was added to the wells and APC-PCI complex formation was monitored using BM chemiluminescence substrate. The luminescence intensity corresponds to the time point of 120 min incubation of HS02-52G aptamer was considered as 100% value. Aptamers HS02-52G and AD02-52 have been used as positive and negative controls, respectively. Results are shown as means of duplicates.

Abbreviations

A260	Absorbance at 260 nM
A280	Absorbance at 280 nM
APC	Activated protein C
ATP	Adenosine 5'-triphosphate
B&W	Binding and washing buffer
BSA	Bovine serum albumin
CaR	Capture and release
CE	Capillary electrophoresis
Conc.	Concentration
CTI	Corn trypsin inhibitor
DNA	Deoxyribonucleic acid
dNTPs	Deoxynucleotide triphosphate
D-PBS	Dulbeco's phosphate buffer saline
EGF1	Epidermal growth factor 1
EGF2	Epidermal growth factor 2
ELISA	Enzyme-linked immunosorbent assay
EOF	Electroosmotic flow
EPCR	Endothelial protein C receptor
ESI	Electronic supplementary information
FII	Factor II (prothrombin)
FIIa	Activated factor II (thrombin)
FIX	Factor IX
FIXa	Activated factor IX
FV	Factor V
FVa	Activated factor V
FVII	Factor VII

Abbreviations

FVIIa	Activated factor VII
FVIII	Factor VIII
FVIIIa	Activated factor VIII
FX	Factor X
FXa	Activated factor X
FXI	Factor XI
FXII	Factor XII
FXIIa	Activated factor XII
FXIII	Factor XIII
GPIb α	Platelet glycoprotein Ib alpha chain
HPLC	High performance liquid chromatography
HRP	Horseradish peroxidase
i.D.	Inner diameter
Kd	Dissociation constant
kV	Kilo volt
mA	mili amper
MW	Molecular weight
NOACs	new oral anticoagulants
NGS	Next generation sequencing
o.D.	Outer diameter
OECA	Oligoenzyme capture assay
PAGE	Polyacrylamide gel electrophoresis
PAR-1	Protease activated receptor 1
PAR-3	Protease activated receptor 3
PBS	Phosphate buffer saline
PC	Protein C
PCI	Protein C inhibitor
PCR	Polymerase chain reaction
pM	Picomolar

Abbreviations

PS	Protein S
psi	Pound-force per square inch
rpm	rotate per minute
RT	room temperature
SELEX	Systematic evolution of ligands by exponential enrichment
SMB	Streptavidin magnetic bead
SMB+	Streptavidin magnetic bead loaded with capture molecules
ssDNA	single-stranded DNA
TF	Tissue factor
TFPI	Tissue factor pathway inhibitor
TM	Thrombomodulin
U	Unit
UFH	Unfractionated heparin
UV	ultra violet
V_{inj}	Volume of injection
WB	washing buffer
WB+	washing buffer containing 1mg/ml BSA
λ_{em}	emmission wavelength
λ_{ex}	excitation wavelength

Bibliography

1. Norris, L. A. Blood coagulation. *Best practice & research. Clinical obstetrics & gynaecology* **17**, 369–383 (2003).
2. Adams, R. L. & Bird, R. J. Review article: Coagulation cascade and therapeutics update: relevance to nephrology. Part 1: Overview of coagulation, thrombophilias and history of anticoagulants. *Nephrology (Carlton, Vic.)* **14**, 462–470 (2009).
3. Rodgers, G. M. & Shuman, M. A. Prothrombin is activated on vascular endothelial cells by factor Xa and calcium. *Proc. Natl. Acad. Sci. USA* **80**, 7001–7005 (1983).
4. Nesheim, M. E., Taswell, J. B. & Mann, K. G. The contribution of bovine Factor V and Factor Va to the activity of prothrombinase. *The Journal of biological chemistry* **254**, 10952–10962 (1979).
5. Dahlback, B. Blood coagulation. *Lancet (London, England)* **355**, 1627–1632 (2000).
6. Maroney, S. A. & Mast, A. E. New insights into the biology of tissue factor pathway inhibitor. *Journal of thrombosis and haemostasis : JTH* **13 Suppl 1**, S200-7 (2015).
7. Stenflo, J. A new vitamin K-dependent protein. Purification from bovine plasma and preliminary characterization. *The Journal of biological chemistry* **251**, 355–363 (1976).
8. Griffin, J. H., Fernandez, J. A., Gale, A. J. & Lo Mosnier. Activated protein C. *Journal of thrombosis and haemostasis : JTH* **5 Suppl 1**, 73–80 (2007).
9. Ikezoe, T. Thrombomodulin/activated protein C system in septic disseminated intravascular coagulation. *Journal of intensive care* **3**, 1 (2015).
10. Long, G. L. Structure and evolution of the human genes encoding protein C and coagulation factor IX. *Journal of cellular biochemistry* **33**, 185–190 (1987).
11. Manithody, C., Fay, P. J. & Rezaie, A. R. Exosite-dependent regulation of factor VIIIa by activated protein C. *Blood* **101**, 4802–4807 (2003).
12. Rezaie, A. R. Exosite-dependent regulation of the protein C anticoagulant pathway. *Trends in cardiovascular medicine* **13**, 8–15 (2003).
13. Muller, J. *et al.* An exosite-specific ssDNA aptamer inhibits the anticoagulant functions of activated protein C and enhances inhibition by protein C inhibitor. *Chemistry & biology* **16**, 442–451 (2009).
14. Yang, L., Manithody, C. & Rezaie, A. R. Contribution of basic residues of the 70-80-loop to heparin binding and anticoagulant function of activated protein C. *Biochemistry* **41**, 6149–6157 (2002).

Bibliography

15. Rosing, J. *et al.* Effects of protein S and factor Xa on peptide bond cleavages during inactivation of factor Va and factor VaR506Q by activated protein C. *The Journal of biological chemistry* **270**, 27852–27858 (1995).
16. Fay, P. J. Regulation of factor VIIIa in the intrinsic factor Xase. *Thrombosis and haemostasis* **82**, 193–200 (1999).
17. Thorelli, E., Kaufman, R. J. & Dahlback, B. Cleavage of factor V at Arg 506 by activated protein C and the expression of anticoagulant activity of factor V. *Blood* **93**, 2552–2558 (1999).
18. Castoldi, E. *et al.* Impaired APC cofactor activity of factor V plays a major role in the APC resistance associated with the factor V Leiden (R506Q) and R2 (H1299R) mutations. *Blood* **103**, 4173–4179 (2004).
19. Cramer, T. J., Griffin, J. H. & Gale, A. J. Factor V is an anticoagulant cofactor for activated protein C during inactivation of factor Va. *Pathophysiology of haemostasis and thrombosis* **37**, 17–23 (2010).
20. Mosnier, L. O., Zlokovic, B. V. & Griffin, J. H. The cytoprotective protein C pathway. *Blood* **109**, 3161–3172 (2007).
21. Feistritzer, C. & Riewald, M. Endothelial barrier protection by activated protein C through PAR1-dependent sphingosine 1-phosphate receptor-1 crossactivation. *Blood* **105**, 3178–3184 (2005).
22. Murakami, K. *et al.* Activated protein C attenuates endotoxin-induced pulmonary vascular injury by inhibiting activated leukocytes in rats. *Blood* **87**, 642–647 (1996).
23. Hosac, A. M. Drotrecogin alfa (activated): the first FDA-approved treatment for severe sepsis. *Proceedings (Baylor University. Medical Center)* **15**, 224–227 (2002).
24. Lai, P. S. *et al.* An updated meta-analysis to understand the variable efficacy of drotrecogin alfa (activated) in severe sepsis and septic shock. *Minerva anesthesiologica* **79**, 33–43 (2013).
25. Alaniz, C. An update on activated protein C (xigris) in the management of sepsis. *P & T : a peer-reviewed journal for formulary management* **35**, 504–529 (2010).
26. Toltl, L. J., Swystun, L. L., Pepler, L. & Liaw, P. C. Protective effects of activated protein C in sepsis. *Thrombosis and haemostasis* **100**, 582–592 (2008).
27. Ellington, A. D. & Szostak, J. W. In vitro selection of RNA molecules that bind specific ligands. *Nature* **346**, 818–822 (1990).
28. Stoltenburg, R., Reinemann, C. & Strehlitz, B. SELEX--a (r)evolutionary method to generate high-affinity nucleic acid ligands. *Biomolecular engineering* **24**, 381–403 (2007).

Bibliography

29. Smuc, T., Ahn, I.-Y. & Ulrich, H. Nucleic acid aptamers as high affinity ligands in biotechnology and biosensorics. *Journal of pharmaceutical and biomedical analysis* **81-82**, 210–217 (2013).
30. Hermann, T. & Patel, D. J. Adaptive recognition by nucleic acid aptamers. *Science (New York, N.Y.)* **287**, 820–825 (2000).
31. Geiger, A., Burgstaller, P., Eltz, H. von der, Roeder, A. & Famulok, M. RNA aptamers that bind L-arginine with sub-micromolar dissociation constants and high enantioselectivity. *Nucleic acids research* **24**, 1029–1036 (1996).
32. Toh, S. Y., Citartan, M., Gopinath, S. C. B. & Tang, T.-H. Aptamers as a replacement for antibodies in enzyme-linked immunosorbent assay. *Biosensors & bioelectronics* **64**, 392–403 (2015).
33. Gold, L., Polisky, B., Uhlenbeck, O. & Yarus, M. Diversity of oligonucleotide functions. *Annual review of biochemistry* **64**, 763–797 (1995).
34. Green, L. S. *et al.* Nuclease-resistant nucleic acid ligands to vascular permeability factor/vascular endothelial growth factor. *Chemistry & biology* **2**, 683–695 (1995).
35. Marro, M. L. *et al.* Identification of potent and selective RNA antagonists of the IFN- γ -inducible CXCL10 chemokine. *Biochemistry* **44**, 8449–8460 (2005).
36. Dougan, H. *et al.* Extending the lifetime of anticoagulant oligodeoxynucleotide aptamers in blood. *Nuclear medicine and biology* **27**, 289–297 (2000).
37. Tuerk, C. & Gold, L. Systematic evolution of ligands by exponential enrichment: RNA ligands to bacteriophage T4 DNA polymerase. *Science (New York, N.Y.)* **249**, 505–510 (1990).
38. Whatley, H. in *Clinical and Forensic Applications of Capillary Electrophoresis*, edited by J. Petersen & A. Mohammad (Humana Press 2001), pp. 21–58.
39. Lauer, H. H. & Rozing, G. P. *High Performance Capillary Electrophoresis: A primer* (Agilent Technologies, Inc., Copyright 2009-2014).
40. *Agilent 7100 capillary electrophoresis system- users manual* (Agilent Technologies, Inc., 2009).
41. Szeitner, Z., Andras, J., Gyurcsanyi, R. E. & Meszaros, T. Is less more? Lessons from aptamer selection strategies. *Journal of pharmaceutical and biomedical analysis* **101**, 58–65 (2014).
42. Mosing, R. K., Mendonsa, S. D. & Bowser, M. T. Capillary electrophoresis-SELEX selection of aptamers with affinity for HIV-1 reverse transcriptase. *Analytical chemistry* **77**, 6107–6112 (2005).
43. Ashley, J. & Li, S. F. Y. Three-dimensional selection of leptin aptamers using capillary electrophoresis and implications for clone validation. *Analytical biochemistry* **434**, 146–152 (2013).

Bibliography

44. Svobodova, M., Pinto, A., Nadal, P. & O' Sullivan, C. K. Comparison of different methods for generation of single-stranded DNA for SELEX processes. *Analytical and bioanalytical chemistry* **404**, 835–842 (2012).
45. Marimuthu, C., Tang, T.-H., Tominaga, J., Tan, S.-C. & Gopinath, S. C. B. Single-stranded DNA (ssDNA) production in DNA aptamer generation. *The Analyst* **137**, 1307–1315 (2012).
46. Holmberg, A. *et al.* The biotin-streptavidin interaction can be reversibly broken using water at elevated temperatures. *Electrophoresis* **26**, 501–510 (2005).
47. Hamedani, N. S. *et al.* Capture and Release (CaR): a simplified procedure for one-tube isolation and concentration of single-stranded DNA during SELEX. *Chemical communications (Cambridge, England)* **51**, 1135–1138 (2015).
48. Warkentin, T. E. & Greinacher, A. Heparin-induced thrombocytopenia and cardiac surgery. *The Annals of thoracic surgery* **76**, 2121–2131 (2003).
49. Ieko, M., Naitoh, S., Yoshida, M. & Takahashi, N. Profiles of direct oral anticoagulants and clinical usage-dosage and dose regimen differences. *Journal of intensive care* **4**, 19 (2016).
50. Bauer, K. A. Pros and cons of new oral anticoagulants. *Hematology / the Education Program of the American Society of Hematology. American Society of Hematology. Education Program* **2013**, 464–470 (2013).
51. Funk, D. M. A. Coagulation assays and anticoagulant monitoring. *Hematology / the Education Program of the American Society of Hematology. American Society of Hematology. Education Program* **2012**, 460–465 (2012).
52. Crowther, M. A. & Warkentin, T. E. Bleeding risk and the management of bleeding complications in patients undergoing anticoagulant therapy: focus on new anticoagulant agents. *Blood* **111**, 4871–4879 (2008).
53. Gonsalves WI, Gupta V, Patnaik MM. Management of Bleeding Complications in Patients on New Oral Anticoagulants. *Journal of Hematology and Transfusion* **2**, 1015–1021 (2014).
54. Gopinath, S. C. B. Anti-coagulant aptamers. *Thrombosis research* **122**, 838–847 (2008).
55. Kuliczkowski, W., Floyd, J., Malinin, A. & Serebruany, V. Aptamers: the emerging class of future anticoagulation for vascular disease. *Expert review of cardiovascular therapy* **8**, 503–507 (2010).
56. Muller, J. *et al.* Monitoring of plasma levels of activated protein C using a clinically applicable oligonucleotide-based enzyme capture assay. *Journal of thrombosis and haemostasis : JTH* **10**, 390–398 (2012).

Bibliography

57. Bock, L. C., Griffin, L. C., Latham, J. A., Vermaas, E. H. & Toole, J. J. Selection of single-stranded DNA molecules that bind and inhibit human thrombin. *Nature* **355**, 564–566 (1992).
58. Kubik, M. F., Stephens, A. W., Schneider, D., Marlar, R. A. & Tasset, D. High-affinity RNA ligands to human alpha-thrombin. *Nucleic acids research* **22**, 2619–2626 (1994).
59. Tasset, D. M., Kubik, M. F. & Steiner, W. Oligonucleotide inhibitors of human thrombin that bind distinct epitopes. *Journal of molecular biology* **272**, 688–698 (1997).
60. Rusconi, C. P. *et al.* RNA aptamers as reversible antagonists of coagulation factor IXa. *Nature* **419**, 90–94 (2002).
61. Oney, S. *et al.* Antidote-controlled platelet inhibition targeting von Willebrand factor with aptamers. *Oligonucleotides* **17**, 265–274 (2007).
62. Huang, R.-H., Fremont, D. H., Diener, J. L., Schaub, R. G. & Sadler, J. E. A structural explanation for the antithrombotic activity of ARC1172, a DNA aptamer that binds von Willebrand factor domain A1. *Structure (London, England : 1993)* **17**, 1476–1484 (2009).
63. Diener, J. L. *et al.* Inhibition of von Willebrand factor-mediated platelet activation and thrombosis by the anti-von Willebrand factor A1-domain aptamer ARC1779. *Journal of thrombosis and haemostasis : JTH* **7**, 1155–1162 (2009).
64. Gal, S. W. *et al.* Selection of a RNA aptamer that binds to human activated protein C and inhibits its protease function. *European journal of biochemistry / FEBS* **252**, 553–562 (1998).
65. Muller, J., Wulffen, B., Potzsch, B. & Mayer, G. Multidomain targeting generates a high-affinity thrombin-inhibiting bivalent aptamer. *Chembiochem : a European journal of chemical biology* **8**, 2223–2226 (2007).
66. Muller, J., Becher, T., Mayer, G. & Potzsch, B. Aptamer-Based Enzyme Capture Assay for Measurement of Plasma Thrombin Levels. *Methods in molecular biology (Clifton, N.J.)* **1380**, 179–189 (2016).
67. Gopinath, S. C., Shikamoto, Y., Mizuno, H. & Kumar, P. K. A potent anti-coagulant RNA aptamer inhibits blood coagulation by specifically blocking the extrinsic clotting pathway. *Thrombosis and haemostasis* **95**, 767–771 (2006).
68. Li, W. *et al.* Development of aptamer oligonucleotides as anticoagulants and antithrombotics for cardiovascular diseases: current status. *Thrombosis research* **134**, 769–773 (2014).
69. Chan, M. Y. *et al.* Phase 1b randomized study of antidote-controlled modulation of factor IXa activity in patients with stable coronary artery disease. *Circulation* **117**, 2865–2874 (2008).

Bibliography

70. Dyke, C. K. *et al.* First-in-human experience of an antidote-controlled anticoagulant using RNA aptamer technology: a phase 1a pharmacodynamic evaluation of a drug-antidote pair for the controlled regulation of factor IXa activity. *Circulation* **114**, 2490–2497 (2006).
71. Povsic, T. J. *et al.* Pegnivacogin results in near complete FIX inhibition in acute coronary syndrome patients: RADAR pharmacokinetic and pharmacodynamic substudy. *European heart journal* **32**, 2412–2419 (2011).
72. Lincoff, A. M. *et al.* Effect of the REG1 anticoagulation system versus bivalirudin on outcomes after percutaneous coronary intervention (REGULATE-PCI): a randomised clinical trial. *The Lancet* **387**, 349–356.
73. Nimjee, S. M. *et al.* A novel antidote-controlled anticoagulant reduces thrombin generation and inflammation and improves cardiac function in cardiopulmonary bypass surgery. *Molecular therapy : the journal of the American Society of Gene Therapy* **14**, 408–415 (2006).
74. Gilbert, J. C. *et al.* First-in-human evaluation of anti von Willebrand factor therapeutic aptamer ARC1779 in healthy volunteers. *Circulation* **116**, 2678–2686 (2007).
75. Markus, H. S. *et al.* The von Willebrand inhibitor ARC1779 reduces cerebral embolization after carotid endarterectomy: a randomized trial. *Stroke; a journal of cerebral circulation* **42**, 2149–2153 (2011).
76. Berezovski, M. *et al.* Nonequilibrium capillary electrophoresis of equilibrium mixtures: a universal tool for development of aptamers. *Journal of the American Chemical Society* **127**, 3165–3171 (2005).
77. Mendonsa, S. D. & Bowser, M. T. In vitro selection of high-affinity DNA ligands for human IgE using capillary electrophoresis. *Analytical chemistry* **76**, 5387–5392 (2004).
78. Ravelet, C., Grosset, C. & Peyrin, E. Liquid chromatography, electrochromatography and capillary electrophoresis applications of DNA and RNA aptamers. *Journal of chromatography. A* **1117**, 1–10 (2006).
79. Wang, J., Rudzinski, J. F., Gong, Q., Soh, H. T. & Atzberger, P. J. Influence of target concentration and background binding on in vitro selection of affinity reagents. *PLoS one* **7**, e43940 (2012).
80. *ProteomeLab™ PA 800 user's information* (Beckman Coulter, Inc., Copyright 2004).
81. Ellington, A. D. & Szostak, J. W. Selection in vitro of single-stranded DNA molecules that fold into specific ligand-binding structures. *Nature* **355**, 850–852 (1992).
82. Espelund, M., Stacy, R. A. & Jakobsen, K. S. A simple method for generating single-stranded DNA probes labeled to high activities. *Nucleic acids research* **18**, 6157–6158 (1990).

Bibliography

83. Wilson, R. Preparation of single-stranded DNA from PCR products with streptavidin magnetic beads. *Nucleic acid therapeutics* **21**, 437–440 (2011).
84. Civit, L., Fragoso, A. & O'Sullivan, C. K. Evaluation of techniques for generation of single-stranded DNA for quantitative detection. *Analytical biochemistry* **431**, 132–138 (2012).
85. Gyllensten, U. B. & Erlich, H. A. Generation of single-stranded DNA by the polymerase chain reaction and its application to direct sequencing of the HLA-DQA locus. *Proceedings of the National Academy of Sciences of the United States of America* **85**, 7652–7656 (1988).
86. Kurien, B. T. & Scofield, R. H. Extraction of nucleic acid fragments from gels. *Analytical biochemistry* **302**, 1–9 (2002).
87. Owczarzy, R. *et al.* IDT SciTools: a suite for analysis and design of nucleic acid oligomers. *Nucleic acids research* **36**, W163-9 (2008).
88. Mendonsa, S. D. & Bowser, M. T. In vitro evolution of functional DNA using capillary electrophoresis. *Journal of the American Chemical Society* **126**, 20–21 (2004).
89. Katona, E. *et al.* Interaction of factor XIII subunits. *Blood* **123**, 1757–1763 (2014).
90. Paul, A., Avci-Adali, M., Ziemer, G. & Wendel, H. P. Streptavidin-coated magnetic beads for DNA strand separation implicate a multitude of problems during cell-SELEX. *Oligonucleotides* **19**, 243–254 (2009).
91. Zuker, M. Mfold web server for nucleic acid folding and hybridization prediction. *Nucleic acids research* **31**, 3406–3415 (2003).
92. Bouwens, E. A. M., Stavenuiter, F. & Mosnier, L. O. Mechanisms of anticoagulant and cytoprotective actions of the protein C pathway. *Journal of thrombosis and haemostasis : JTH* **11 Suppl 1**, 242–253 (2013).
93. Crawley, J. T. & Efthymiou, M. Cytoprotective effect of activated protein C: specificity of PAR-1 signaling. *Journal of thrombosis and haemostasis : JTH* **6**, 951–953 (2008).
94. Yang, L., Bae, J.-S., Manithody, C. & Rezaie, A. R. Identification of a specific exosite on activated protein C for interaction with protease-activated receptor 1. *The Journal of biological chemistry* **282**, 25493–25500 (2007).
95. Tairaku, S. *et al.* Prenatal genetic testing for familial severe congenital protein C deficiency. *Human genome variation* **2**, 15017 (2015).
96. Sharma, S., Anbazhagan, J. & Plakkal, N. Neonatal purpura fulminans due to protein C deficiency. *Archives of disease in childhood. Fetal and neonatal edition* **100**, F453 (2015).
97. Broekmans, A. W. Hereditary protein C deficiency. *Haemostasis* **15**, 233–240 (1985).

Bibliography

98. Vincent, J.-L. Organ dysfunction in patients with severe sepsis. *Surgical infections* **7 Suppl 2**, S69-72 (2006).
99. Richardson, M. A. *et al.* Treatment of sepsis-induced acquired protein C deficiency reverses Angiotensin-converting enzyme-2 inhibition and decreases pulmonary inflammatory response. *The Journal of pharmacology and experimental therapeutics* **325**, 17–26 (2008).
100. Cohen, M. J. *et al.* Critical role of activated protein C in early coagulopathy and later organ failure, infection and death in trauma patients. *Annals of surgery* **255**, 379–385 (2012).
101. Johansson, P. I. *et al.* Disseminated intravascular coagulation or acute coagulopathy of trauma shock early after trauma? An observational study. *Critical care (London, England)* **15**, R272 (2011).
102. Ettingshausen, C. E. *et al.* Replacement therapy with protein C concentrate in infants and adolescents with meningococcal sepsis and purpura fulminans. *Seminars in thrombosis and hemostasis* **25**, 537–541 (1999).
103. Kroiss, S. & Albisetti, M. Use of human protein C concentrates in the treatment of patients with severe congenital protein C deficiency. *Biologics : targets & therapy* **4**, 51–60 (2010).
104. Andreou, A. P. *et al.* Protective effects of non-anticoagulant activated protein C variant (D36A/L38D/A39V) in a murine model of ischaemic stroke. *PloS one* **10**, e0122410 (2015).
105. Bae, J.-S., Yang, L., Manithody, C. & Rezaie, A. R. Engineering a disulfide bond to stabilize the calcium-binding loop of activated protein C eliminates its anticoagulant but not its protective signaling properties. *The Journal of biological chemistry* **282**, 9251–9259 (2007).
106. Heeb, M. J. & Griffin, J. H. Physiologic inhibition of human activated protein C by alpha 1-antitrypsin. *The Journal of biological chemistry* **263**, 11613–11616 (1988).
107. Heeb, M. J., Espana, F. & Griffin, J. H. Inhibition and complexation of activated protein C by two major inhibitors in plasma. *Blood* **73**, 446–454 (1989).
108. Berg, D. T. *et al.* Engineering the proteolytic specificity of activated protein C improves its pharmacological properties. *Proceedings of the National Academy of Sciences of the United States of America* **100**, 4423–4428 (2003).
109. Dupont, D. M. *et al.* Protein-binding RNA aptamers affect molecular interactions distantly from their binding sites. *PloS one* **10**, e0119207 (2015).
110. Sperandio, O. *et al.* Identification of novel small molecule inhibitors of activated protein C. *Thrombosis research* **133**, 1105–1114 (2014).

Bibliography

111. Brummel-Ziedins, K. E., Whelihan, M. F., Rivard, G. E. & Butenas, S. Activated protein C inhibitor for correction of thrombin generation in hemophilia A blood and plasma. *Journal of thrombosis and haemostasis : JTH* **9**, 2262–2267 (2011).
112. Butenas, S., Orfeo, T., Kalafatis, M. & Mann, K. G. Peptidomimetic inhibitors for activated protein C: implications for hemophilia management. *Journal of thrombosis and haemostasis : JTH* **4**, 2411–2416 (2006).
113. Hamedani, N. S. & Muller, J. Capillary Electrophoresis for the Selection of DNA Aptamers Recognizing Activated Protein C. *Methods in molecular biology (Clifton, N.J.)* **1380**, 61–75 (2016).
114. Tolle, F. & Mayer, G. Preparation of SELEX Samples for Next-Generation Sequencing. *Methods in molecular biology (Clifton, N.J.)* **1380**, 77–84 (2016).
115. Kikin, O., D'Antonio, L. & Bagga, P. S. QGRS Mapper: a web-based server for predicting G-quadruplexes in nucleotide sequences. *Nucleic acids research* **34**, W676–82 (2006).
116. Hemker, H. C. *et al.* Calibrated automated thrombin generation measurement in clotting plasma. *Pathophysiology of haemostasis and thrombosis* **33**, 4–15 (2003).

Acknowledgement

Most of all I would like to thank Prof. Dr. Bernd Pötzsch, who supported me throughout the work on my thesis and gave me advice, guidance and motivation.

I would like to express my sincerest gratitude to Prof. Dr. Johannes Oldenburg for giving me the opportunity to perform my PhD thesis in institute of Experimental Haematology and Transfusion Medicine.

I also would like to express my gratitude towards Dr. Jens Müller for scientific advices, teaching me his valuable experiences and his support in accompanying my thesis. His ability to transfer enthusiasm and knowledge has provided the basis for me to accomplish this work.

Furthermore I thank Prof. Dr. Diana Imhof for being the second referee of this thesis.

I also would like to express my gratitude towards Prof. Dr. Günter Mayer for the possibility to work in the S1 lab in Kekule institute.

I wish to thank Ms Simone Fischer and Ms Simone Gasper for their excellent technical assistance.

I also thank all my colleagues in institute of Experimental Haematology and Transfusion Medicine of University clinic Bonn for their support, understanding and making a friendly working environment.

Last but not least I wish to express my deepest gratitude to my husband and my parents who have supported and encouraged me entire my life with care and love.

Curriculum Vitae

CONTACT INFORMATION

Name: Nasim Shahidi Hamedani

Address: Graf-stauffenbergstraße 10, 53115 Bonn, Germany

Telephone: 0049 228 97375566

Cell Phone: 015129197352

Email: nasim.shahidi_hamedani@ukb.uni-bonn.de

CONFERENCE PRESENTATIONS AND AWARDS

- 1) **Hamedani NS**, Muller J, Fischer S, Oldenburg J, Mayer G and Potzsch B, FXIIIAa-targeting aptamers as diagnostic tools, 60th annula meeting society of thrombosis and haemostasis research (GTH 2016), Münster, Germany.
- 2) **Hamedani NS**, Fischer S, Oldenburg J, Mayer G, Potzsch B and Muller J Aptamers targeting activated protein C show different functions despite sharing the same binding site, 60th annula meeting society of thrombosis and haemostasis research (GTH 2016), Münster, Germany.
- 3) **Hamedani NS**, Muller J, Fischer S, Steiner R, Pezeshkpoor B, Rohrbach F, Oldenburg J, Mayer G and Potzsch B, Selection and characterization of DNA aptamers against activated factor XIII, 59th annula meeting society of thrombosis and haemostasis research (GTH 2015), Düsseldorf, Germany.
- 4) **Hamedani NS**, Krammer R, Muller J, Rühl H, Oldenburg J and Potzsch B. Fibrinogen protects activated factor XIII from early inactivation in human plasma. 58th annula meeting society of thrombosis and haemostasis research (GTH 2014), Wien, Austria.
- 5) **Hamedani NS**, Muller J, Potzsch B and Oldenburg J. Selection of high affinity DNA aptamer for activated protein C using capillary electrophoresis. 13th Iranian pharmaceutical sciences congress (IPSC 2012), Isfahan, Iran.
- 6) **Shahidi Hamedani N**, Abnous K, Ramezani M, Preparation and evaluation of transfection efficiency of nanoparticles of polyethylenimine-aptamer conjugates for prostate cancer siRNA delivery. 8th Nanotechnology Iranian Students Conference (NISC 2010), Mashhad, Iran. Best poster award.

- 7) **Shahidi Hamedani N**, Abnous K, Ramezani M, Targeted delivery of plasmid to ALL t-cells using aptamer PEI non-covalent conjugate. 3rd International congress on nanoscience and nanotechnology (ICNN2010), Shiraz, Iran.
- 8) **Shahidi Hamedani N**, Abnous K, Ramezani M, 2010, Nanoparticle-based targeted gene delivery to ALL T-cells using aptamer-PEI non covalent conjugates. 12th Iranian pharmaceutical sciences congress (IPSC 2010), Zanjan, Iran. Best Paper Award.

LIST OF PUBLICATIONS

- 1) **Hamedani NS**, Rühl H, Zimmermann JJ, Heiseler T, Oldenburg J, Mayer G, Pötzsch B, Müller J. In Vitro Evaluation of Aptamer-Based Reversible Inhibition of Anticoagulant Activated Protein C as a Novel Supportive Hemostatic Approach, 2016, *Nucleic Acid Ther.*, 26(6): 355-362.
- 2) Pezeshkpoor B, Castoldi E, Mahler A, Hanel D, Müller J, **Hamedani NS**, Biswas A, Oldenburg J, Pavlova A, Identification and functional characterization of a novel F5 mutation (Ala512Val, FVB onn) associated with activated protein C resistance, *J Thromb Haemost.* 2016 Apr 19 doi: 10.1111/jth.13339. [Epub ahead of print]
- 3) **Hamedani NS** and Muller J, Capillary Electrophoresis for the Selection of DNA Aptamers Recognizing Activated Protein C, 2016, *Methods in molecular biology* (Clifton, N.J.) 1380, 61-75.
- 4) **Hamedani NS**, Blumke F, Tolle F, Rohrbach F, Ruhl H, Oldenburg J, Mayer G, Pötzsch B, Muller J, Capture and Release (CaR): a simplified procedure for one-tube isolation and concentration of single-stranded DNA during SELEX, 2015, *Chemical communications* (Cambridge, England) 51: 1135–1138.
- 5) **Shahidi Hamedani N**, Shier W.T, Moghadam ariaee F, Abnous K, Ramezani M, Targeted gene delivery with non covalent electrostatic conjugates of sgc-8c aptamer and polyethylenimine, 2013, *The journal of gene medicine*, 15: 261-269.
- 6) Jalalian SH, Taghdisi SM, **Shahidi Hamedani N**, Kalat SA, Lavaee P, Zandkarimi M, Ghows N, Jaafari MR, Naghibi S, Danesh NM, Ramezani M, Abnous K, Epirubicin loaded super paramagnetic iron oxide nanoparticle-aptamer bioconjugate for combined colon cancer therapy and imaging in vivo, 2013, *European Journal of Pharmaceutical Sciences*, 50(2): 191-197.